(2)

PLANNED MONOLAYER ASSEMBLIES BY ADSORPTION

Final Technical Report

by

Jacob Sagiv

September 1988

United States Army

EUROPEAN RESEARCH OFFICE OF THE U.S. ARMY

London, England

CONTRACT NUMBER DAJA45-84-C-0055

Contractor: The Weizmann Institute
Attn: Ms. N. Guter
Office of Research Contracts and Projects
76 100 Rehovot, Israel

Unclassified
SECURITY CLASSIFICATION OF THIS PAGE

ADA205088

REPORT DOCUMENTATION PAGE

Form Approved
OMB No 0704-0188
Exp Date Jun 30 1986

1a. REPORT SECURITY CLASSIFICATION Unclassified	1b. RESTRICTIVE MARKINGS
2a. SECURITY CLASSIFICATION AUTHORITY	3. DISTRIBUTION / AVAILABILITY OF REPORT Approved for public release; distribution unlimited
2b. DECLASSIFICATION / DOWNGRADING SCHEDULE	
4. PERFORMING ORGANIZATION REPORT NUMBER(S)	5. MONITORING ORGANIZATION REPORT NUMBER(S) R&D 4501-MS-01
6a. NAME OF PERFORMING ORGANIZATION The Weizmann Institute of Science 6b. OFFICE SYMBOL (If applicable) 6	7a. NAME OF MONITORING ORGANIZATION European Research Office (USARDSG-UK)
6c. ADDRESS (City, State, and ZIP Code) Department of Isotope Research 76100 Rehovot Israel	7b. ADDRESS (City, State, and ZIP Code) Box 65 FPO NY 09510-1500
8a. NAME OF FUNDING / SPONSORING European Research Office USARDSG-UK 8b. OFFICE SYMBOL (If applicable) (RM)	9. PROCUREMENT INSTRUMENT IDENTIFICATION NUMBER DAJA45-84-C-0055
8c. ADDRESS (City, State, and ZIP Code) Box 65 FPO NY 09510-1500	10. SOURCE OF FUNDING NUMBERS PROGRAM ELEMENT NO. 61102A; PROJECT NO 1L161102BH57; TASK NO; WORK UNIT ACCESSION NO

11. TITLE (Include Security Classification)
(U) Planned Monolayer Assemblies by Adsorption

12. PERSONAL AUTHOR(S)
Dr. Jacob Sagiv

13a. TYPE OF REPORT	13b. TIME COVERED	14. DATE OF REPORT (Year, Month, Day)	15 PAGE COUNT
Final	FROM 1984 TO 1988	1988 September	13

16. SUPPLEMENTARY NOTATION

17 COSATI CODES			18. SUBJECT TERMS (Continue on reverse if necessary and identify by block number)
FIELD	GROUP	SUB-GROUP	
11	03		
07	04		

19. ABSTRACT (Continue on reverse if necessary and identify by block number)

Based on previous experimental results obtained in our laboratories, studies have been carried out with the main purpose of developing organic monolayer and multilayer films of ordered organic molecules that might show real potential as ultrathin protective or passivating coatings for certain practical applications. The research has focused on three interrelated issues: (i) a comparative study of the stability and structural perfection of some representative monolayer systems obtained by the Langmuir-Blodgett method and by self-assembly, and an evaluation of their performance as ultrathin barriers; (ii) an investigation of possible routes to the efficient in-situ chemical modification of preassembled monolayers; (iii) an exploration of the possible construction of high-quality multilayer structures via chemically-controlled self-assembly. The results demonstrate that high-quality mono and multilayer films may be obtained via self-assembly, provided certain conditions related to the mode of film-to-surface binding and

CONT. OVERLEAF.....

20. DISTRIBUTION / AVAILABILITY OF ABSTRACT	21. ABSTRACT SECURITY CLASSIFICATION
☒ UNCLASSIFIED/UNLIMITED ☒ SAME AS RPT. ☒ DTIC USERS	Unclassified
22a. NAME OF RESPONSIBLE INDIVIDUAL Dr. Wilbur C. Simmons	22b TELEPHONE (Include Area Code) 01-409 4423
	22c OFFICE SYMBOL AMXSN-UK-RM

DD FORM 1473, 84 MAR 83 APR edition may be used until exhausted. All other editions are obsolete.

SECURITY CLASSIFICATION OF THIS PAGE
Unclassified

cont'd

the geometry of the film forming molecules are fulfilled. For example, highly stable solid-supported monolayer barriers, capable of efficiently blocking the passage of ions and molecules from an adjacent fluid phase, could be engineered on various solid substrates using long chain silanes that bind covalently to the underlying surface, while polymerizing laterally to form a compact two-dimensional network. Good quality multilayer structures could be successfully prepared by self-assembly using bifunctional long chain silanes provided with non polar functions which may be modified through appropriate surface chemical reactions conducted on the preassembled film. Finally, the present research demonstrates the superior performance of certain self-assembling monolayers, in terms of stability and degree of structural perfection, as compared to analogous films prepared by the Langmuir-Blodgett method.

1. STATEMENT OF THE PROBLEM AND BACKGROUND

The research consisted of a series of studies performed with the general purpose of developing organized self-assembling mono and multilayer organic films that might have practical applicability as ultrathin protective or passivating coatings on various solids, including semiconductor materials. The project has been initiated on the basis of previous experimental results obtained in this laboratory, which indicated that ordered solid-supported monolayers reminiscent of Langmuir-Blodgett (LB) films (deposited on solids by mechanical transfer of monolayers initially formed as floating films on water) may be obtained directly on various polar solids via spontaneous molecular self-assembly (SA) from solution. Compared to the mechanical procedures involved in the deposition of LB monolayers, the spontaneous self-assembly process presents a number of intrinsic advantages, particularly important with regard to possible practical applications. The SA approach is free of some of the inherent limitations of the LB method, while offering new options for the utilization of ordered organic monolayers.

Preliminary evidence obtained in this laboratory pointed to the remarkably improved performance of SA monolayers as regarding their stability under adverse physical and chemical conditions. This encouraged us to pursue a research program aiming at the preparation of ultrathin organic films of unusual robustness and structural integrity. A study of the <u>in-situ</u> chemical modification of preformed SA films has also been undertaken, with the purpose of extending our synthetic capabilities towards the construction of novel types of ordered mono and multilayer films with planned structure and properties. These studies were directly related to another objective of the present re-

search - the development of high quality multilayer structures via self-assembly. As shown previously by us, the self-assembly approach may, in principle, be extended to the preparation of ordered multilayers, using a stepwise process consisting of monolayer deposition by self-assembly followed by its subsequent chemical modification, in order to generate surface binding sites for the anchoring of the next layer in the structure.

Obviously, the chemical modification of a preformed film is limited by the film structural stability under the conditions required by the respective chemical reactions. Thus, highly resistant and structurally stable films are required for this purpose, which demonstrates the interrelation between the different main directions of the present research: (i) studies on the stability and structural perfection of organic monolayers and development of more resistant such films; (ii) development of chemical routes to the efficient in-situ chemical modification of preassembled monolayers; (iii) construction of planned high quality multilayer structures via self-assembly. A comparison of SA and analogous LB films, with regard to their stability and degree of structural perfection, was also considered essential within the present research, in order to provide a common basis for the evaluation of the performance of ordered organic monolayers, in general.

2. SUMMARY OF MAIN RESULTS

Most of the experimental work, including the comparative investigation of SA and analogous LB systems, has been done on monolayers of long chain surfactants, some of which were partially or totally fluorinated. Such surfactants may form Langmuir monolayers on water as well as self-assemble on solids.

Some surfactants containing aromatic moieties have also been synthesized and investigated as SA systems.

a. Studies on the Stability, Structural Integrity, and Barrier Performance of LB and SA Monolayers

Experiments have been carried out to determine the thermal behavior of some representative monolayer systems,[1] their resistance to extraction by solvents and exposure to various corrosive reagents at ambient as well as elevated temperatures.[2,3] The performance of monolayers as diffusion barriers, i.e. protective/passivating coatings preventing the passage of undesired molecular or ionic species from the surrounding environment, has also been investigated.[3,4] The main findings are summarized below:

* In general, SA systems have shown superior properties, as compared to analogous LB films, in all above mentioned tests.

* SA silane monolayers stabilized by intralayer (lateral) and layer-to-substrate covalent bonds, display remarkably improved performance, in terms of stability, structural integrity, and barrier efficiency, as compared to ionic fatty acid films.[1,3,4]

* For example, monolayers of long chain silanes on aluminium mirrors maintain their highly ordered solid-like state up to temperatures in excess of 150°C,[1] such monolayers on silicon may be extracted for hours with various solvents, including boiling toluene (110°C), or exposed to concentrated hydrochloric acid at 100°C and $LiAlH_4$ in boiling THF (67°C), without showing any sign of structural deterioration.

* Studies on the penetrability of monolayers, performed by means of "penetration reactions" (reactions of ionic or molecular species diffusing from an

outer fluid phase with a monolayer inner function, or the underlying solid sibstrate itself), demonstrate that highly efficient protective barriers may be produced on Si and ZnSe using long chain silane monolayers.[3,4] Long chain thiols show similar performance on gold.[5] It has been demonstrated that oriented, tightly packed monolayers of long chain amphiphiles may behave as perfect barriers, provided they are free of pinholes and their highly ordered structure is preserved under exposure to the penetrating species.[4] The barrier performance of monolayers is thus a function of both their structural integrity and stability. Obviously, the morphology and chemical nature of the coated solid are important factors in this respect. It thus appears that the improved behavior of mixed thiol-silane monolayers on gold (monolayers of this type may be prepared behaving as perfect barriers for ions as well as water itself) is a consequence of both their improved surface coverage and stability, resulting from the combined use of a laterally polymerizable (silane) and a surface attached monomeric (thiol) component.

* The encouraging results obtained in the preparation of stable, pinhole-free monolayer barriers enabled us to construct and demonstrate, for the first time, the functioning of efficient ion-specific electrode coatings of molecular thickness.[5] Such electrochemical monolayer membranes are prepared as mixed monolayers, incorporating a specific ion-binding ("active") component within the matrix formed by a nonspecific ("blocking") component, which functions as a barrier for undesired ionic species.

b. Investigation of Surface Reactions for the In-Situ Chemical Modification of Preassembled Monolayers

A number of surface reactions involving monolayer functions have been investigated during this project: hydrolysis of ester functions, reduction of ester functions, oxidation of ethylenic double bonds with $KMnO_4$ in aqueous and organic solutions. The usefulness of such reactions as synthetic tools for the modification of surface properties, or for the activation of exposed monolayer surfaces, depends on the structural stability of the monolayers to be modified, the time required for complete conversion of the reacting functions, and the distribution of the reaction products.

Main findings:

* Ionically bonded fatty acid monolayers, of either the LB or SA type, do not withstand the conditions required by above mentioned reactions, and, thus, may not be modified using such surface chemical transformations.[4]

* Covalently bonded silane monolayers are considerably more resistant on Si than on ZnSe or Ge. Thus, while such reactions (or solvent extractions) may be carried out with Si substrates at elevated temperatures (above 100°C),[3] silane monolayers on ZnSe or Ge are usually resistant under exposure to similar treatments only at the ambient temperature. This may have to do with the nature of the monolayer-to-surface bonding or the possible slight dissolution of the support itself (for ZnSe).[4]

* The ester hydrolysis must be conducted in acidic (HCl) media, as hot NaOH or KOH solutions cause damage to silane monolayers, most probably through the hydrolytic breaking of (Si-O-Si) bonds.

* With terminal functions, all studied reactions are complete within times of the order of 30 min., leading to a single reaction product[2-4] (the situation is more ambiguous with aqueous $KMnO_4$).[4]

* Monolayer inner functions may also be affected, and the reaction brought to completion, provided the monolayer is cleaved at the position of the reacting function. In this case, much longer reaction times are required (many hours), the reaction mechanism involving lateral propagation from edges and layer defects.[3]

c. Construction of Planned Multilayer Structures via Self-Assembly

The main problems involved in the construction of planned multilayer structures via chemically-controlled self-assembly are related to the stability of the interlayer bonding under the conditions required for the chemical activation of the outer film surface, and the necessity of preserving the molecular order with increasing member of deposited layers, i.e. avoiding accumulation of structural defects from layer to layer.

We have investigated a number of possible routes to the construction of planned SA multilayer structures, using long chain silanes with terminal double bonds[3] or ester functions, aliphatic[2] as well as aromatic.[3] Chemical surface activation has been achieved by the conversion of terminal double bonds to hydroxyls via hydroboration,[3] the oxidation of double bonds to carboxyls by organic permanganate[3] (followed in some cases by reduction with $LiAlH_4$ to terminal hydroxyls), the acidic hydrolysis of ester functions to terminal carboxyls,[3] and $LiAlH_4$ reduction of ester functions to terminal hydroxyls.[2,3]

Results obtained in the course of the present research project demonstrate that, if adequately applied, each of the above mentioned chemical activation routes may, in fact, lead to multilayer structures of good quality. It became apparent that some of the difficulties previously reported by us[2,6] originated in the purity of the monolayer forming compounds and the contamination of the activated film surface by traces of photochemically generated phosgene present in the rinsing solvent (chloroform).

Two examples of multilayer construction, involving the hydroboration of the terminal double bond of a long chain aliphatic silane, and the reduction of a long chain silane with an aromatic ester function, are given in ref. 3. It is quite obvious from these examples that sterical factors play an important role in the engineering of SA multilayer structures. Thus, to avoid accumulation of structural defects, which may then interfere with the smooth deposition of additional layers on top of each other, it is important to maintain the orientation and tight molecular packing of each layer. Apparently, this ensures that the intralayer polymerization proceeds to the extent that lateral "bridging" can compensate for missing binding sites or other structural defects in the underlying layer. In this manner, each layer becomes independent of that lying underneath it, and the accumulation of structural defects with the deposition of additional layers is thus avoided. Based on these results, studies have been initiated, and are presently in progress, aiming at the construction of SA multilayer films provided with oriented aromatic chromophores as intrinsic part of their structure (see "3rd Periodic Report").

CONCLUSIONS AND RECOMMENDATIONS

The main objectives of the herewith summarized research project have been successfully accomplished, the results demonstrating real possibilities for certain technological applications of self-assembled mono and multilayer films;

1. The performance of covalently bonded silane monolayers, in terms of degree of structural perfection and stability, may meet the specifications required for a range of practical applications, including their utilization as protective/passivating coatings.

2. Since the chemical nature and morphology of the coated solid play active roles in the mode and strength of layer-to-surface binding, also affecting the structural perfection of a monolayer coating, one must regard the solid substrate as an integral part of any monolayer system formed via self-assembly. The performance of a monolayer barrier is thus to be evaluated only with reference to a particular substrate, the same monolayer components behaving differently on different substrates. As the various analytical methods employed during the present project were not universally applicable to each of the studied solid substrates, it is rather difficult to establish quantitative correlations between the various monolayer/substrate systems with regard to their barrier efficiencies. For example, while quantitative FTIR spectroscopy in the Total Internal Reflection mode could be applied to Si and ZnSe, the powerful electrochemical methods were applicable to Au substrates only.

To develop a protective or passivating monolayer coating for a specific application, it will, therefore, be necessary to prepare and test it in direct relation to the particular application for which it is intended. In general,

the results obtained during the present studies demonstrate that useful monolayer barriers may actually be engineered using techniques of monolayer self-assembly.

3. Studies performed in the course of this research project indicate that high quality multilayer structures are obtainable via self-assembly, provided the right type of monolayer-forming components and proper experimental conditions are employed.

While some general hints emerge from these studies as to what may work and what not, additional basic research will be certainly required to establish reliable rules regarding the construction of SA multilayers. Further research will also be required to develop any particular new system which might present interest for a particular type of application. It is reasonable to assume that the gradual accumulation of more experimental data in this area will shorten the research effort necessary for the development of new and more complex SA systems.

If the prospect of investing a large effort in the development of novel SA film systems may be discouraging, one should be reminded that the alternative LB route is, in fact, not shorter if films meeting a particular set of specifications are to be produced. Thus, despite the considerable research effort so far invested in LB films all over the world, no technological applications of such systems have been yet reported. On the basis of the present results, it appears that chances are much better to reach this goal by the self-assembly approach.

REFERENCES

1. S.R. Cohen, R. Naaman and J. Sagiv, "Thermally induced disorder in organized organic monolayers on solid substrates", J. Phys. Chem. 90, 3054 (1986).
2. M. Pomeratnz, A. Segmüller, L. Netzer and J. Sagiv, "Coverage of Si substrates by self-assembling monolayers and multilayers, as measured by IR, wettability and X-ray diffraction", Thin Solid Films 132, 153 (1985).
3. R. Maoz, L. Netzer, J. Gun and J. Sagiv, "Self-assembling monolayers in the construction of planned supramolecular structures and as modifiers of surface properties", Proceedings of NATO Advanced Research Workshop on "Properties and Applications of 2-Dimensional Organic Films: Langmuir Blodgett Films and Related Structures", Val de Courcelle (Paris) France, 5-9 June 1988, J. Chim. Phys., in press.
4. R. Maoz and J. Sagiv, "Penetration controlled reactions in organized monolayer assemblies. I. Aqueous permanganate interaction with monolayer and multilayer films of long chain surfactants", Langmuir 3, 1034 (1987).
5. R. Maoz and J. Sagiv, "Penetration controlled reactions in organized monolayer assemblies. II. Aqueous permanganate interaction with self-assembling monolayers of long chain surfactants", Langmuir 3, 1045 (1987).
6. I. Rubinstein, S. Steinberg, Y. Tor, A. Shanzer and J. Sagiv, "Ionic recognition and selective response in self-assembling monolayer membranes on electrodes", Nature 332, 426 (1988).

7. L. Netzer, R. Iscovici and J. Sagiv, "Adsorbed monolayers versus Langmuir-Blodgett monolayers - why and how? II. Characterization of built-up films constructed by stepwise adsorption of individual monolayers", Thin Solid Films 100, 67 (1983).

SELF-ASSEMBLING MONOLAYERS IN THE CONSTRUCTION OF PLANNED SUPRAMOLECULAR STRUCTURES AND AS MODIFIERS OF SURFACE PROPERTIES

Rivka Maoz, Lucy Netzer, Julio Gun and Jacob Sagiv

Department of Isotope Research

The Weizmann Institute of Science

76100 Rehovot, Israel

ABSTRACT

Organized monolayer structures prepared on polar solids via spontaneous adsorption from organic solutions (self-assembly) exhibit some rather unique features, particularly relevant with regard to possible technological applications of such systems.

The outstanding stability of covalently bonded monolayers under exposure to a variety of adverse physical and chemical agents allows well known methods of synthetic organic chemistry to be applied to their *in-situ* chemical modification. This offers interesting new opportunities for the engineering of planned film structures, directly on the desired solid surface.

Proceedings of the NATO Advanced Research Workshop on "Properties and Applications of 2-Dimensional Organic Films: LB Films and Related Structures", Val de Courcelle (Paris), France, 5-9 June 1988, J. Chim. Phys., in press.

Examples will be given to illustrate the key roles of molecular organization and mode of film-to-surface binding in the chemical manipulation of preassembled films, while briefly discussing some related aspects of the process of molecular self-assembly at solid-liquid interfaces. The discussion will focus on three different directions of application:

1. Preparation of stable organic surfaces with well defined outer functionality.
2. Construction of planned multilayer structures via self-assembly.
3. Construction of monolayer barriers and utilization of "penetration" reactions as sensitive probes of the penetrability and structural integrity of monolayers films.

INTRODUCTION

Organized monolayer films have long been considered attractive for a variety of applications of scientific interest, however, it is only recently that research in this area has entered the critical stage of evaluating the technological feasibility of some of these applications[1].

Formation of ordered monolayers via self-assembly[2-10], i.e. spontaneous adsorption from a bulk fluid phase (usually organic solution) onto a polar solid contacting the fluid, presents some rather unique features, which, apart from their theoretical significance, are particularly valuable from the point of view of possible technological applications of monolayer systems. Thus, being a spontaneous molecular process, the

self-organization of molecules at fluid-solid interfaces should necessarily lead to stabilized (low free energy) structures, at least under the conditions prevailing during their formation. The process does not involve mechanical operations, meaning that the quality of self-assembled films is not affected by macroscopic mechanical factors, and, therefore, should not depend on the availability of sophisticated deposition equipment. Ordered self-assembling monolayers may, in principle, be prepared on a large variety of smooth polar solids, regardless of their size, shape, or state of dispersion[3]. Furthermore, as water is not required in the formation of these monolayers, the use of water-sensitive materials is also allowed, as well as that of monolayer components not necessarily possessing the amphiphilic character required for formation of insoluble Langmuir monolayers at water-gas interfaces[10,11]. Finally, the direct anchoring of the film to the underlying solid substrate is one of the most important features characteristic of self-assembly. Since the driving force in the process of monolayer formation on solid surfaces is largely provided by the attractive interactions between the adsorbate molecules and the solid, the specific mode of binding to the solid plays key roles in the dynamics of film formation as well as in the stabilization of the final film structure[11,12]. As we have shown[3,11-17], the layer-to-surface and intralayer covalent bonding achieved in self-assembled silane monolayers results in remarkably improved film stability. Covalently bonded silane monolayers were found to be highly resistant to adverse conditions, such as prolonged extrac-

tions by good solvents[11-13], high temperatures[14], and treatments by corrosive chemicals[13,15]. Such monolayers are expected to meet the stringent stability requirements posed by a variety of applications of technological interest. In addition, the high structural stability conferred by covalent bonding offers interesting new synthetic possibilities, through the in situ chemical modification of preassembled films, directly on the desired solid surface[15-17] (see below).

Research conducted in this laboratory over the past several years has aimed at elucidating a number of basic questions regarding the process of monolayer formation via self-assembly[3,8,12,13], while exploring the feasibility and general problematics of the chemical manipulation of preassembled film structures[15-17]. The purpose of this paper is to briefly discuss a number of examples illustrating possibilities for the use of self-assembling monolayers in three different directions of application bearing technological relevance.

1. MODIFICATION OF SURFACE PROPERTIES - PREPARATION OF STABLE ORGANIC SURFACES WITH WELL DEFINED OUTER FUNCTIONALITY

Some examples of important scientific and technological applications that should benefit from the availability of organic surfaces with well defined outer functionality (in terms of the chemical nature, density and orientation of the exposed functions) are listed below:

* Fundamental studies of physical and chemical forces operating at interfaces[1,18].
* Coupling of two surfaces (adhesion)[19].

* Prevention of adhesion - low energy surfaces[20-22].

* Biocompatible surfaces[6,23,24].

* Epitaxial control of crystal growth[25].

The use of oriented monolayers exposing the desired functions provides an attractive straightforward route to the preparation of such surfaces. However, the usefulness of this approach is limited by the usual low stability of monolayer coatings. For example, unless polymerized under water[24,26] or under a hydrophilic coating[24], Langmuir-Blodgett monolayers exposing polar outer functions undergo the well known turn-over rearrangement (to a non polar outer surface) when pulled out of the water through the water-air interface[27]. Surface-bound monolayers prepared by self-assembly offer a satisfactory solution to the problem of stability of monolayer coatings. The modification of the chemical nature of a solid surface upon coating with such monolayers may, in principle, be achieved in two different ways:

a) The monolayer forming molecules are designed such as to orient on the surface with the desired function pointing outwards.

b) The desired surface function is introduced via the in situ chemical modification of preassembled monolayers made of appropriate bifunctional constituents (see Figure 1).

Figure 1 here

The first route is usually applicable to the preparation of low-energy non-polar surfaces (except for cases where the anchoring to the sur-

face is highly specific and effected through moieties having poor general reactivity or adsorptivity, like thiols or sulphides on gold[6,9,10]), while the second one allows stable surfaces with polar outer functionality to be produced. In the following, examples will be given illustrating the use of the first route in the preparation of fluorinated surfaces and of the second one in the preparation of surfaces with exposed carboxylic or hydroxylic groups.

Fluorinated Surfaces

Surfaces exposing closely packed ($-CF_3$) groups exhibit the highest so far observed liquidophobicity (highest contact angles with respect to water as well as organic liquids)[20]. Fluorinated monolayers are of interest for the preparation of highly non-adherent (low energy) surfaces, as inert protective coatings, and also in connection with their special electrical properties[28].

Highly oleophobic fluorinated surfaces prepared in the past by adsorption of perfluorinated fatty acids[20] had low stability, particularly in contact with water, which limited considerably their usefulness as hydrophobic coatings. Looking for a convenient simple route to the synthesis of fluorinated surfactants suitable for preparation of stable monolayers with the desired structural properties, we have used intrachain ester functions to obtain partially fluorinated long chain surfactants in which a hydrocarbon chain segment serves as spacer between the terminal fluorocarbon one and a silane or carboxyl head group (Compounds

(B), (C)). It was anticipated that the packing density and orientation of such partially fluorinated chains would be determined by the bulkier fluorocarbon segments[20,21], thus producing monolayers with densely packed outer ($-CF_3$) groups. The long chain acid (C), structurally analogous to the silane (B), lends itself to preparation of monolayers via both self-assembly (SA) and the Langmuir-Blodgett (LB) method[21], which provided us with the important additional option of comparing the two types of films[3,13] (see also section 3 below).

Formulas of Compounds (A), (B), (C) here

The formation and structure of SA monolayers of a series of partially fluorinated long chain and fluorinated short chain surfactants, such as (B), (C) and (A), have been investigated using Fourier transform infrared (FTIR) spectroscopy in the internal reflection (ATR)[3] and external reflection (reflection-absorption-RA)[4,7,8,13] modes, and contact angle measurements[3-5,9,20]. Glass, aluminum, ZnSe, Ge and Si were employed as solid substrates. The SA monolayers were compared with LB monolayers of compound (C) deposited on the respective substrates from the water-air interface[3,13].

It was found that the silane (B) forms covalently bonded SA monolayers exhibiting surface energies in the range of the lowest values (highest contact angles) so far reported[20], while displaying remarkably higher stability, under exposure to both organic solvents and water, than previously reported fluorinated acid monolayers[20]. The fluorocarbon

chain segments in such monolayers appear to actually approach a state of dense packing with rather good perpendicular orientation on the surface, while the hydrocarbon segments are more disordered, as expected from the difference in the cross sections of the fluorocarbon and hydrocarbon chains[20,21]. Short chain fluorinated surfactants such as the silane (A) or the corresponding acid tend to adsorb as partially oriented multilayers, possibly as a result of their low solubility in the hydrocarbon solvents employed in these experiments.

Table 1 here

Figure 2 here

Examples of ATR spectra and the respective contact angle values are given in Figure 2 and Table I for some representative films of compounds (A), (B) and (C), and also for a monolayer of n-octadecyltrichlorosilane (OTS)[3,12] on Ge. The significantly higher contact angles measured on films of the long chain silane (B), as compared with those of the other fluorinated compounds, point to the more uniform orientation and possibly denser molecular packing of the former[3,12]. This conclusion is corroborated by the IR data. According to the integrated intensities of the ($-CH_2-$) stretch bands around 2900 cm^{-1} (compare curve (B) with that of OTS in Figure 2), compound (B) forms an oriented SA monolayer with a packing density of the order of 33 $Å^2$/molecule[21]. The intensity of the ($-CF_2-$) stretch band at 1151 cm^{-1} in curve (B) is ca. 1.7 times higher

than that of the analogous LB monolayer in curve (C), while the corresponding ($-CH_2-$) bands at 2922 cm^{-1} differ by a factor of only 1.17. This points to differences in both the density and the molecular orientation of the two films[3], the SA silane monolayer being denser and having better perpendicular orientation of its fluorocarbon segments. Further evidence supporting these conclusions is obtained from the analysis of the RA spectra of the respective monolayers on Al (not shown). Compared to OTS, the broadening and blue-shift (from 2918 cm^{-1} to 2922 cm^{-1}) of the ($-CH_2-$) stretch bands of (B) and (C) are both indicative of the looser packing and less ordered arrangement of the hydrocarbon segments[30] in these partially fluorinated amphiphiles. Finally, the integrated intensity of the 1151 cm^{-1} band in curve (A) is seen to be ca. 10 times larger than that in curve (C), clearly demonstrating the multilayer nature of the adsorbed film formed by the short chain silane (A).

Surfaces with Exposed Carboxylic or Hydroxylic Groups

Figure 3 here

The surface hydrolysis and reduction of a bifunctional monolayer with a silane head group and a terminal aromatic ester function (C_{17}SPE) are schematically depicted in Figure 3. As demonstrated by the ATR spectra in Figures 4 and 5, these surface modification reactions can be carried out to completion within reasonable times, without affecting the integrity of the reacted monolayers. The advancing contact angles for H_2O

and bicyclohexyl change accordingly[9,16,17], from initial values of ca. 90°and 31°, to final values of ca. 55°and 0°on the acid surface, and 50°and 0° on the alcohol surface, respectively. It should be noted that the presence of the terminal benzene ring imposes a somewhat looser chain packing in these monolayers, as compared with that reached in monolayers of normal long chain amphiphiles such as OTS[3].

Figures 4 and 5 here

Hydroxyl and carboxyl reach surfaces prepared by this method are perfectly stable under water as well as in air or in organic solvents, and may thus be used in various applications, among others, in the construction of SA multilayer organizates[16,17] (Figure 1, see also below).

2. CONSTRUCTION OF PLANNED MULTILAYER STRUCTURES VIA SELF-ASSEMBLY

Some of the most attractive possible applications of organized monolayer assemblies follow from their precisely defined architecture, in terms of the position and orientation of individual molecular constituents in space. Many of these applications require that ordered structures thicker than one monolayer be assembled. Examples include the fabrication of piezo, pyroelectric and non-linear optical elements, molecular insulators, conductors, and, in the more distant future, the eventual assembly of more sophisticated elements for molecular electronic devices[1]. Therefore, developing methods for the construction of planned layered assemblies of gradually increasing complexity, suffi-

ciently resistant for applications of practical interest, constitutes a major objective in monolayer research today[1]. As we have shown[16,17], combining the basic process of monolayer self-assembly with the in situ chemical modification (activation) of preassembled monolayers, provides a promising new synthetic approach to the construction of such structures (Figure 1). The chemical activation of the outer monolayer surface, realized through the use of bifunctional monolayer constituents, plays the role of a controllable triggering system allowing sequential deposition of discrete monolayers in a growing multilayer structure. The required stability of the resulting structure may be achieved by inter and intralayer covalent bonding of its constituents. We should emphasize that the use of monolayer constituents with "inert" outer functions, convertible into "active" ones upon appropriate surface chemical treatment, is essential if precise control on the deposition and orientation of each monolayer is to be maintained.

Our first attempts to construct SA multilayer films according to the scheme in Figure 1 met with some difficulties[16,17], which now appear to have originated in technical problems related to the purity of the monolayer forming compounds and the contamination of the exposed film surface following the chemical activation steps. As demonstrated by the examples given below, if adequately applied, the basic adsorption-surface-chemical-activation approach depicted in Figure 1 may yield high quality self-assembled multilayer structures (Experimental details will be provided in a number of forthcoming publications).

Figure 6 here

Figure 6 shows IR spectra recorded during the construction of a 5-layers film of a long chain (C_{19}) silane-terminal double bond surfactant (NTS), using the previously reported general method of double bonds conversion to terminal hydroxyls (via hydroboration and treatment with basic H_2O_2) and interlayer coupling through covalent (Si-O-C) bridges[16]. As evidenced by the absorbance intensities in Fig. 6, within the experimental error, each deposited layer represents a complete monolayer of densely packed and perpendicularly oriented NTS molecules, no systematic variations in the amount of material and its orientation being detectable from layer to layer. This is confirmed by the constant high contact angles measured after the deposition of each of the five layers (103°-105° for H_2O, 50°-52° for bicyclohexyl, 44°-46° for n-hexadecane)[3,16]. Thus, the stepwise film growth process appears to proceed smoothly and independent of the total number of superimposed layers[16,17].

Figure 7 here

A different example of multilayer construction using the same basic approach is given in Figure 7. The surface activation of this aromatic ester monolayer, realized via its reduction to the respective terminal alcohol (Figure 3), involves removal of the terminal benzene ring. This is seen to result in a surfactant with a molecular cross section smaller than that of the initial one. Some of the "sterical matching" difficulties arising from the use of such a bifunctional surfactant, featuring a

terminal function bulkier than its main hydrocarbon core (Figure 1), are apparent in Figure 7. In order to preserve the orientation of the paraffinic chains following removal of the aromatic end groups, and thus allow regular deposition of ordered layers on top of each other, it was necessary to introduce OTS molecules as "filler" material into the free space between the chains of the C_{17}SPE molecules. Using this strategy, a multilayer film made of 9 superimposed monolayers was constructed on a Si ATR plate, each layer containing besides C_{17}SPE the equivalent of ca. 10% of a complete OTS monolayer.

ATR spectra recorded after deposition of the first, third and sixth layer in this nine layers film are shown in Figure 8. The step-by-step growth in the thickness of the film is evidenced by the corresponding growth in the absorbance of the ($-CH_2-$) stretch bands[3,16,17] around 2900 cm^{-1}, while the constancy of the carbonyl stretch band at 1761 cm^{-1} demonstrates the basic equivalence of each of the respective C_{17}SPE monolayers in the multilayer film. It should be further noted that the carbonyl band disappears following each reduction step (see Figures 3, 5), only the last deposited (unreduced) monolayer in the growing multilayer film retaining the ester function (Figure 7). The stepwise film growing process, according to Figure 7, is, finally, confirmed by the alternation in the contact angles following each adsorption and reduction step[16,17]. The H_2O advancing contact angle was found to alternate between ca. 90° and 50° and the bicyclohexyl angle between ca. 26° and 0° for each layer, except for the first one, on which the initial bicyclo-

hexyl contact angle was ca. 30° This points to a possible slight difference in the orientation of the molecules in each of the upper layers as compared with the first one.

Figure 8 here

Further work is now in progress aiming at the construction of aromatic multilayer structures designed such that their molecular packing and orientation are not drastically affected by the surface chemical activation of each layer. UV and polarized UV spectroscopy are used to determine the chemical transformations and the orientation of the aromatic moieties in these films.

3. CONSTRUCTION OF MONOLAYER BARRIERS. UTILIZATION OF "PENETRATION" REACTIONS AS SENSITIVE PROBES OF THE PENETRABILITY AND STRUCTURAL INTEGRITY OF MONOLAYER FILMS

Ordered solid-like monolayers of long chain amphiphiles are expected to behave as efficient ultrathin diffusion barriers for various ionic and molecular species. This follows from the exceptionally high density and rigidity of such films, achieved through the uniform alignment and tight packing of their molecular constituents. The possibility of engineering efficient monolayer barriers is attractive for a number of novel applications, including the development of ultrathin protective coatings, high resolution electron-beam resists, ultrathin selective membranes, and selective monolayer-modified electrodes[1]. However, the lit-

erature presents apparently contradictory evidence regarding the penetrability of monolayer and multilayer films[15,29]. An extensive comparative study of the penetrability of some mono and multilayer LB films and SA monolayers recently carried out in this laboratory[15,29] demonstrates that the passage of molecular and ionic species across a tightly packed monolayer assembly of oriented long chain amphiphiles occurs through fortuitous structural defects in the assembly, or through defects generated under the action of the penetrating species. The penetrability of the films was probed by monitoring the extent of $KMnO_4$ oxidative attack on intralayer located ethylenic double bonds. Both aqueous[29] and organic[15] solutions of $KMnO_4$ were examined. As before, FTIR-ATR spectroscopy and contact angle measurements were employed to reveal the chemical and structural transformations undergone by the films upon their exposure to the penetrating reagents. Some of the main results of this investigation are listed below:

* SA monolayers of long chain acid salts were found to be less penetrable than analogous LB films containing from one to three superimposed monolayers. This is a consequence of the higher degree of perfection and higher structural stability of the SA monolayers.
* It is possible to produce SA acid salt monolayers displaying high barrier efficiencies when exposed to the $KMnO_4$ solutions for times of the order of several minutes. Longer exposure times result in gradual deterioration of the ordered structure of such ionic films, with a corresponding drastic increase in their penetrability.

* Covalently bonded SA monolayers of both saturated and unsaturated long chain silanes are highly stable and impenetrable (in their tightest mode of packing) in the aqueous permanganate environment. Saturated silane monolayers display similar behaviour also in the organic permanganate.
* Unsaturated silane monolayers undergo in the organic reagent very slow oxidative cleavage of the chains at the position of the double bonds, via a mechanism of lateral propagation starting from edges and layer defects. The process ends in the formation of an oriented shorter chain monolayer with exposed carboxylate functions (Figure 9).

Figure 9 here

The ATR spectra in Figure 10, taken before and after exposure of an unsaturated silane monolayer to the organic permanganate reagent for 2 and 6 hours, confirm the gradual cleavage of the chains, as suggested in Figure 9.

For comparison, Figure 11 shows ATR spectra of complete and incomplete monolayers of the same unsaturated silane as in Figure 9 taken during their exposure to the aqueous permanganate reagent. According to the decrease in the absorbance of the (C=C) band at 964 cm^{-1}, more than 60% of the ethylenic functions in the incomplete monolayer are oxidized within 3 minutes, while no measurable change in the absorbance of this band is observed in the complete (densely packed) monolayer even after

30 to 90 minutes exposure to the reagent (only the 30 min. spectrum is shown in Figure 11). The penetration of the aqueous permanganate ion into the inner core of a monolayer is thus clearly seen to depend on its packing density, being efficiently blocked by layers approaching their tightest mode of packing. Except for the decrease in the (C=C) band absorbance of the incomplete monolayer, practically no other spectral changes are observed in Figure 11, thus demonstrating the structural stability of these silane monolayers in the aqueous $KMnO_4$ solution.

Figures 10 and 11 here

The present results emphasize the important role of film structural stability, besides its degree of structural perfection, in the engineering of useful monolayer barriers. Covalently bonded silane monolayers were found to exhibit remarkably superior performance in such applications as compared to ionically bonded acid films. It is further demonstrated that "penetration" reactions are very useful as sensitive probes of the penetrability of monolayer films, while supplying additional valuable information on their overall structural stability. Finally, the lateral cleavage of unsaturated silane monolayers by the organic permanganate reagent suggests interesting synthetic possibilities for the preparation of oriented short chain monolayers with outer polar functionality. In general, neither the LB method nor the self-assembly from solution allow such structures to be directly produced.

CONCLUDING REMARKS

Examples were presented demonstrating the potential of monolayer self-assembly in a range of possible applications. The attention has been focused on three main issues bearing particular relevance with regard to the possible technological utilization of monolayer systems:

* The stability of organic monolayers.
* The degree of structural perfection attainable in solid-supported films.
* The availability of film building methods enabling construction of organized assemblies with the desired molecular architecture.

As far as the compactness, integrity and film structural stability are concerned, it is now possible to produce covalently bonded SA monolayers of improved quality as compared to related LB films. Such monolayers are promising as molecular barriers and in applications demanding modification of surface properties. The enhanced stability of covalently bonded SA monolayers allows a variety of chemical modification reactions to be directly conducted on preassembled films, thus offering new synthetic options in the construction of more complex layered assemblies.

The NTS compound (Fig. 6) was a gift sample kindly supplied by Kazufumi Ogawa of Matsushita Electric Ind. Co., LTD., Osaka, Japan.

Partial support of this work by a grant from the European Research Office of the U.S. Army is gratefully acknowledged.

References

1. J.D. Swalen, D.L. Allara, J.D. Andrade, E.A. Chandross, S. Garoff, J. Israelachvili, T.J. McCarthy, R. Murray, R.F. Pease, J.F. Rabolt, K.J. Wynne, and H. Yu, Langmuir, 1987, 3, 932-950.
2. W.C. Bigelow, D.L. Pickett, and W.A. Zisman, J. Colloid Sci. 1946, 1, 513-538.
3. R. Maoz and J. Sagiv, J. Colloid Interface Sci., 1984, 100, 465-496.
4. D.L. Allara and R.G. Nuzzo, Langmuir, 1985, 1, 45-52; ibid. 52-66.
5. S. Garoff, R.B. Hall, H.W. Deckman, and M.S. Alvarez, Proc. Electrochem. Soc., 1985, 85-8,112-121.
6. T. Diem, B. Czajka, B. Weber and S.L. Regen, J. Am. Chem. Soc., 1986, 108, 6094-6095.
7. H.O. Finklea, L.R. Robinson, A. Blackburn, B. Richter, D. Allara and T. Bright, Langmuir, 1986, 2, 239-244.
8. E. Sabatani, I. Rubinstein, R. Maoz and J. Sagiv, J. Electroanal. Chem., 1987, 219, 365-371.
9. C.D. Bain and G.M. Whitesides, Science, 1988, 240, 62-63, and references cited therein.
10. I. Rubinstein, S. Steinberg, Y. Tor, A. Shanzer and J. Sagiv, Nature, 1988, 332, 426-429.
11. J. Sagiv, J. Am. Chem. Soc., 1980, 102, 92-98;
    J. Sagiv, Isr. J. Chem., 1979, 18, 339-345;
    J. Sagiv, Isr. J. Chem. 1979, 18, 346-353.

12. J. Gun and J. Sagiv, J. Colloid Interface Sci., 1985, 112, 457-472.

13. J. Gun, R. Iscovici and J. Sagiv, J. Colloid Interface Sci., 1984, 101, 201-213.

14. S.R. Cohen, R. Naaman and J. Sagiv, J. Phys. Chem., 1986, 90, 3054-3056.

15. R. Maoz and J. Sagiv, Thin Solid Films, 1985, 132, 135-151.

16. L. Netzer and J. Sagiv, J. Am. Chem. Soc., 1983, 105, 674-676;
L. Netzer, R. Iscovici and J. Sagiv, Thin Solid Films, 1983, 99, 235-241;
L. Netzer, R. Iscovici and J. Sagiv, Thin Solid Films, 1983, 100, 67-76.

17. M. Pomerantz and A. Segmüller, L. Netzer and J. Sagiv, Thin Solid Films, 1985, 132, 153-162.

18. See, for example: R.M. Pashley, P.M. McGuiggan, B.W. Ninham, D.F. Evans, Science, 1985, 229, 1088-1089.

19. See for example: E.G. Shafrin and W.A. Zisman, Advan. Chem. Ser., 1969, 87, 20-37.

20. F. Shulman and W.A. Zisman, J. Colloid. Sci., 1952, 7, 465-481; E.G. Shafrin and W.A. Zisman, J. Phys. Chem., 1962, 66, 740-748, and references cited therein.

21. M.K. Bernett and W.A. Zisman, J. Phys. Chem., 1963, 67, 1534-1540.

22. F.P. Bowden and D. Tabor, Mechanism of boundary lubrication, in:"The Friction and Lubrication of Solids", Clarendon Press, Oxford, 1950, 200-227;

O. Levine and W.A. Zisman, J. Phys. Chem., 1957, 61, 1068-1077.

23. J.A. Hayward, A.A. Durrani, C.J. Shelton, D.C. Lee and D. Chapman, Biomaterials, 1986, 7, 126-131, and references cited therein.

24. O. Albrecht, D.S. Johnston, C. Villaverde and D. Chapman, Biochim. Biophys. Acta, 1982, 687, 165-169.

25. E.M. Landau, M. Levanon, L. Leiserowitz, M. Lahav and J. Sagiv, Nature, 1985, 318, 353-356.

26. V. Enkelmann and J.B. Lando, J. Polymer Sci., 1977, 15, 1843-1854.

27. E.P. Honig, J. Colloid Interface Sci., 1973, 43, 66-72, and references cited therein.

28. E.E. Polymeropoulos and J. Sagiv, J. Chem. Phys., 1978, 69, 1836-1847.

29. R. Maoz and J. Sagiv, Langmuir, 1987, 3, 1034-1044;

ibid, 1045-1051.

30. L. Rothberg, G.S. Higashi, D.L. Allara and S. Garoff, Chem. Phys. Letters, 1987, 133, 67-72, and references cited therein.

Table 1. Equilibrium Advancing Contact Angles Measured on the Films of Figure 2

Film[a]	n-Hexadecane	Bicyclohexyl	H_2O
A, OTS/Ge	45°	51°	112°
(A) A, PFDTS/Ge	70°	78°	112°
(B) A, $C_{10}(F)C_{13}SE(11)/Ge$	81°	88°	124°
(C) L, $C_{10}(F)C_{12}AE/Ge$	71°	75°	108°

[a]A and L designate films produced by self-assembly (Adsorption) and the LB method, respectively.

Figure captions

Fig. 1. Schematic representation of the utilization of bifunctional monolayer constituents in the preparation of organic surfaces with polar outer functionality, and in the construction of planned self-assembling multilayer structures. The *in situ* chemical modification (activation) of the preassembled film is a key feature in both applications. Active functions are defined as those carrying potential for binding to the surface, or to which an additional monolayer may bind.

Fig. 2. FTIR-ATR spectra of SA films (Adsorbed, A) of compounds (A), (B) and OTS, and of a LB monolayer (L) of the Cd^{++} salt of compound (C) on Germanium. The LB monolayer was quantitatively transferred at a constant pressure of 20 dyne/cm and a nominal area/molecule of 31 $Å^2$. The SA films were prepared under conditions leading to saturation of the adsorption and maximal contact angles for each of the respective compounds[3,12]. For OTS, only the 3000-2800 cm^{-1} spectral region is shown.

Fig. 3. Surface hydrolysis or reduction of the ester function of a bifunctional silane-ester surfactant (C_{17}SPE) in a covalently bonded SA monolayer, according to the general approach formulated in Figure 1 (lateral and layer-to-surface (-Si-O-) bonds are schematically shown). Quantitative modification of the exposed ester functions is achieved under the indicated reaction conditions without affecting the integrity of the underlying portion of the monolayer.

Fig. 4. FTIR-ATR spectra on silicon of a monolayer of the silane-ester surfactant (C_{17}SPE) shown in Figure 3, before (lower curve) and after HCl hydrolysis of the ester function to the respective terminal acid. The quantitative disappearance of the ester carbonyl band and the appearance of a carboxylic acid band are evident at 1757 and 1713 cm^{-1}, respectively. The integrity of the monolayer is preserved under the conditions of the reaction, as confirmed by the invariance of the ($-CH_2-$) stretch bands around 2900 cm^{-1}.

Fig. 5. Spectra as in Figure 4, taken before (lower curve) and after $LiAlH_4$ reduction of the ester function to the respective terminal alcohol. Note the quantitative disappearance of the ester carbonyl band at 1758 cm^{-1} and the invariance of the ($-CH_2-$) bands around 2900 cm^{-1}.

Fig. 6. FTIR-ATR spectra of a 5-layers film of nonadecenyltrichlorosilane (NTS) on silicon, showing (from the left) the (C-H) stretch region of the entire film and the individual contributions of each of the five monolayers in the structure. The individual contributions are difference spectra, each n-th layer representing the mathematical subtraction of the spectrum recorded after the deposition of n-1 layers from that of the corresponding n-layers film. Formula of NTS, bound to the surface and laterally polymerized via convalent (-Si-O-) bonds, is depicted in the insert.

Fig. 7. Construction of a SA multilayer film of C_{17}SPE (see compound formula in Figure 3) according to the general approach formulated in

Figure 1. The interlayer binding is realized through the formation of (Si-O-C) bridges, involving the reaction of the exposed hydroxyl groups of the activated monolayer with the chlorosilyl groups of the adsorbing molecules. One OTS molecule (C_{18}) is schematically shown to fill the free space between the paraffinic chains of two C_{17}SPE (C_{17}) molecules (see text for details).

Fig. 8. FTIR-ATR spectra on silicon taken after deposition of one, three and six C_{17}SPE monolayers in a multilayer film constructed according to the procedure outlined in Figure 7.

Fig. 9. Oxidative cleavage of the chain of a surface immobilized unsaturated long chain silane (1) by the crown-ether-$KMnO_4$ complex in benzene. Terminal aldehyde functions (3) are further oxidized to carboxylates (2).

Fig. 10. FTIR-ATR spectra of a complete monolayer of the unsaturated silane surfactant shown in Figure 9 on ZnSe: (a) before exposure to organic $KMnO_4$; (b), (c) after exposure to the reagent for two and six hours, respectively; (d) after treatment of (c) with HCl. The gradual cleavage of the chains (at C_{13}=C_{14}), with the formation of a surface immobilized C_{13} silane-terminal acid salt monolayer and the concomitant detachment from the surface of the shorter C_9 acid segment (Figure 9), is evident from the gradual disappearance of the (C=C) and ($-CH_3$) bands at 963 and 2957 cm^{-1}, respectively, the reduction in the intensities of the ($-CH_2-$) bands at 2919 and 2851 cm^{-1}, and the simultaneous appearance

of carboxylate ($-COO^-$) bands at 1549 and 1558 cm^{-1} (curves (a) - (c)). The disappearance of the carboxylate bands and the appearance of a free carboxyl band at 1702 cm^{-1}, upon acidification of the surface, is evident in curve (d). The progression of weak bands visible in curve (d) between 1186-1239 cm^{-1} points to the rigid all-trans conformation of the chains in the residual C_{13} monolayer[4,13,14].

Fig. 11. Spectra as in Figure 10 for complete (lower part) and incomplete monolayers of the unsaturated silane surfactant of Figure 9, before and after exposure to aqueous $KMnO_4$ for the indicated periods of time (see text for details).

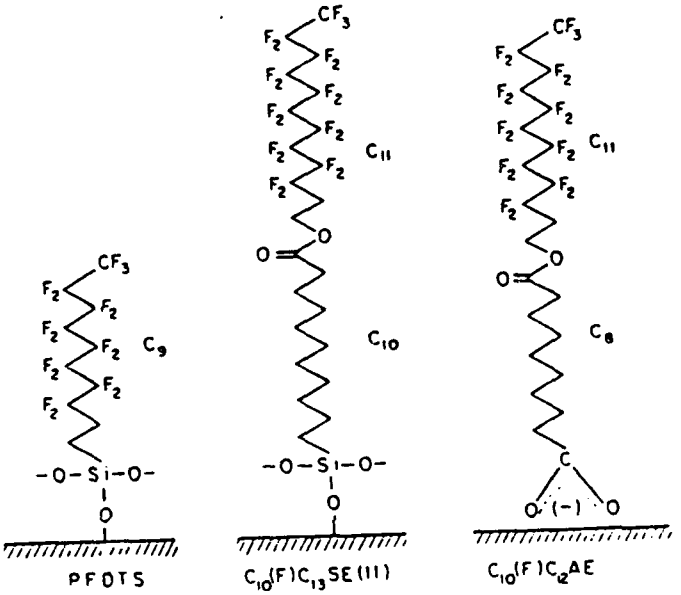
CF3
F2
C9
C11
C10
C8
O
C
(-)
-O-Si-O-
PFDTS
C10(F)C13SE(11)
C10(F)C12AE
(A)
(B)
(C)

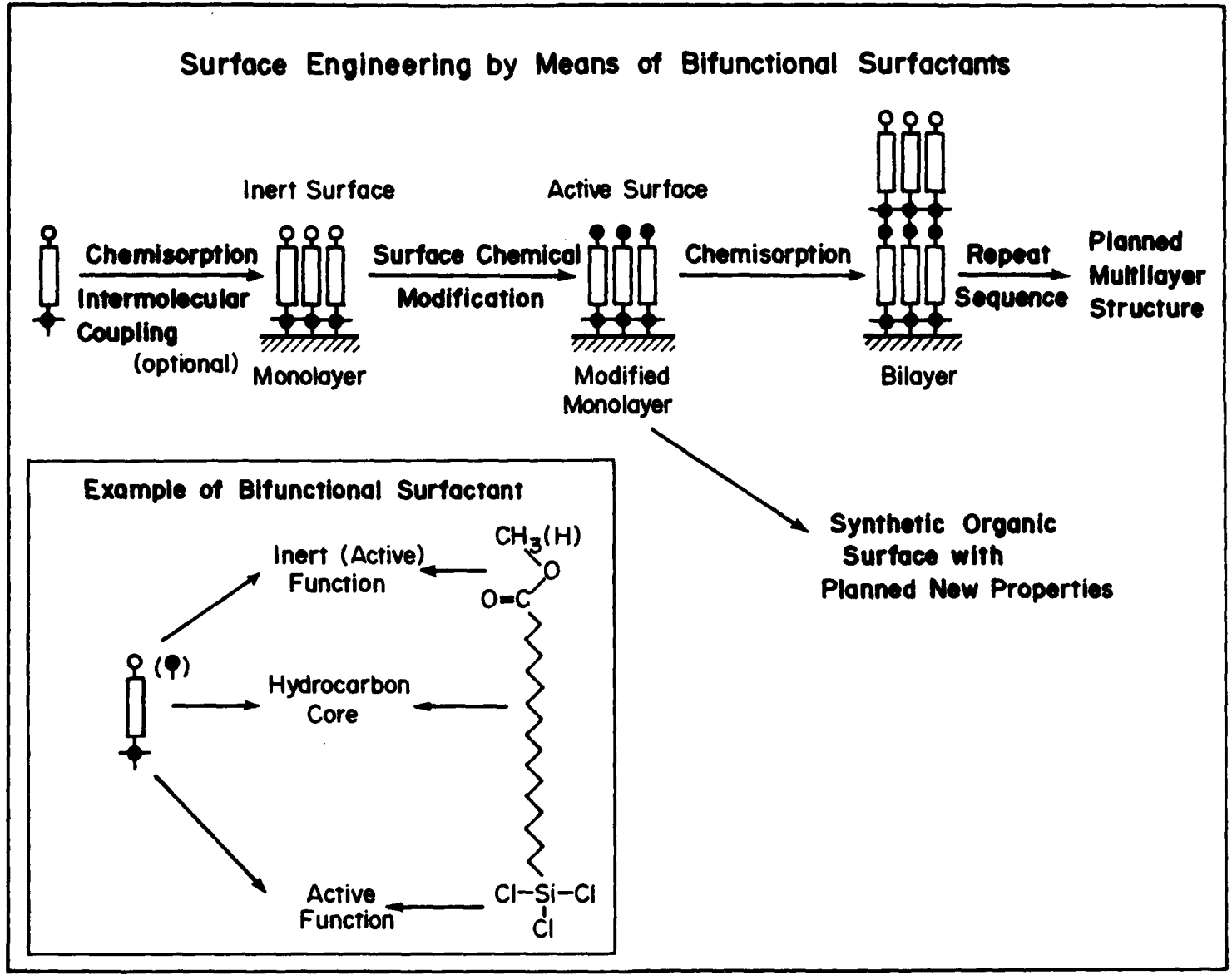
Surface Engineering by Means of Bifunctional Surfactants
Inert Surface
Active Surface
Chemisorption
Intermolecular
Coupling
(optional)
Monolayer
Surface Chemical
Modification
Modified
Monolayer
Chemisorption
Bilayer
Repeat
Sequence
Planned
Multilayer
Structure
Synthetic Organic
Surface with
Planned New Properties
Example of Bifunctional Surfactant
CH3(H)
Inert (Active)
Function
O=C
(●)
Hydrocarbon
Core
Active
Function
Cl–Si–Cl
Cl

Fig. 1

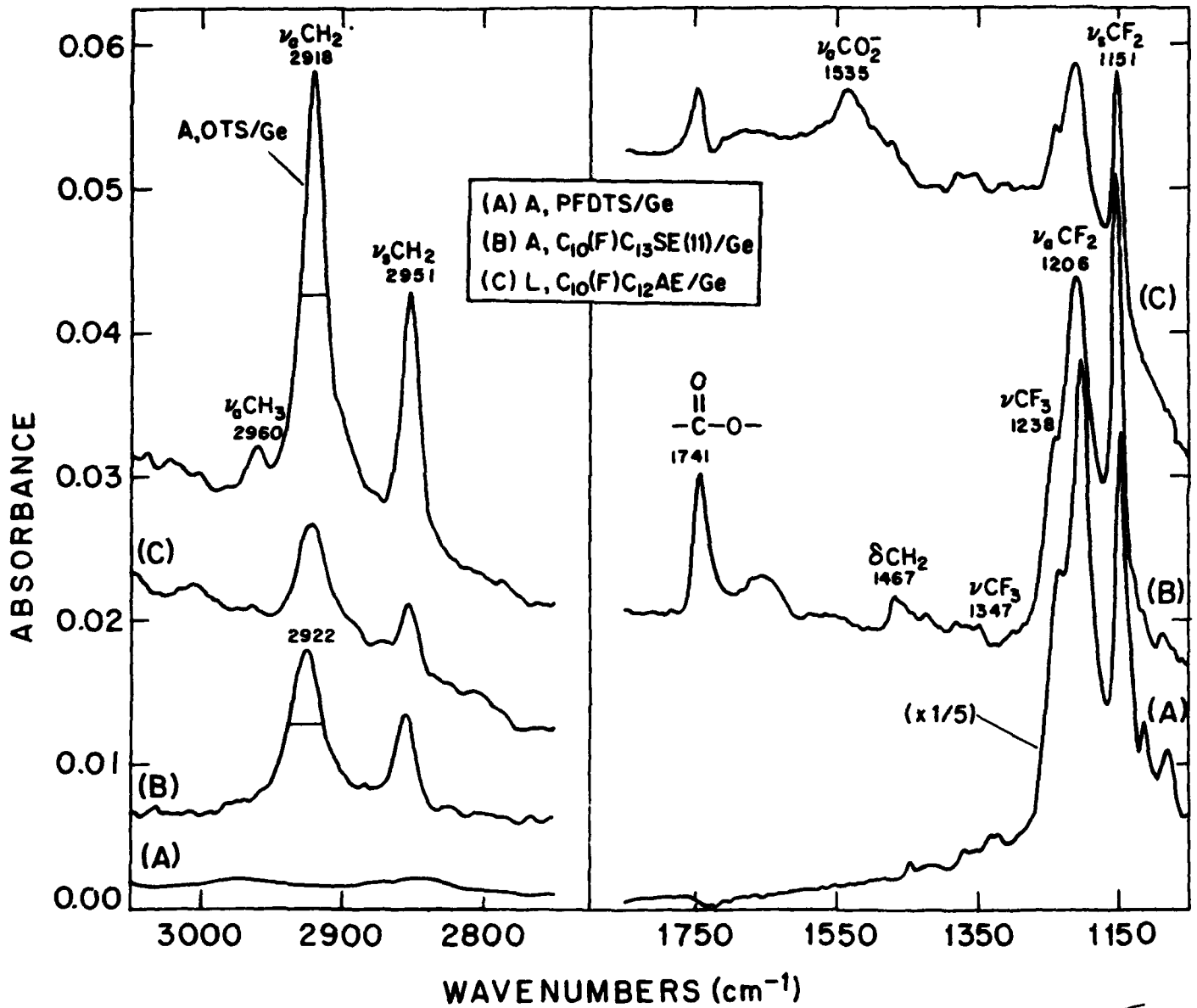
0.06
0.05
0.04
0.03
0.02
0.01
0.00
ABSORBANCE
3000
2900
2800
1750
1550
1350
1150
WAVENUMBERS (cm⁻¹)
$\nu_a CH_2$ 2918
$\nu_s CH_2$ 2951
$\nu_a CH_3$ 2960
A, OTS/Ge
2922
(A) A, PFDTS/Ge
(B) A, $C_{10}(F)C_{13}SE(11)/Ge$
(C) L, $C_{10}(F)C_{12}AE/Ge$
(A)
(B)
(C)
$\nu_a CO_2^-$ 1535
$\nu_s CF_2$ 1151
$\nu_a CF_2$ 1206
νCF_3 1238
O
II
−C−O−
1741
δCH_2 1467
νCF_3 1347
(x 1/5)

Fig. 2

Fig. 2

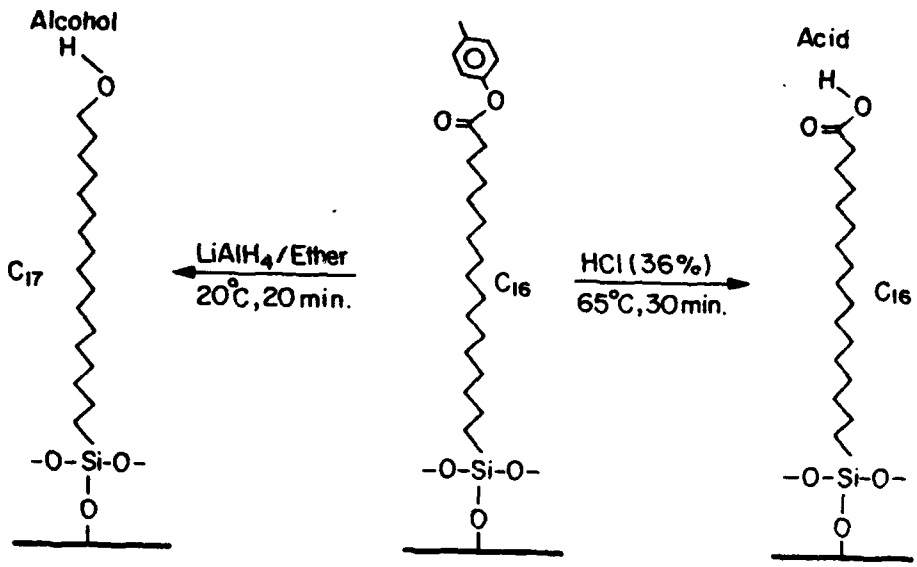
Alcohol
H
O
C_{17}
-O-Si-O-
O
$LiAlH_4$/Ether
20°C, 20 min.
O
O
C_{16}
-O-Si-O-
O
HCl (36%)
65°C, 30 min.
Acid
H
O
O
C_{16}
-O-Si-O-
O

Fig. 3

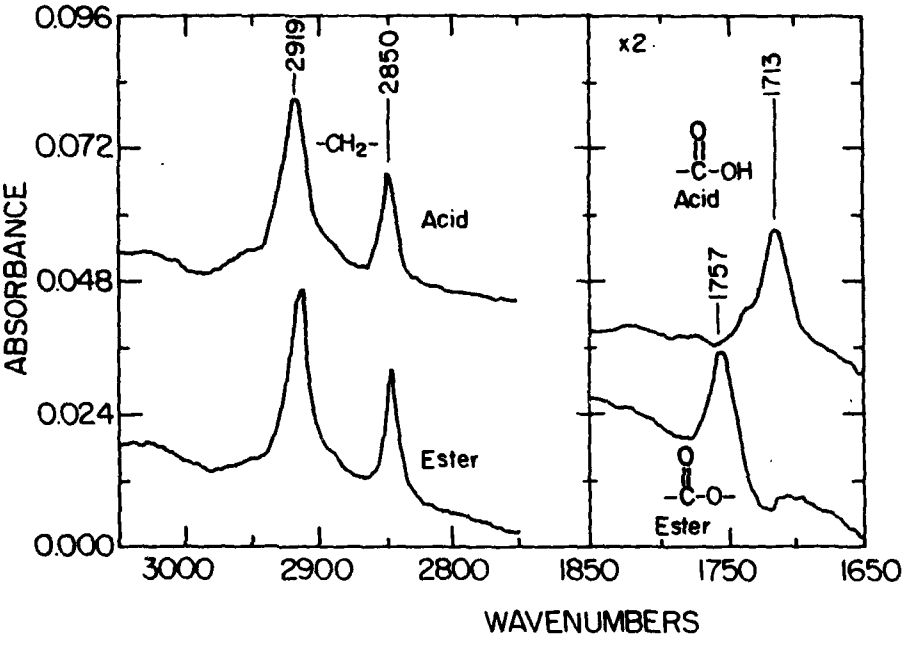
0.096
0.072
0.048
0.024
0.000
ABSORBANCE
2919
2850
-CH2-
Acid
Ester
x2
1713
-C-OH
Acid
1757
-C-O-
Ester
3000
2900
2800
1850
1750
1650
WAVENUMBERS

Fig. 4

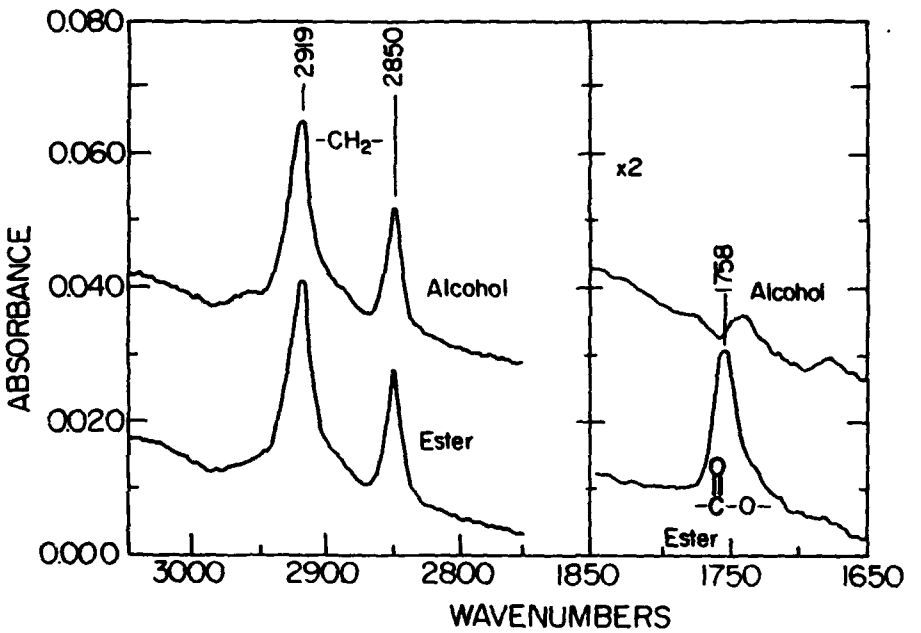
0.080
0.060
0.040
0.020
0.000
ABSORBANCE
2919
2850
-CH2-
Alcohol
Ester
x2
1758
Alcohol
-C-O-
Ester
3000
2900
2800
1850
1750
1650
WAVENUMBERS

Fig. 5

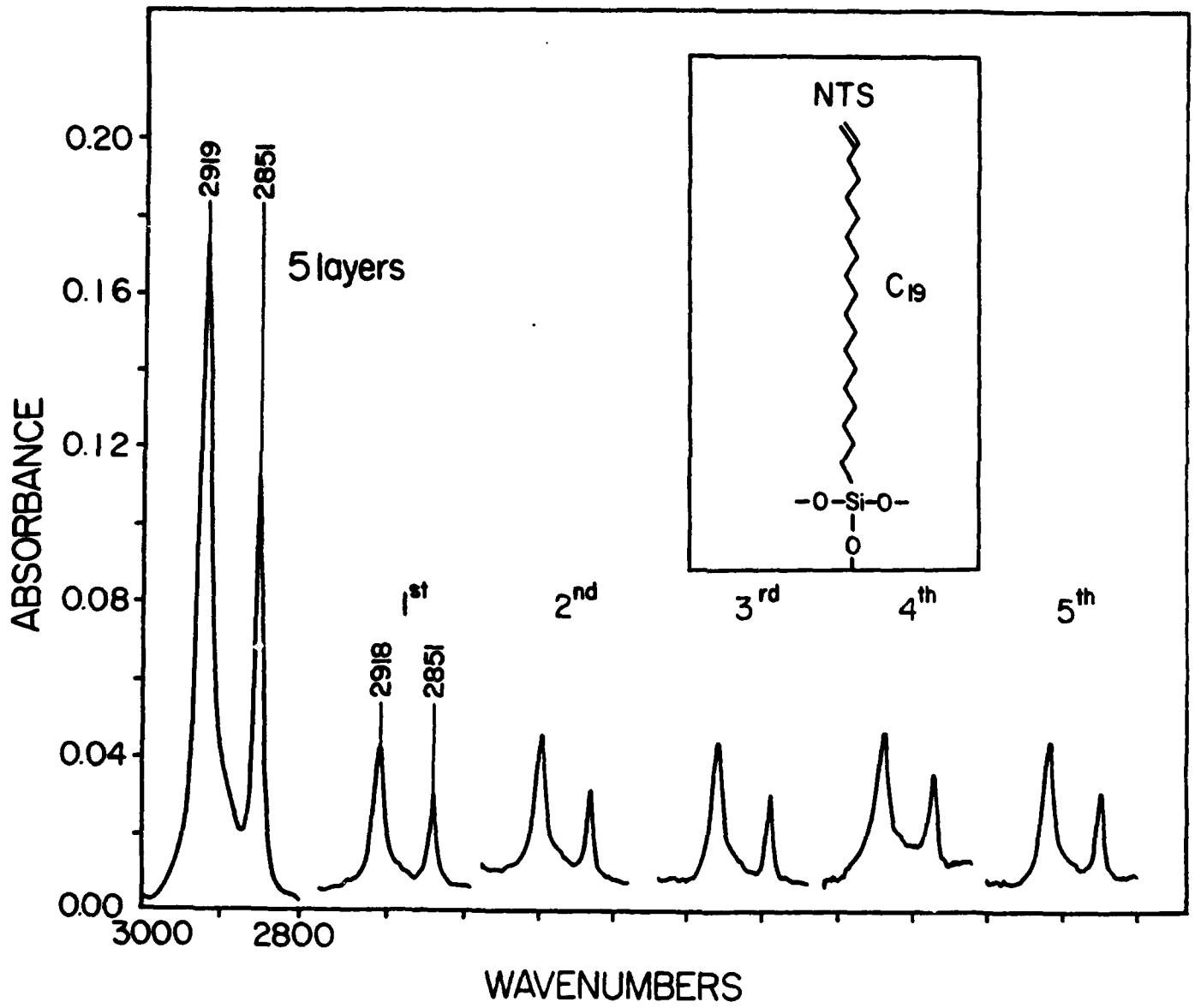
NTS
C_{19}
-O-Si-O-
O
0.20
0.16
0.12
0.08
0.04
0.00
ABSORBANCE
2919
2851
5 layers
1st
2nd
3rd
4th
5th
2918
2851
3000
2800
WAVENUMBERS

Fig. 6

Fig. 6

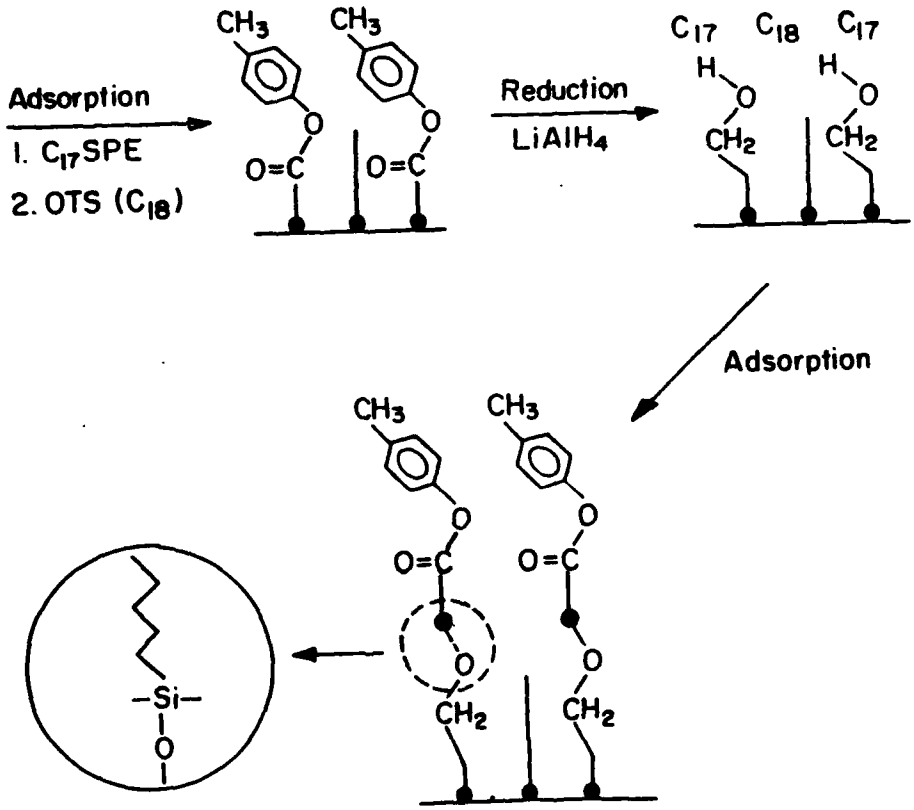
Adsorption
1. C_{17}SPE
2. OTS (C_{18})
CH_3
CH_3
O
O=C
Reduction
$LiAlH_4$
C_{17}
C_{18}
C_{17}
H
O
CH_2
Adsorption
-Si-
O

Fig. 7

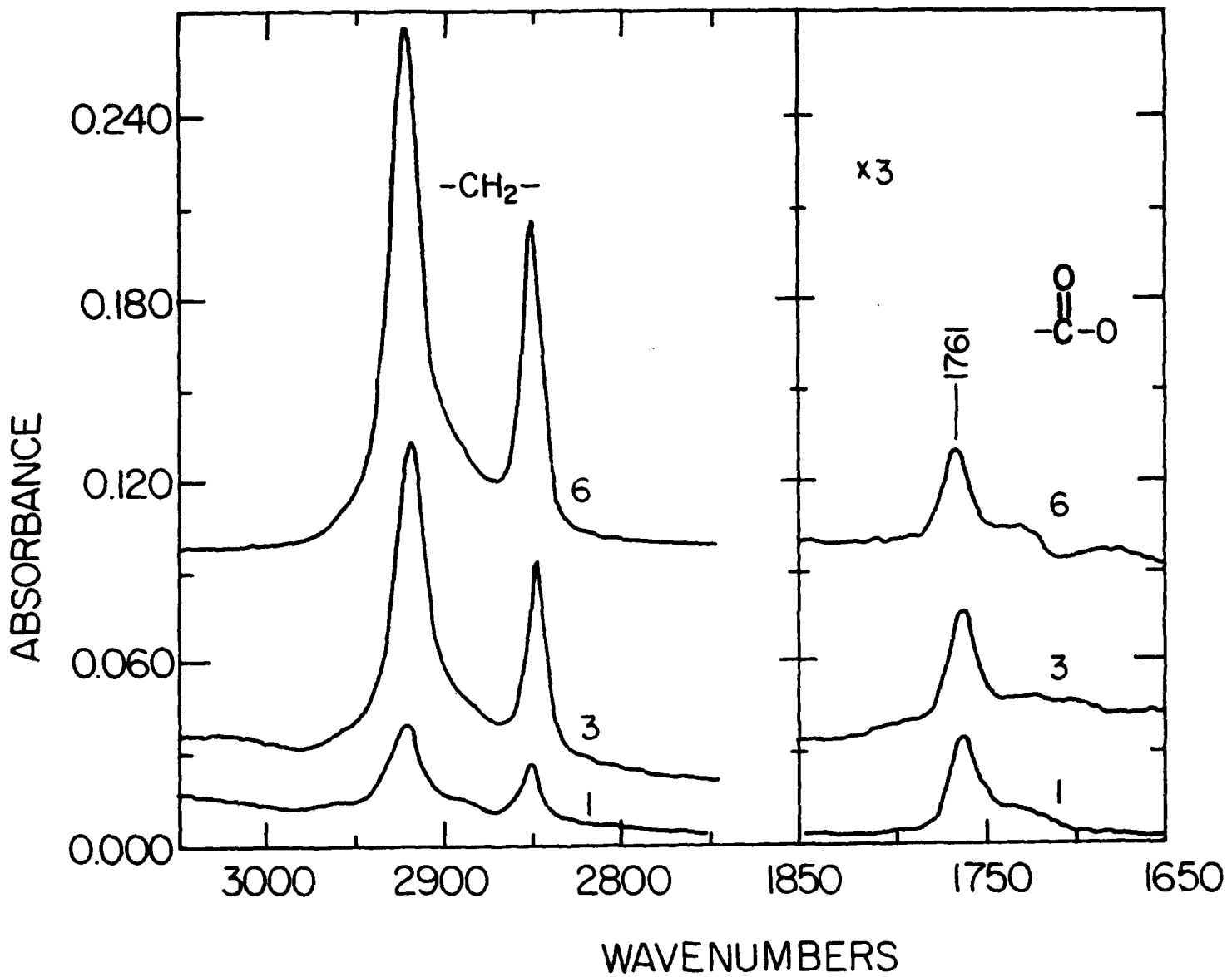
0.240
0.180
0.120
0.060
0.000
ABSORBANCE
-CH2-
x3
1761
O
-C-O
6
3
1
3000
2900
2800
1850
1750
1650
WAVENUMBERS

Fig. 8

Fig. 9

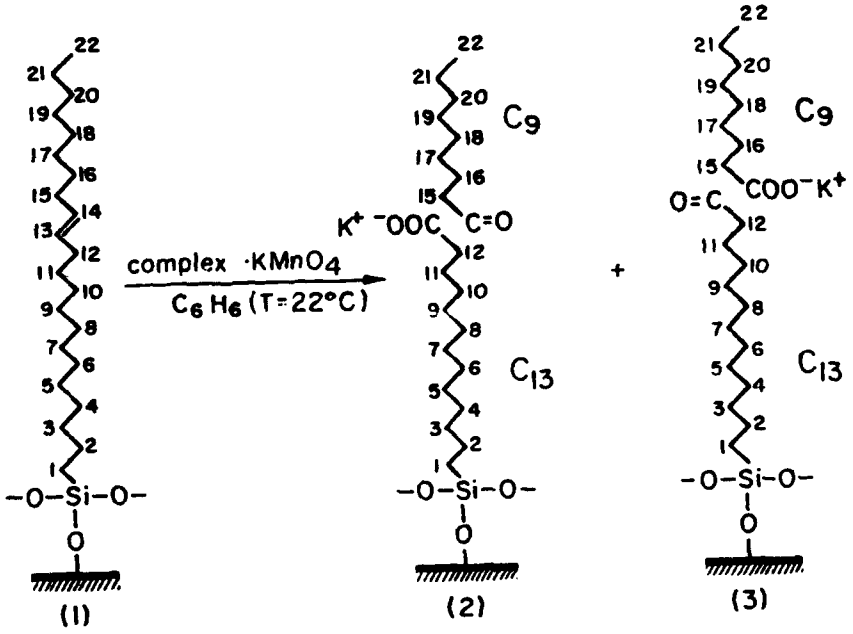

complex·KMnO4 = 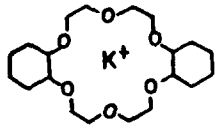 MnO_4^-

Fig 9

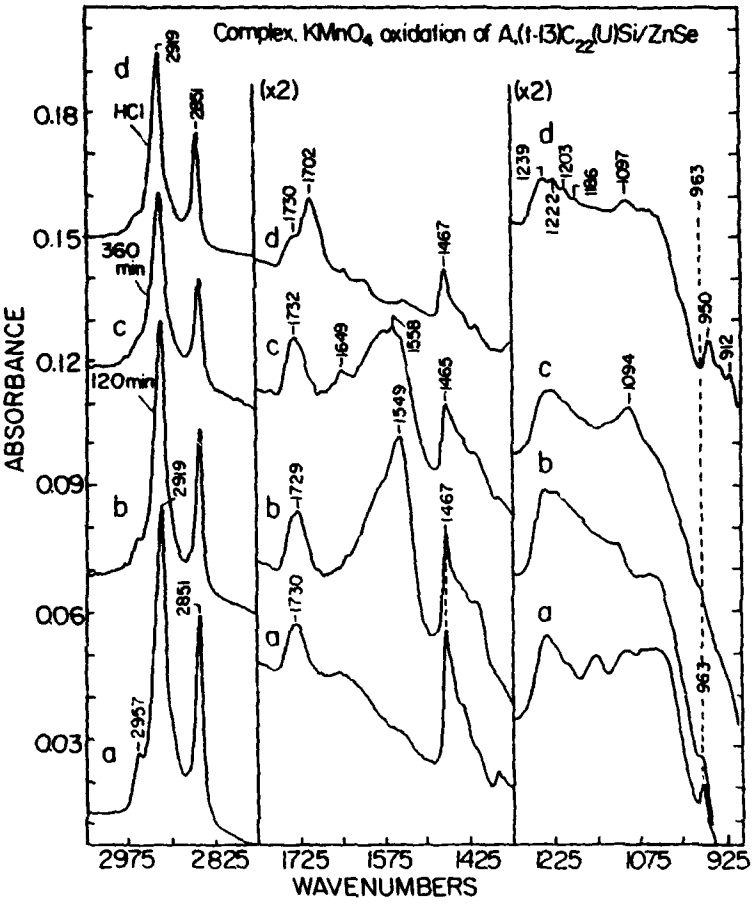
Complex. KMnO4 oxidation of A,(1-13)C22(U)Si/ZnSe
(x2)
(x2)
ABSORBANCE
0.18
0.15
0.12
0.09
0.06
0.03
HCl
360 min
120min
2957
2919
2851
1730
1702
1732
1649
1558
1549
1467
1729
1465
1239
1222
1203
1186
1097
1094
963
950
912
2975
2825
1725
1575
1425
1225
1075
925
WAVENUMBERS

Fig. 10

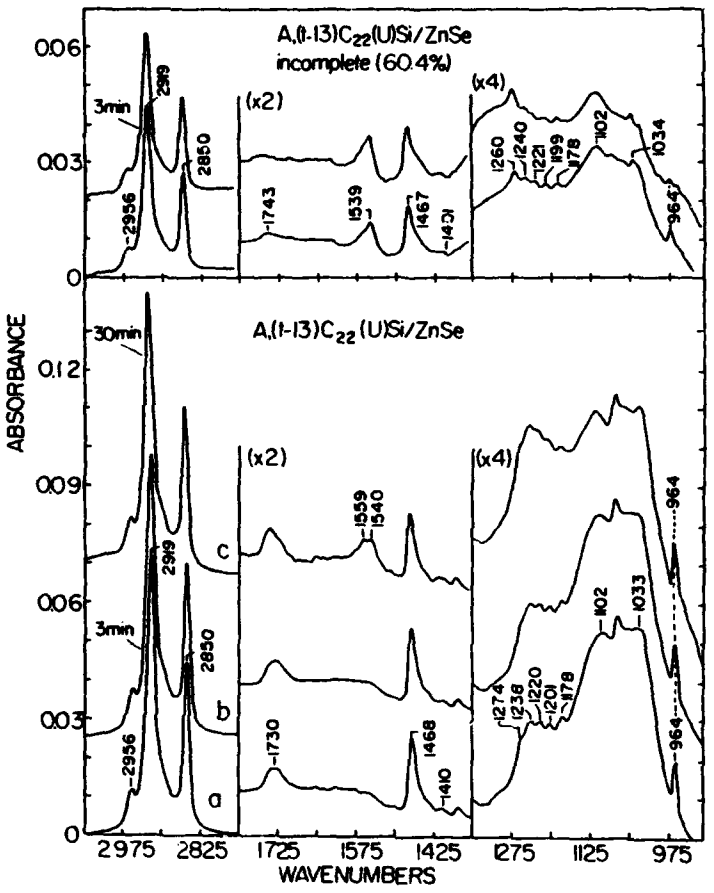
A,(I-13)C22(U)Si/ZnSe
incomplete (60.4%)
3min
2919
2850
2956
(x2)
1743
1539
1467
1431
(x4)
1260
1240
1221
1199
1178
1102
1034
964
30min
A,(I-13)C22 (U)Si/ZnSe
1559
1540
c
b
a
1730
1468
1410
1274
1238
1220
1201
1178
1102
1033
964
ABSORBANCE
0.06
0.03
0
0.12
0.09
2975
2825
1725
1575
1425
1275
1125
975
WAVENUMBERS

Fig. 11

Reprinted from Nature, Vol. 332, No. 6163, pp. 426-429, 31 March 1988

Ionic recognition and selective response in self-assembling monolayer membranes on electrodes

Israel Rubinstein*, Suzi Steinberg*, Yitzhak Tor†, Abraham Shanzer† & Jacob Sagiv‡

Departments of * Materials Research, † Organic Chemistry and ‡ Isotope Research, The Weizmann Institute of Science, Rehovot 76100, Israel

Communication in living organisms is governed by cell bilayer membranes, which selectively recognize a specific component in the presence of others and accordingly respond. The functioning of such molecular-size barriers involves molecular and quantum processes deriving from a precise, purpose-oriented architecture, and attempts have been made to create artificial supramolecular structures exhibiting similar properties[1-9]. In particular, chemically modified electrodes, coated with various types of organic layers[10-18], have been used to control the access of electroactive species from solution, but such systems have so far lacked some of the important features of real, molecular-size membranes. Here we present the first example of an electrode coated with a stable, ion-selective artificial membrane having the thickness of just one molecule, which successfully mimics basic structural and functional principles of the natural bilayer membrane. This monolayer membrane, produced by molecular self-assembly on gold, can recognize a selected metal ion in the presence of other ions, and thus induces a specific electrode response. It consists of synthetic 'receptor sites', designed to impart the desired selectivity, embedded within an inert monolayer matrix which blocks vacant sites on the surface and so prevents the passage of undesired species. The supporting gold electrode permits electrochemical analysis of the membrane structure and performance. Such monolayer membranes may aid the study of elementary charge transfer processes at liquid–solid interfaces, and contribute to future molecular-based technologies.

Impermeable one-molecule-thick barriers for ions and water have recently been produced on gold[19-21] using techniques of monolayer self-assembly[19-25]. Achieving ion selectivity in such systems is more complex, as the 'active' element providing the desired selectivity may not form film structures that are compact enough to prevent leakage of other, undesired species. We show here the feasibility of an approach based upon the use of self-assembled mixed monolayers, containing both 'active' (monolayer-forming ligand) and 'blocking' (surface-sealing long-chain amphiphile) components[25], so that a specific response for metal ions forming 1:1 complexes with the ligand is achieved.

The ligand used was 2,2'-thiobisethyl acetoacetate, $S(CH_2CH_2OCOCH_2COCH_3)_2$ (TBEA, Fig. 1), designed and synthesized as 'active' component. The two β-keto ester groups of TBEA form a tetradentate chelating centre, and the sulphur bridge was designed to anchor the ligand to a gold surface[19,20,23,24,26]. Surface-bound tetradentate TBEA is an excellent candidate for the formation of 1:1 complexes with divalent metal ions, such as Cu^{2+}, but is geometrically unsuited for binding trivalent metal ions, such as Fe^{3+}, that require octahedral coordination. Therefore, in terms of geometric discrimination (and also electrochemical suitability), Cu^{2+} and Fe^{3+} are convenient ionic probes to test the selectivity of the present monolayer-coated electrodes.

Figure 2*a* shows a cyclic voltammogram of a bare gold electrode in H_2SO_4 solution containing Cu^{2+} and Fe^{3+}. The $Fe^{3+/2+}$ reduction–oxidation peaks are marked with arrows; the small peaks around −0.15 V correspond to underpotential deposition (UPD) of a monolayer of Cu on Au[27] and the peaks at −0.55 V (reduction) and −0.40 V (oxidation) correspond to deposition–dissolution of bulk Cu. Examination of an electrode coated with

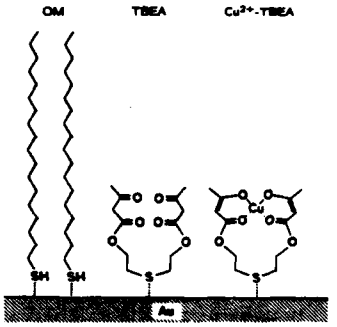

Fig. 1 Schematic representation of TBEA, Cu^{2+}-TBEA complex, and *n*-octadecyl mercaptan (OM), adsorbed on gold substrate. Note that ligand binds Cu^{2+} in the enol form upon losing two protons, and thus the complex is neutral. TBEA was prepared by the 4-dimethylaminopyridine (DMAP)-catalysed reaction[29] of 2,2'-thiobisethanol with diketene. Gold electrodes were prepared by sputter-deposition of ~1,000 Å gold on glass microscope slides[19,21], followed by annealing for 15 min at 420 °C, which reduces the gold-surface roughness.

only TBEA (Fig. 2*b*) indicates a film structure not sufficiently compact to prevent leakage of Fe^{3+} through uncovered portions of the electrode. (TBEA was adsorbed on gold by immersion in a solution containing 3.3×10^{-2} M TBEA in bicyclohexyl:chloroform, 4:1 v/v, for 3.5 h; the resulting electrodes are denoted Au/TBEA.) Evidently the introduction of an appropriate 'blocking' element is necessary for the proper functioning of the system. It was expected that addition of a surface-sealing monolayer component to the adsorption solution might result in a continuous mixed monolayer barrier with ion-selective sites embedded within a compact, electrochemically inert matrix. Previous experience[19-21] pointed to *n*-octadecyl mercaptan, $CH_3(CH_2)_{17}SH$ (OM, Fig. 1) as a suitable such component. Thus mixed monolayer membranes were prepared on gold substrates by co-adsorption of the two components from a solution containing 2.0×10^{-2} M TBEA + 2.0×10^{-2} M OM in bicyclohexyl:chloroform, 4:1 v/v, for 3.5 h. These electrodes are denoted Au/(TBEA+OM).

The performance of the mixed (TBEA+OM) monolayer membranes was compared with that of gold electrodes coated with the same ligand, but sealed with a thin electrodeposited polymeric film (~10–15 Å thick) of 1-naphthol (NP), known to suppress electrochemical reactivity[28] (Fig. 2*c*). Figure 2*e* and *f* show, respectively, voltammetric curves of an Au/(TBEA+NP) electrode in Cu^{2+} solution and in a mixed solution of Cu^{2+} and Fe^{3+}. Although the electrode is inert to Fe^{3+}, Cu^{2+} peaks are clearly observed. The voltammogram of the soluble Fe^{3+}-ethylacetoacetate complex in Fig. 2*i* indicates that the absence of $Fe^{3+/2+}$ peaks in Fig. 2*c* and *f* is not due to a possible shift in the redox potentials of complexed Fe^{3+}.

The qualitative behaviour of a typical Au/(TBEA+OM) electrode, shown in Fig. 2*d* and *g* for solutions containing Fe^{3+} or both Cu^{2+} and Fe^{3+} ions, respectively, is similar to that of Au/(TBEA+NP) (Fig. 2*c* and *f*); however, a considerably decreased background, virtually coinciding with the baseline, in Fig. 2*d* and *g*, indicates a clear improvement of the barrier properties for the mixed monolayer membrane. Thus the selective complexation of Cu^{2+} enables its penetration into the monolayer and electron exchange with the underlying electrode, whereas hydrated Fe^{3+} remains in the bulk solution at considerably greater distance from the electrode, which precludes its electrochemical reduction in the applied voltage range. Fe^{3+} forms a red complex with *dissolved* TBEA, possibly an oligomeric octahedral complex. For steric reasons, this should be prevented when the ligand is bound to the surface in an oriented monolayer. Total suppression of voltammetric response

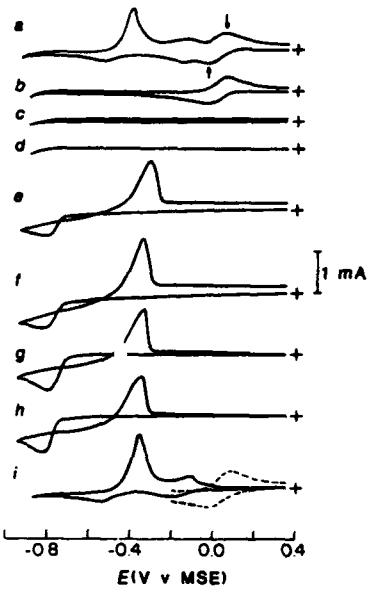

Fig. 2 Cyclic voltammograms in 0.1 M H_2SO_4 containing 1.0 mM Cu^{2+}, 3.0 mM Fe^{3+}, or both (scan rate: 0.10 V s^{-1}; electrode area: 0.63 cm^2; MSE is mercurous sulphate reference electrode, +0.400 V versus saturated calomel electrode). *a*, Au *in* $Cu^{2+}+Fe^{3+}$; *b*, Au/TBEA (~80% coverage) in Fe^{3+}; *c*, Au/(TBEA+NP) in Fe^{3+}; *d*, Au/(TBEA+OM) in Fe^{3+}; *e*, Au/(TBEA+NP) in Cu^{2+}; *f*, Au/(TBEA+NP) in $Cu^{2+}+Fe^{3+}$; *g*, Au/(TBEA+OM) in $Cu^{2+}+Fe^{3+}$; *h*, Au/(TBPA+OM) in $Cu^{2+}+Fe^{3+}$; *i*, Au in 0.1 M H_2SO_4 containing 0.4 M ethyl acetoacetate and either Cu^{2+} (solid line) or Fe^{3+} (broken line). The ligand coverage was estimated from the minimal amount of charge required to block Au/(TBEA) with naphthol polymer (towards Fe^{3+}) compared to that required to block a bare electrode of the same geometric area. Surface coverages of *ca.* 80% with TBEA are typical. Essentially the same curves as *c* and *d* are obtained, respectively, for Au/NP and Au/OM in either Cu^{2+}, Fe^{3+}, or $Cu^{2+}+Fe^{3+}$. For *c*, *e*, *f*, naphthol polymer (NP) was deposited in a stirred solution containing 1.0 mM 1-naphthol in 0.5 M H_2SO_4 by passing a constant anodic current for 2.0 $\mu A\ cm^{-2}$ for 4.5 min. This corresponds to about 10 layers of NP deposited at ligand-uncovered sites of the electrode, which results in a NP film thickness comparable with that of the ligand monolayer itself.

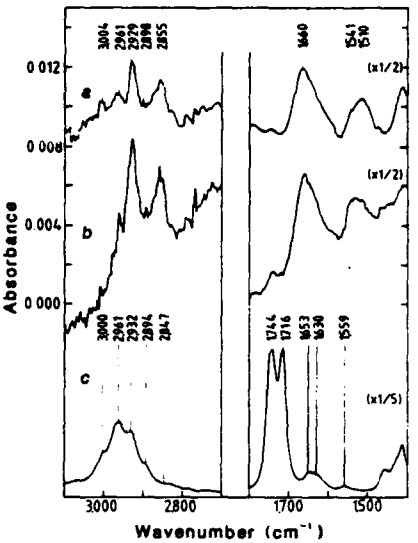

Fig. 3 RA-FTIR spectra of: *a*, Cu^{2+}-TBEA complex in a Au/(Cu^{2}-TBEA+OM) electrode (specimen obtained by immersion of Au/(TBEA+OM) in saturated aqueous copper acetate solution adjusted to *p*H 7.5 with sodium acetate, for 1.5 h at 40–45 °C); *b*, TBEA in the electrode of *a*, after electrochemical removal of the Cu^{2+} by cycling three times in 0.1 M H_2SO_4 between +0.35 V and −0.75 V (v. MSE); *c*, TBEA in bulk liquid. The spectra in *a* and *b* were produced by a weighted subtraction of Au/OM spectrum from the spectra of the respective electrodes in *a* and *b*. The spectral features in the 3,000–2,800 cm^{-1} region represent various C—H stretch modes[19,23]. The peaks at 1,744 and 1,716 cm^{-1} are C=O stretch modes of the ester and ketone functions, respectively, of TBEA in the keto form (ref. 30, pp. 150 and 204). The features between 1,660 and 1,510 cm^{-1} are characteristic of the Cu^{2+}-acetoacetate complex (ref. 30, pp. 165 and 209), the bands around 1,660 cm^{-1} (*a*, *b*) and 1,653–1,630 cm^{-1} (*c*) thus being assigned to the conjugated ester and double bond of TBEA in the enol form (ref. 30, pp. 165 and 209) (see Fig. 1). The spectra in *a* and *b* were taken with parallel polarized radiation in the reflection–absorption (RA) mode, at an angle of incidence of 75° and a resolution of 4 cm^{-1} (ref. 19). The spectrum in *c* was taken in the transmission mode, at the same resolution, using a thin film of pure TBEA between two NaCl windows.

is also observed with other ions, which are either trivalent (for instance, Ce^{3+}) or sterically incompatible (for instance, VO^{2+}).

The monolayers on gold were characterized by contact-angle measurements[19,22,24,26], reflection–absorption Fourier transform infrared (RA-FTIR) spectroscopy[19,20,23], and various electrochemical measurements[19,21], a full discussion of which is beyond the scope of this paper. Indirect electrochemical evidence indicates ~50% ligand coverage in the present (TBEA+OM) mixed monolayers. Surprisingly high contact angles for Au/(TBEA+OM), indicative of a rather unusual mode of film packing (typical values: 108°, 59° and 57° for water, bicyclohexyl and *n*-hexadecane, respectively, with no hysteresis) and significant contact angle variations are observed after Cu^{2+} uptake and removal. Figure 3 shows selected infrared spectra for the Au/(TBEA+OM) system, from which a number of general conclusions can be drawn: (1) complexed TBEA (enol form) can be detected spectroscopically in the monolayer on gold; (2) the enol form is preserved upon electrochemical removal of the Cu^{2+}; (3) differences in the relative intensities of the various C–H stretch peaks in Fig. 3*a*, *b* and *c* are indicative of non-random orientation of TBEA on the surface[19,23]; (4) the system appears stable towards electrochemical treatment.

Common prominent features in Fig. 2*f* and *g*, which may be correlated with structural characteristics of an ordered Cu^{2+}-selective monolayer barrier, are: (1) the complete absence of $Fe^{3+/2+}$ peaks; (2) the absence of Cu UPD peaks; (3) the negative shift of the bulk Cu deposition peak by ~0.25 V; (4) the existence of a loop when the voltammetric scan direction is reversed. The absence of Cu UPD peaks indicates that Cu atoms are deposited inside the organized monolayer at some distance from the surface, not in direct contact with the gold substrate. The shift in the bulk Cu deposition potential and the voltammetric loop are indicative of the preferred perpendicular orientation of the ligand. In a monolayer where TBEA molecules are oriented normal to the substrate plane (as in Fig. 1), the complexed Cu^{2+} ions are held at a distance of ~7 Å from the Au surface, which introduces a tunnelling barrier for electron transfer with the underlying electrode (assuming that quantum-mechanical tunnelling governs electron transfer over distances of this order of magnitude). However, reduced Cu atoms are not complexed and may be deposited within the ligand 'cavity' closer to the electrode, thus lowering the energy barrier for further electron transfer. Voltammetrically, the initial barrier is manifested as an increased overpotential for the reduction, i.e. a negative shift of the reduction potential, whereas the easier electron transfer provided by the first layer of deposited Cu atoms gives rise to an autocatalytic effect, appearing as an enhanced reduction current (and thus a loop) on the reverse scan. Experiments with

decreasing reversal potentials (not shown) indicate that even sub-monolayer amounts of Cu atoms may cause such appreciable catalytic effects.

From the negative shift of the Cu^{2+} reduction peak potential, observed with Au/(TBEA+OM) relative to a bare gold electrode (Figs 2*g* and *i*), and considering a tunnelling mechanism for the electron exchange with the metal, one can estimate the potential shifts to be expected for varying distances between Cu^{2+} and the underlying electrode. To verify these expectations, a new ligand molecule which contains an additional methylene group, 3,3'-thiobispropyl acetoacetate, $S(CH_2CH_2CH_2OCOCH_2COCH_3)_2$ (TBPA), was prepared and tested under identical electrochemical conditions. Assuming a similar orientation of the two ligands with respect to the substrate, the metal ion with TBPA should be located 0.5–1.0 Å further away from the gold surface than with TBEA. Indeed, this results in a reduction peak potential more negative by ~0.030 V for the deposition of Cu with TBPA (Fig. 2*g* and *h*), which agrees qualitatively with the proposed tunnelling mechanism.

Thus we have demonstrated the possible use of spontaneous molecular organization at liquid–solid interfaces for the preparation of solid-supported functional monolayer structures. Structure–function interrelations in supramolecular organizates of this type appear to be advantageously revealed by electrochemical techniques. Such artificial self-assembled systems are of particular significance in view of their resemblance to the natural bilayer membranes (with respect to their molecular dimensions, mode of organization, and spontaneous formation), while offering high stability and the option of systematic modification.

I.R. was supported partly by a grant from Yeda Fund of the Weizmann Institute; J.S. was supported partly by a grant from the European Research Office of the U.S. Army; I.R. holds the Victor L. Erlich Career Development Chair.

Received 25 August 1987; accepted 14 January 1988.

1. Kuhn, H. *J. Photochem.* **10**, 111–132 (1979).
2. Polymeropoulos, E. E., Möbius, D. & Kuhn, H. *Thin Solid Films* **68**, 173–190 (1980).
3. Fromherz, P. & Arden, W. *J. Am. chem. Soc.* **102**, 6211–6218 (1980).
4. Lehn, J.-M. *Science* **227**, 849–856 (1985).
5. Arrhenius, Th. S., Blanchard-Desce, M., Dvolaitzky, M., Lehn, J.-M. & Malthete, J. *Proc. natn. Acad. Sci. USA* **83**, 5355–5359 (1986).
6. Kumano, A., Niwa, O., Kajiyama, T., Takayanagi, M. & Kunitake, T. *Polymer J.* **16**, 461–470 (1984).
7. Ringsdorf, H., Schmidt, G. & Schneider, J. *Thin Solid Films* **152**, 207–222 (1987).
8. Proc. 2nd Int. Conf. on Langmuir-Blodgett Films, Schenectady, 1985 *Thin Solid Films* **132**, 1–249 (1985).
9. Fendler, J. H. *J. Membrane Sci.* **38**, 323–346 (1987).
10. Mu[illegible] W. in *Electroanalytical Chemistry* Vol. 13 (ed. Bard, A. J.) 191–368 (Dekker, New York, 1984).
11. Eaves, J. G., Munro, H. S. & Parker, D. *Inorg. Chem.* **26**, 644–650 (1987).
12. Takeuki, E. S. & Osteryoung, J. *Analyt. Chem.* **57**, 1770–1771 (1985).
13. Kimura, K., Kumami, K., Kitazawa, S. & Shono, T. *Analyt. Chem.* **56**, 2369–2372 (1984).
14. Fujihira, M. in *Topics in Organic Electrochemistry* (ed. Fry, A. J. & Britton, W. E.) 255–294 (Plenum, New York, 1986).
15. Facci, J. S. *Langmuir* **3**, 525–530 (1987).
16. Okahata, Y., Enna, G., Taguchi, K. & Seki, T. *J. Am chem. Soc.* **107**, 5300–5301 (1985).
17. Martin, C. R., Rubinstein, I. & Bard, A. J. *J. Am. chem. Soc.* **104**, 4817–4824 (1982).
18. Rubinstein, I. & Rubinstein, I. *J. phys. Chem.* **91**, 235–241 (1987).
19. Sabatani, E., Rubinstein, I., Maoz, R. & Sagiv, J. *J. electroanalyt. Chem.* **219**, 365–371 (1987).
20. Finklea, H. O., Avery, S., Lynch, M. & Furtsch, T. *Langmuir* **3**, 409–413 (1987).
21. Sabatani, E. & Rubinstein, I. *J. phys. Chem.* **91**, 6663–6669 (1987).
22. Maoz, R. & Sagiv, J. *J. Colloid Interface Sci.* **100**, 465–496 (1984).
23. Nuzzo, R. G., Fusco, F. A. & Allara, D. L. *J. Am. chem. Soc.* **109**, 2358–2368 (1987).
24. Diem, T., Czajka, B., Weber, B. & Regen, S. L. *J. Am. chem. Soc.* **108**, 6095–6096 (1986).
25. Sagiv, J. *Israel J. Chem.* **18**, 346–353 (1979).
26. Holmes-Farley, S. R., Reamey, R. H., McCarthy, Th. J., Deutch, J. & Whitesides, G. M. *Langmuir* **1**, 725–740 (1985).
27. Kolb, D. M. in *Advances in Electrochemistry and Electrochemical Engineering* Vol. 11 (ed. Gerischer, H. & Tobias, C. W.) 155 (Wiley, New York, 1978).
28. Babai, M., Gottesfeld, S. & Gileadi, E. *Israel J. Chem.* **13**, 110–117 (1979).
29. Wilson, S. R. & Price, M. F. *J. org. Chem.* **49**, 722–725 (1984).
30. Bellamy, L. J. *The Infra-red Spectra of Complex Molecules* (Wiley, New York, 1975).

Reprinted from LANGMUIR, 1987, 3, 1034.

Penetration-Controlled Reactions in Organized Monolayer Assemblies. 1. Aqueous Permanganate Interaction with Monolayer and Multilayer Films of Long-Chain Surfactants

Rivka Maoz and Jacob Sagiv*

Department of Isotope Research, The Weizmann Institute of Science, 76100 Rehovot, Israel

Received December 6, 1986. In Final Form: May 26, 1987

The extent of oxidation of unsaturated monolayer constituents by aqueous $KMnO_4$ is employed to probe the penetration of ions from an aqueous phase into organized monolayer assemblies of some long-chain acid and silane surfactants. The study comprises solid-supported Langmuir–Blodgett (LB) and self-assembled (SA) monolayers as well as a series of LB built-up (multilayer) films, the molecular architecture of which was planned such as to furnish evidence on the depth of penetration of the permanganate ion into the inner core of a compact film assembly. A combined analysis of the structural stability and the reactivity of the films, as revealed by FTIR–ATR spectroscopy and wettability observations, suggests a defect-controlled mechanism for the passage of ions across tightly packed monolayers and multilayers of oriented long-chain surfactants. The barrier efficiency of the investigated films is thickness independent, in the range between one to three superimposed monolayers, being determined by the structural perfection of the films and their stability under the action of the penetrating species, solely. Self-assembled monolayers are found to be more stable and less penetrable than each of the presently studied monolayer or trilayer LB assemblies. Wetting of a monolayer- or multilayer-covered polar solid by water or by the aqueous permanganate solution is shown to require establishment of direct contacts between the bulk liquid and the underlying solid surface and lateral diffusion of the liquid in the film–solid interface.

Introduction

Organized monolayer structures produced on polar solid surfaces via spontaneous adsorption from organic solutions (self-assembling monolayers) are supramolecular organizates resembling, in some respects, the well-known Langmuir–Blodgett (LB) built-up films while displaying other distinct and rather unique features.[1-10] Apart from their relevance in the study of molecular self-organization, in general, much of the interest in self-assembling (SA) monolayers stems from their potential in a wide range of scientific and technological applications.[3]

So far, most of the published material on SA monolayers has focused on their formation and structure as derived by various physical methods.[1-10] The chemical properties and reactivity of self-assembling monolayers have only briefly been touched, mainly in relation to their binding to the solid surface[2,4,7-10] and to their chemical modification, as required in the construction of planned multilayer structures.[3] The present series of papers is intended to

(1) Bigelow, W. C.; Pickett, D. L.; Zisman, W. A. *J. Colloid Sci.* **1946**, *1*, 513.
(2) Maoz, R.; Sagiv, J. *J. Colloid Interface Sci.* **1984**, *100*, 465.
(3) (a) Netzer, L.; Iscovici, R.; Sagiv, J. *Thin Solid Films* **1983**, *99*, 235; (b) **1983**, *100*, 67.
(4) (a) Nuzzo, R. G.; Allara, D. L. *J. Am. Chem. Soc.* **1983**, *105*, 4481. (b) Allara, D. L.; Nuzzo, R. G. *Langmuir* **1985**, *1*, 45; (c) **1985**, *1*, 52.
(5) (a) Sandroff, C. J.; Garoff, S.; Leung, K. P. *Chem. Phys. Lett.* **1983**, *96*, 547. (b) Garoff, S.; Hall, R. B.; Deckman, H. W.; Alvarez, M. S. *Proc. Electrochem. Soc.* **1985**, *85-89*, 112.
(6) For example, see: (a) Shafrin, E. G.; Zisman, W. A. *Adv. Chem. Ser.* **1960**, *87*, 20 and references cited therein. (b) Bewig, K. W.; Zisman, W. A. *J. Phys. Chem.* **1963**, *67*, 130. (c) Brockway, L. O.; Jones, R. L. *Adv. Chem. Ser.* **1964**, *43*, 275. (d) Bartell, L. S.; Betts, J. R. *J. Phys. Chem.* **1960**, *64*, 1075. (e) Gaines, G. L., Jr. *J. Colloid Sci.* **1960**, *15*, 321. (f) Young, J. R. *Aust. J. Chem.* **1955**, *8*, 173.
(7) (a) Chapman, J. A.; Tabor, D. *Proc. R. Soc. London, A* **1957**, *242*, 96. (b) Bowden, F. P.; Tabor, D. *The Friction and Lubrication of Solids*; Clarendon: Oxford, 1950; Chapter X.
(8) Gun, J.; Iscovici, R.; Sagiv, J. *J. Colloid Interface Sci.* **1984**, *101*, 201.
(9) Boerio, F. J.; Chen, S. L. *J. Colloid Interface Sci.* **1980**, *73*, 176.
(10) (a) Finklea, H. O.; Robinson, L. R.; Blackburn, A.; Richter, B.; Allara, D.; Bright, T. *Langmuir* **1986**, *2*, 239. (b) Sabatani, E.; Rubinstein, I.; Maoz, R.; Sagiv, J. *J. Electroanal. Chem.* **1987**, *219*, 365.

0743-7463/87/2403-1034$01.50/0

report results of a study of some model surface reactions involving the penetration of a reagent from an adjacent fluid phase into the inner core of a more or less ordered monolayer structure. Useful information was derived from a comparative investigation of LB and self-assembled systems, the emphasis being, however, on the latter.

The study of "penetration-controlled" reactions was considered of particular interest for several reasons: (a) Following the behavior of an organized molecular assembly under exposure to a penetrating reagent may serve as a sensitive tool for probing its three-dimensional architecture, structural integrity, and overall stability under the action of the reagent. Information derived from such studies is essential in the evaluation of a number of interesting potential applications (scientific as well as technological) of self-assembling monolayers depending on their performance as molecular diffusion barriers. (b) Information on monolayer penetrability is demanded in the selection of appropriate synthetic strategies for the construction of self-assembling multilayer structures.[3] (c) Conducting chemical reactions in a highly ordered and anisotropic environment, such as that provided by an organized monolayer assembly, has been shown to give rise to various catalytic and selectivity effects.[11-13] The impenetrability, or selective penetrability, of a given monolayer system may lead to interesting such effects.[14-18] As, in principle, the self-assembly method allows ordered monolayers to be prepared on large-area particulate supports,[3] such systems might become useful in preparative-scale synthetic applications.

The quite extensive literature devoted to the penetrability of monolayers, including monolayers at water–gas interfaces as well as solid-supported built-up films, presents apparently contradictory data regarding the efficiency of monolayers as molecular diffusion barriers.[19-27,30,31] For example, carefully prepared monolayers of saturated long-chain fatty acids (C_{17} to C_{20}) at the water–air interface were reported to reduce the rate of water evaporation by factors as high as 10^4 relative to that from the free water surface,[21] and built-up films of cadmium arachidate ca. six monolayers thick were found to block completely access of water to the underlying surface,[23] while, on the other hand, relatively large molecules were reported to diffuse without difficulty through a large number of monolayers in LB built-up assemblies of same or similar surfactants.[23-26]

As built-up LB films are metastable structures, susceptible to alterations of their planned architecture,[27-29] much of the apparent inconsistency found in the literature on monolayer penetrability might originate in inherent difficulties associated with the proper structural characterization of the studied systems or in the interpretation of the observed effects. In spite of these difficulties, one may expect, on the basis of theoretical considerations and existing experimental evidence, that closely packed solid-like monolayers of long-chain surfactants, immobilized on a solid surface and strongly anchored to it, should behave as efficient barriers with respect to diffusion of ions and molecules exceeding a certain critical size. This expectation follows from the proposed mechanism of diffusion through Langmuir monolayers at the water–gas interface, according to which the lateral mobility of the surfactant molecules in the layer plane is an essential factor in the statistical formation of interchain gaps through which water or other gas molecules may move across the film.[19,21,30] Furthermore, to rationalize the observed penetrability of some solid-supported built-up films, models were proposed invoking variable degrees of film fluidity,[22,25] lateral diffusion in the interlayer hydrophilic planes,[16,26] or other types of motion of the film-forming molecules,[20,23,27] while rigid films of cadmium arachidate (three to five monolayers thick) deposited on flat solids by the LB method were reported to provide efficient protection to the underlying surface against a number of corrosive chemicals in aqueous solution.[31]

Since both the film packing density and its strength of anchoring to the underlying solid substrate may be easily controlled and varied in monolayers prepared by spontaneous adsorption from solution,[2,5,32] it was anticipated that a comparative investigation of self-assembling and related LB monolayers might help solve some of the basic questions regarding the penetrability of monolayers.

The first three papers in this series deal with solid-supported monolayers and multilayer films of saturated and unsaturated long-chain fatty acids and silanes (with terminal and intrachain ethylenic double bond functions) exposed to aqueous and organic $KMnO_4$ solutions. The investigation was carried out in parallel on LB mono- and multilayer films and analogous SA monolayers prepared on several different flat substrates. Fourier transform infrared–attenuated total reflection (FTIR–ATR) spectroscopy, including measurements with linearly polarized radiation,[3] and wettability observations[2] were used to determine the initial composition and structure of the films and to follow the chemical and structural transformations produced upon their exposure to the permanganate solutions. The planning of the experiments sought to answer the following specific questions: (a) How stable are the various studied film assemblies under exposure to the liquid reagent, and what are the chemical and structural

(11) Fendler, J. H. *Membrane Mimetic Chemistry*; Wiley-Interscience: New York, 1982.
(12) Tieke, B.; Lieser, G. *J. Colloid Interface Sci.* **1982**, *88*, 471 and references cited therein.
(13) Barraud, A.; Rosilio, C. *Ann. Chim.* **1975**, *10*, 195.
(14) Fukuda, K.; Shibasaki, Y.; Nakahara, H. *Thin Solid Films* **1983**, *99*, 87.
(15) (a) Horsey, B. E.; Whitten, D. G. *J. Am. Chem. Soc.* **1978**, *100*, 1293. (b) Whitten, D. G.; Eaker, D. W.; Horsey, B. E.; Schmehl, R. H.; Worsham, P. R. *Ber. Bunsenges. Phys. Chem.* **1978**, *82*, 558 and references cited therein.
(16) Schmehl, R. H.; Shaw, G. L.; Whitten, D. G. *Chem. Phys. Lett.* **1978**, *55*, 549.
(17) Eden, Ch.; Shaked, A. *Isr. J. Chem.* **1975**, *13*, 1.
(18) Ogawa, H.; Chihara, T.; Taya, K. *J. Am. Chem. Soc.* **1985**, *107*, 1365.
(19) *Retardation of Evaporation by Monolayers*; La Mer, V. K., Ed.; Academic: New York, 1962.
(20) Ross, G. D.; Quinn, J. A. *J. Colloid Interface Sci.* **1968**, *27*, 198.
(21) Archer, R. J.; La Mer, V. K. *J. Phys. Chem.* **1955**, *59*, 200.
(22) Windreich, S.; Silberberg, A. *J. Colloid Interface Sci.* **1980**, *77*, 427.
(23) Sobotka, H. *J. Colloid Sci.* **1956**, *11*, 435 and references cited therein.
(24) Kuhn, H.; Möbius, D. *Angew. Chem., Int. Ed. Engl.* **1971**, *10*, 620.
(25) Richard, M. A.; Deutch, J.; Whitesides, G. M. *J. Am. Chem. Soc.* **1978**, *100*, 6613.
(26) Mercer-Smith, J. A.; Whitten, D. G. *J. Am. Chem. Soc.* **1979**, *101*, 6620.
(27) Sobotka, H. *J. Phys. Chem.* **1955**, *62*, 527.
(28) Kopp, F.; Fringeli, U. P.; Mühlethaler, K.; Günthard, Hs. H. *Biophys. Struct. Mech.* **1978**, *1*, 75 and references cited therein.
(29) Gaines, G. L., Jr. *Thin Solid Films* **1980**, *68*, 1.
(30) Quickenden, T. I.; Barnes, G. T. *J. Colloid Interface Sci.* **1978**, *67*, 415 and references cited therein.
(31) Beischer, D.; Oschsel, G. *Z. Electrochem. Angew. Phys. Chem.* **1942**, *49*, 310.
(32) Gun, J.; Sagiv, J. *J. Colloid Interface Sci.* **1986**, *112*, 457.

transformations produced by the $KMnO_4$ oxidation of the unsaturated monolayers? How does the reactivity of a film correlate with its structural stability? (b) How does the efficiency of the double bond attack by permanganate correlate with structural features of the film, such as its density of packing or the location of the double bond below the exposed film surface? (c) Are the rigidity of the film and the immobilization of the film constituent molecules (strength of anchoring to the solid surface) important in preventing the penetration of the reagent into the film? (d) What is the relative importance of molecular diffusion across the film, versus passage through defects, and lateral diffusion in the interlayer planes or in the film–substrate interface? (e) What is the role of the hydrophobic effect[33] in inhibiting penetration of ions from an aqueous phase into the nonpolar region of the film?

The experimental material included in this first paper in the series is intended to provide a comparative picture of the behavior of monolayers (LB and SA) and LB built-up multilayer assemblies, under exposure to aqueous permanganate, while the following paper[34] in this issue is devoted to a detailed investigation of the aqueous permanganate interaction with monolayer films only. The third paper[35] deals with monolayer films treated with $KMnO_4$ in organic solution.

Experimental Section

Materials. Except where otherwise stated, all materials were identical with those employed in the previous work.[2] The following surfactants were used in the preparation of films for this study:[36] arachidic acid [C_{20}, $CH_3(CH_2)_{18}COOH$], *n*-octadecyltrichlorosilane [OTS, $CH_3(CH_2)_{17}SiCl_3$], *trans*-13-docosenoic acid [brassidic acid, (t-13)C_{22}(u), $CH_3(CH_2)_7CH{=}CH(CH_2)_{11}COOH$], *trans*-13-docosenyltrichlorosilane [(t-13)C_{22}(u)Si, $CH_3(CH_2)_7CH{=}CH(CH_2)_{12}SiCl_3$],[37] and 17-octadecenoic acid [(t-17)C_{18}(u), $CH_2{=}CH(CH_2)_{15}COOH$].[38]

Film Preparation and $KMnO_4$ Treatment. LB monolayer and built-up multilayer films of the acid cadmium salts were prepared as described before.[2] Transfer curves were recorded during the deposition of the LB monolayers for each of the specimens prepared for this study.[2] Continuous quantitative transfer (transfer ratios in the range 1.00 ± 0.05)[2] has been achieved in all reported samples. The SA monolayers were prepared by adsorption (at the ambient temperature) from solutions in bicyclohexyl (BCH), at concentrations ensuring formation of complete monolayers of the respective compounds.[2] As before,[2] LB and SA films are denoted by L and A (adsorbed), respectively.

The permanganate reagent was a 1.2 M solution of analytical grade $KMnO_4$ in doubly distilled water at neutral pH. Exposure of the films to the reagent was usually performed by keeping the film-coated ATR plates in a horizontal position and spreading a thick layer of the $KMnO_4$ solution over their entire radiation-sampled area.[2] After the desired exposure time had elapsed (3 min in this study), the permanganate solution was removed by suction and the surface rinsed several times with pure water, using the same spreading–suction procedure. The surface was finally allowed to slowly air-dry under a glass cover. Treatments with pure water, HCl, and NaOH solutions were performed in an analogous manner. This procedure was adopted in order to avoid the possibility of eventual contamination of the measured film surface by traces of surface-active material accumulated on the free surface of the water or reagent solution.[39]

IR and Contact Angle Measurements. IR–ATR and contact angle measurements were performed as described before.[2] The test liquids used in the contact angle measurements were, as in previous work,[2,3,22] *n*-hexadecane (HD), bicyclohexyl (BCH), and water. The contact angles were usually determined after recording the respective IR spectra, in order to reduce the danger of possible contamination of the films by traces of the test liquids.[22] All reported spectra were obtained at a resolution of 4 cm^{-1} and represent the net contributions of the respective organic films. The estimated reproducibility of the absorbance and contact angle measurements is indicated in the plots either by error bars or by the size of the displayed data points.

Planning of the Experiments and Interpretation of Experimental Data. In order to explore the depth of penetration of $KMnO_4$ into an organized film assembly, films from one to several superimposed monolayers were constructed, with the reactive double bond functions located at variable positions below the outer film surface. Films made of saturated amphiphiles only (C_{20} and OTS) were also examined, with the purpose of checking the behavior of monolayers devoid of reactive ethylenic functions under exposure to the reagent.

In addition to organized mono- and multilayer assemblies with planned architecture, relatively thick, polycrystalline films of (t-13)C_{22}(u) were also prepared on ZnSe by casting a measured volume of the surfactant solution in chloroform on the ZnSe surface and then letting the solvent evaporate. It was hoped that a comparative study of the two types of films would allow us to evaluate the role of planned molecular organization and structural homogeneity in the process of film penetration.

The main oxidation products of olefins by aqueous $KMnO_4$ were reported to be diols, ketols, diketones, and cleavage products of the carbon–carbon double bond, their relative distribution depending on the conditions of the reaction.[40-44] The reaction has been extensively studied mainly on cis compounds, such as oleic acid ((c-9)C_{18}(u)), for which the distribution of products was found to be pH dependent in bulk aqueous solutions,[40,41] while in water emulsions it is pH independent and also different from that in homogeneous solutions.[42] No significant pH dependence was found in the oxidation of the trans double bond in elaidic acid ((t-9)C_{18}(u)) in aqueous solutions above pH 9, the main products being the ketol and diol.[41] The oxidation of oleic acid in monolayers spread on dilute acidic permanganate solution was reported to lead to the quick formation of the *cis*-epoxy acid, with subsequent partial cleavage of the C=C bond to shorter water-soluble acid fragments.[43] It is also of interest to note that the oxidation of the brassidic acid (trans isomer) in Langmuir monolayers spread on aqueous permanganate solutions could be almost completely inhibited by compressing the monolayers to their solid phase, while no such dependence of the reaction on compression could be found for the respective cis isomer (erucic acid).[44] This effect was interpreted as evidence that the close packing of the chains achieved in the monolayer of the trans isomer efficiently prevents contact of the reactive ethylenic function with the liquid permanganate in the underlying subphase.[44]

On the basis of the above available data on the $KMnO_4$ oxidation of olefins it could be anticipated that IR spectroscopy should furnish evidence on the oxidation of monolayer double bond functions mainly through the disappearance of the ethylenic

(33) Menger, F. M.; Doll, D. W. *J. Am. Chem. Soc.* **1984**, *106*, 1109.
(34) Maoz, R.; Sagiv, J. *Langmuir*, following paper in this issue.
(35) Maoz, R.; Sagiv, J. *Thin Solid Films* **1985**, *132*, 135.
(36) The abbreviated notations used for the film-forming surfactants are as in ref 2. For example, (t-13)C_{22}(u)Si indicates the presence of unsaturation (u) at position 13 in a chain of 22 carbon atoms (C_{22}), with trans (t) configuration of the double bond and a silane (Si) head group.
(37) The synthesis of (t-13)C_{22}(u)Si is described in ref 24.
(38) The 17-octadecenoic acid was a gift sample obtained from Prof. G. M. Whitesides.[39]

(39) Some of the first investigated specimens, exposed to the $KMnO_4$ solution by immersion in the bulk liquid followed by withdrawal through the liquid–air interface, were found to display higher CH_2 and CH_3 peak absorbances after exposure to the reagent. This enhancement of the methylene and methyl band intensities comes, most likely, from traces of organic material picked up from the surface of the liquid. Possible sources of such surface contamination may be weakly bonded film material removed from the unpolished edges of the ATR plate (these edges are not sampled by the IR beam[2]) or traces of hexadecane or bicyclohexyl retained on the film surface during the contact angle measurements.[22]
(40) Wolfe, S.; Ingold, C. F. *J. Am. Chem. Soc.* **1981**, *103*, 938 and references cited therein.
(41) Coleman, J. E.; Ricciuti, C.; Swern, D. *J. Am. Chem. Soc.* **1956**, *78*, 5342.
(42) Garti, N.; Avni, E. *Colloids Surf.* **1982**, *4*, 33.
(43) Iwahashi, M.; Toyoki, K.; Watanabe, T.; Muramatsu, M. *J. Colloid Interface Sci.* **1981**, *79*, 21 and references cited therein.
(44) Maradem, J.; Rideal, E. K. *J. Chem. Soc.* **1938**, 1163.

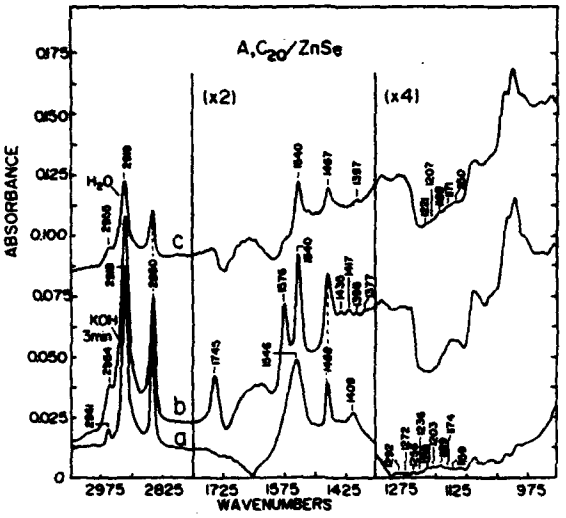

Figure 1. Example of spectral changes observed in the ATR infrared spectrum of a C_{20} monolayer adsorbed on ZnSe upon exposure to aqueous KOH and water: (a) before exposure to KOH; (b) after a 3-min exposure to the KOH solution (1% in water); (c) after rinsing the KOH-treated film with pure water. Note the appearance of a potassium carboxylate peak at 1576 cm^{-1} after the KOH treatment (curve b) and its disappearance, accompanied by a reduction in the intensities of all other bands, following the H_2O rinse (curve c). The origin of the 1745-cm^{-1} peak in curve b is not clear. It may represent a measurement artifact due to distortions of the base line in this spectral region[38] (compare curves a, b, c).

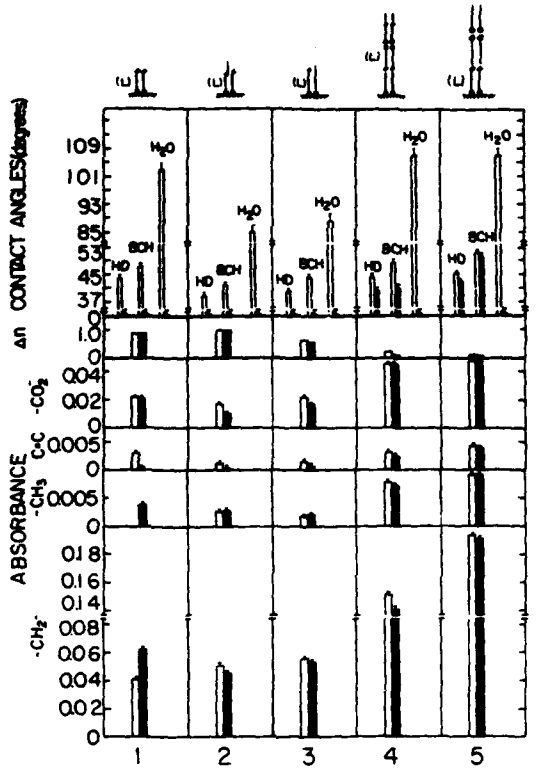

Figure 2. IR absorbance and contact angles of LB film assemblies containing terminal double bond functions (on ZnSe), before and after a 3-min exposure to the permanganate solution: 1, (*t*-17)C_{18}(u) monolayer; 2, (*t*-17)C_{18}(u) + (*t*-13)C_{22}(u) mixed monolayer (see also Figure 4); 3, (*t*-17)C_{18}(u) + C_{20} mixed monolayer; 4, (*t*-13)C_{22}(u)/(*t*-17)C_{18}(u)/C_{20}/ZnSe trilayer (see also Figure 4); 5, C_{20}/C_{20}/(*t*-17)C_{18}(u)/ZnSe trilayer (Figure 3). Lower part: $-CH_3$, $-CH_2$, C=C, and $-CO_2^-$ represent ATR peak absorbances at ca. 2919, 2956, 910, and 1540 cm^{-1}, respectively (see Figure 3). □, initial absorbance; ▩, absorbance after exposure to $KMnO_4$. Middle part: Δn is the fraction of reacted terminal double bonds, determined from the decrease in the absorbance of the 910-cm^{-1} peak, relative to its initial value. □, uncorrected; ▩, normalized with respect to the observed change in the absorbance of the respective 2919-cm^{-1} (CH_2) peak after exposure to $KMnO_4$. Upper part: Advancing contact angles. □, initial values; ▩, after exposure to $KMnO_4$.

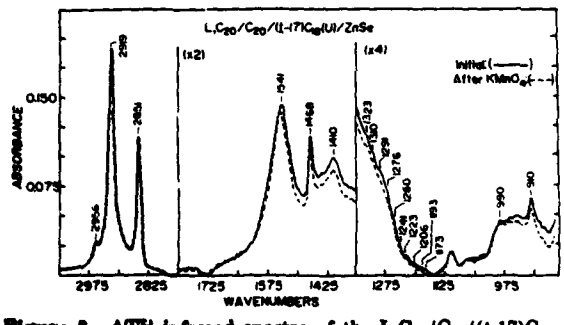

Figure 3. ATR infrared spectra of the L,C_{20}/C_{20}/(*t*-17)C_{18}-(u)/ZnSe trilayer (Figure 2, column 5): (—) before exposure to the $KMnO_4$ reagent; (- - -) after exposure to the reagent for 3 min.

bending band at ca. 964 cm^{-1} (914 cm^{-1} in (*t*-17)C_{18}(u))[2,5] and the eventual appearance of carbonylic functions in the 1500–1700-cm^{-1} region. Changes in the intensity and characteristic appearance of a number of other IR-active bands, associated with the paraffinic chains and with the carboxylate (COO^-) function (in the acid salt films), should also be of help in evaluating the chemical and structural transformations effected by the reagent on the treated films.

The usefulness of wettability observations in the context of the present study follows from the high sensitivity of contact angles to structural and chemical transformations affecting the packing density and orientation of the film-forming molecules,[2,4,5,8,22,45,46] as well as the polarity of the functions exposed on the outer film surface.[2,4,5,22,47,48] Such transformations, induced through the action of the $KMnO_4$ reagent, may be expected to result in more wettable surfaces, i.e., lower contact angles for both organic liquids and water. As noted above, *attempts to assess* the penetrability of an organized film assembly without providing adequate evidence for its structural stability during the experiments under consideration may lead to erroneous conclusions. Wettability observations are particularly important in this respect, providing a sensitive complementary analytical tool in the interpretation of the IR data.

Results and Discussion

Analysis of Wettability Data. Table I summarizes all relevant wettability data collected during this study, including contact angles measured on nonreactive films (C_{20}, OTS) and on a number of reactive multilayer films for which IR spectra were not recorded. Contact angles obtained for some representative reactive films are also plotted in Figures 2 and 4 along with the respective IR data.

(45) (a) Bartell, L. S.; Ruch, R. *J. J. Phys. Chem.* **1956**, *60*, 1231; (b) **1959**, *63*, 1046.
(46) Cohen, S.; Naaman, R.; Sagiv, *J. J. Phys. Chem.* **1986**, *90*, 3054.
(47) Heinze-Farley, S. R.; Rosmay, R. H.; McCarthy, T. J.; Deutch, J.; Whitesides, G. M. *Langmuir* **1985**, *1*, 725.
(48) Maoz, R.; Netzer, L.; Gun, J.; Sagiv, J. Proceedings of the Meeting "New Technological Applications of Phospholipid Bilayers, Thin Films and Vesicles"; Tenerife-Canary Islands, Jan 6–9, 1986; Plenum: New York, in press.

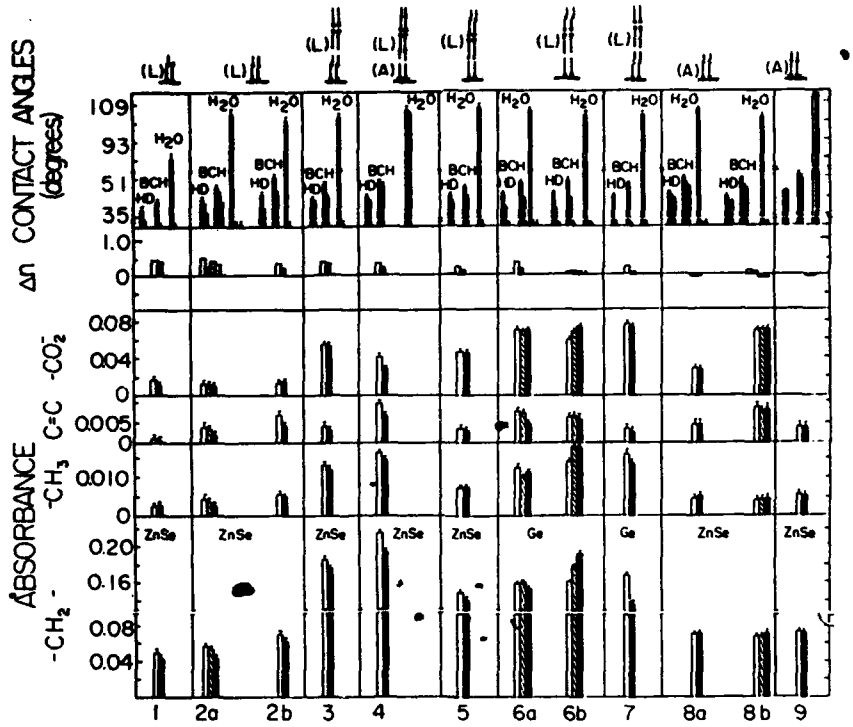

Figure 4. IR absorbance and contact angles of LB and SA films containing the *trans*-13-docosenyl moiety, before and after a 3-min exposure to pure water and/or the $KMnO_4$ solution: 1, L,[(*t*-17)C_{18}(u) + (*t*-13)C_{22}(u)]/ZnSe (see also Figure 2); 2a and 2b, identically prepared samples of L,(*t*-13)C_{22}(u)/ZnSe; 3, L,C_{20}/C_{20}/(*t*-13)C_{22}(u)/ZnSe (Figure 6); 4, L,(*t*-13)C_{22}(u)/(*t*-13)C_{22}(u)/OTS/ZnSe (Figure 7); 5, L,(*t*-13)C_{22}(u)/(*t*-17)C_{18}(u)/C_{20}/ZnSe (see also Figure 2); 6a and 6b, identically prepared samples of L,(*t*-13)C_{22}(u)/C_{20}/C_{20}/Ge (Figure 5; 6b was exposed to H_2O and $KMnO_4$ by immersion in the bulk liquid, followed by withdrawal through the liquid–air interface[38] (see Experimental Section for details)); 7, L,C_{20}/C_{20}/(*t*-13)C_{22}(u)/Ge; 8a and 8b, identically prepared samples of A,(*t*-13)C_{22}(u)/ZnSe. The IR spectrum of 8b displays "unusual" features, indicative of long-range crystalline order;[34] 9, A,(*t*-13)C_{22}(u)/Si/ZnSe. Lower part: $-CH_2^-$, $-CH_3$, C=C, and $-CO_2^-$ represent ATR peak absorbances at ca. 2919, 2957, 964, and 1543 cm^{-1}, respectively (see Figures 5–7). □, initial absorbance; ▨, absorbance after exposure to H_2O; ■ absorbance after exposure to $KMnO_4$. Middle part: Δn is the fraction of reacted internal double bonds, determined from the decrease in the absorbance of the 964-cm^{-1} peak. □, relative to the initial absorbance, uncorrected; ▨, relative to the initial absorbance, normalized with respect to the observed change in the absorbance of the respective 2919-cm^{-1} CH_2 peak after exposure to $KMnO_4$; ▨, relative to the absorbance of the H_2O-treated film, uncorrected; ■, relative to the absorbance of the H_2O-treated film, normalized with respect to the observed change in the absorbance of the respective CH_2 peak after exposure to $KMnO_4$. Small negative Δn values (within ca. −0.05), indicating an increase in the absorbance of the 964-cm^{-1} peak following the $KMnO_4$ treatment, may arise from the statistical spreading of the IR measurements. Upper part: Advancing contact angles. □, initial values; ▨, after exposure to H_2O; ■, after exposure to $KMnO_4$.

The contact angles measured prior to exposure of the films to H_2O or to the $KMnO_4$ solution are in the range characteristic of highly oriented, compact monolayer structures of the respective compounds.[2-4,32,40] A combined analysis of the contact angles and the respective IR data collected after 3-min exposure of the films to the $KMnO_4$ solution (Figures 2 and 4; see discussion below) reveals that, in general, one cannot find a one-to-one correspondence between the extent of oxidation of intralayer-located double bonds and the observed changes in the wetting properties of the respective films.

The wetting properties are found to be strongly dependent on the mode of film-to-surface binding, the thickness of the film (in multilayer structures), and the nature of the solid substrate. Thus, except for (*t*-17)C_{18}(u) monolayers and mixed monolayers containing this compound (Figure 2, columns 1–3; Table I, entries 1–3), in which the almost quantitative oxidation of the unprotected terminal double bonds results in complete wetting by each of the three test liquids, the fatty acid salt monolayers on ZnSe are affected by the 3-min exposure to the $KMnO_4$ solution in a manner causing only a moderate drop in their HD and BCH contact angles, while being completely wetted by H_2O (Table I, entries 16–19; Figure 4). The effect of pure water on these monolayers is similar, although less drastic than that of the $KMnO_4$ reagent. C_{20} (Table I, entry 25) and (*t*-13)C_{22}(u) monolayers display similar wetting properties despite the absence of reactive double bonds in the former films.

No significant effect of water or of the $KMnO_4$ solution on the contact angles of complete silane monolayers adsorbed on ZnSe (OTS as well as (*t*-13)C_{22}(u)Si) could be observed (Table I, entries 27 and 20, respectively; Figure 4). As shown in the following paper in this issue,[34] incomplete OTS/Si monolayers are insensitive to the action of the $KMnO_4$ reagent too, while the significant drop in the contact angles of an incomplete (*t*-13)C_{22}(u)Si/ZnSe monolayer upon exposure to aqueous $KMnO_4$ may be ascribed to the oxidation of the double bonds in this film.

The wettability of multilayer acid salt films is clearly dependent on the number of layers in the film and the nature of the film-forming surfactants. Thus, LB films of C_{20} on Ge thicker than a trilayer retain both their oleophobicity and hydrophobicity upon exposure to the $KMnO_4$ solution (Table I, entries 23, 24), while (*t*-13)C_{22}(u) films display similar behavior only at thicknesses above seven layers (Table I, entries 6–10). Mixed multilayer films containing, besides C_{20}, (*t*-13)C_{22}(u) layers are more

Table I. Film Wettability before and after a 3-min Exposure to Pure H_2O and Aqueous $KMnO_4$

		equilibrium advancing contact angle,[a] deg								
		HD			BCH			H_2O		
no.	film	initial[b]	H_2O[b]	$KMnO_4$[b]	initial[b]	H_2O[b]	$KMnO_4$[b]	initial[b]	H_2O[b]	$KMnO_4$[b]
1	L,(t-17)C_{18}(u)/ZnSe	44		0	49		0	98		0
2	L,[(t-17)C_{18}(u) + C_{20}]/ZnSe	40		0	44		0	88		0
3	L,[(t-17)C_{18}(u) + (t-13)C_{22}(u)]/ZnSe	38		0	42		0	85		0
4	L,(t-13)C_{22}(u)/(t-17)C_{18}(u)/C_{20}/ZnSe	44		40	48		41	107		0[c]
5	L,C_{20}/C_{20}/(t-17)C_{18}(u)/ZnSe	45		43	51		50	107		0[c]
6	L(t-13)C_{22}(u)/Ge	45		0	52		0	108		0[d]
7	L,3[(t-13)C_{22}(u)]/Ge				51		0	103		0[d]
8	L,5[(t-13)C_{22}(u)]/Ge				51		0	105		0[d]
9	L,7[(t-13)C_{22}(u)]/Ge				51		48	104		100
10	L,9[(t-13)C_{22}(u)]/Ge				50		49	103		102
11	L,(t-13)C_{22}(u)/C_{20}/C_{20}/Ge	45	37	0	49	41	0	104	0	0[d]
12	L,(t-13)C_{22}(u)/C_{20}/C_{20}/Ge	44		0	48		0	103		0[d]
13	L,C_{20}/C_{20}/(t-13)C_{22}(u)/Ge				48		0	102		0[d]
14	L,C_{20}/C_{20}/(t-13)C_{22}(u)/C_{20}/C_{20}/Ge				49		0	103		0[d]
15	L,C_{20}/C_{20}/C_{20}/C_{20}/(t-13)C_{22}(u)/Ge				48		0	104		0[d]
16	L,(t-13)C_{22}(u)/ZnSe	44	39	35	48	45	42	105	0[c]	0
17	L,(t-13)C_{22}(u)/ZnSe	45		37	51		45	103		0
18	A,(t-13)C_{22}(u)/ZnSe	45	40	40	51	48	47	108	0[c]	0
19	A,(t-13)C_{22}(u)*/ZnSe[e]	43	40	40	50	47	45	103	0[c]	0
20	A,(t-13)C_{22}(u)Si/ZnSe	45		45	52		51	112		112
21	L,C_{20}/C_{20}/(t-13)C_{22}(u)/ZnSe	43		39	49		43	104		0[c]
22	L,(t-13)C_{22}(u)/(t-13)C_{22}(u)/OTS/ZnSe	44		41	50		48	107		104
23	L,C_{20}/Ge	44		0	51		0	105		0[d]
24	L,3[C_{20}]/Ge				52		51	105		104
25	L,C_{20}/ZnSe	45		45	50		49	105		0
26	A,OTS/Ge	45	45	0	52	52	0	112	111	0[c]
27	A,OTS/ZnSe	45	45	44	49	49	49	112	111	111
28	A,OTS/Si	45	45	45	51	52	52	112	111	112
29	polycrystalline (t-13)C_{22}(u) on ZnSe (ca. 15 monolayers-thick film)									
	immediately after placing the test drop on the surface	45	45	40	48	49	45	103	103	98
	3 min later	43			41			80		
	5 min later (equilibrium)	40			36			78		

[a] The precision of the contact angle measurements is of the order of ±1° for HD and BCH and ±2° for H_2O.[3] [b] Angles determined before (initial) and after a 3-min exposure to H_2O and then to the $KMnO_4$ solution. [c] Partially dry after removal of the bulk liquid from the surface. The water test drops spread on the dry as on the initially wetted portions of the surface. [d] Yellowish precipitate left on the surface upon treatment with $KMnO_4$. The precipitate may be removed by gentle wiping with cotton wool, without removing the underlying organic film. No changes are observed in the HD and BCH contact angles, while the H_2O angle grows to ca. 60° after removal of the precipitate. [e] Specimen listed in column 8b of Figure 4.

wettable than pure C_{20} films (Table I, entries 11–15 and 24).

As may be seen in Figure 4 and Table I (entries 6, 7, 11–13, 16–19, 21, 23, 25), the wettability of (t-13)C_{22}(u) trilayer films and mixed trilayers composed of C_{20} and (t-13)C_{22}(u) layers is similar to that of the respective monolayers; i.e., such films loose their hydrophobicity upon exposure to the $KMnO_4$ solution. In contradistinction to the pure acid–salt trilayers, a mixed trilayer comprised of an LB bilayer of (t-13)C_{22}(u) deposited on top of a self-assembled OTS/ZnSe monolayer maintains its high hydrophobicity following treatment with the $KMnO_4$ solution (Table I, entry 22; Figure 4, column 4). This behavior is obviously associated with the presence of the OTS monolayer underneath the acid salt bilayer in this trilayer film. Coverage of the solid substrate by a covalently bonded silane monolayer has invariably been found to render it nonwettable by water. The surface hydrophobicity is preserved even in the presence of incomplete silane monolayers (including (t-13)C_{22}(u)Si) with appreciably lower packing densities than in closely packed structures.[49]

On the basis of all these observations we may conclude that, in the absence of extensive oxidative attack of the film, two conditions must be fulfilled in order to bring about wetting by water or by the permanganate solution of a polar solid coated with an oriented film assembly: (a) Water must penetrate the film and reach the underlying solid surface. (b) The mobility of the film-forming molecules in the first layer adjacent to the solid surface must not be hindered by covalent intermolecular coupling and/or covalent anchoring to the underlying surface.

Both conditions are fulfilled in monolayers or thin-enough multilayers of ionically bonded fatty acid salts. Water diffusion down to the underlying solid substrate is efficiently blocked by dense C_{20} films thicker than a trilayer, or (t-13)C_{22}(u) films thicker than seven layers,[22,31] which explains the stable hydrophobic character of such films. The hydrophobicity of silane films, particularly that of the incomplete monolayers, is obviously a consequence of the surface immobilization of the silane amphiphiles, effected through their intralayer and layer–surface covalent binding.[2,8,10,32,46]

Films on Ge (Table I, entries 6–15, 23, 24, 26; Figure 4) are seen to be, in general, more wettable than their counterparts on ZnSe (Table I, entries 16–21, 25, 27).[2] This points to weaker anchoring to the Ge surface of both the fatty acid Cd^{2+} salts and silane monolayers. The drastic drop in the HD and BCH contact angles, besides those of H_2O, upon exposure of Ge-supported films to the $KMnO_4$ solution, and the simultaneous appearance of a removable yellowish precipitate on the exposed film surface (see

(49) A detailed discussion of the behavior of incomplete monolayers is given in ref 34.

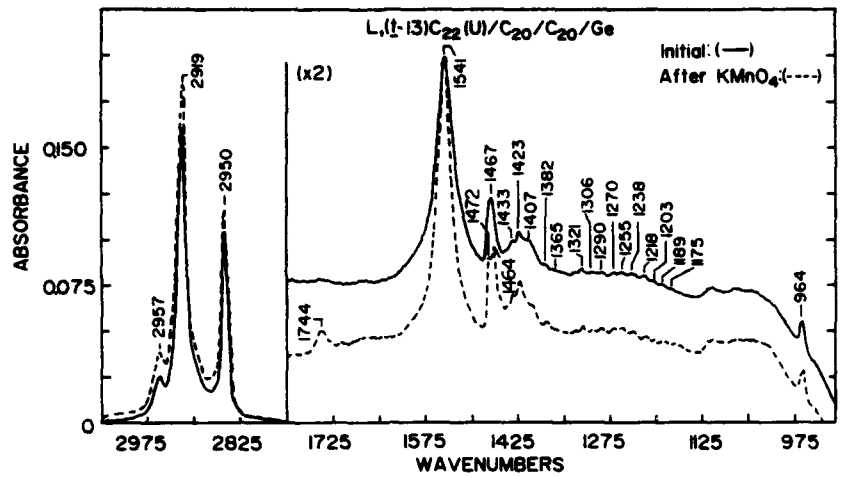

Figure 5. ATR infrared spectra of the $L_n(t\text{-}13)C_{22}(u)/C_{20}/C_{20}/Ge$ trilayer listed in Figure 4, column 6b: (—) before exposure to the $KMnO_4$ reagent; (---) after exposure to the reagent for 3 min.

Ge-supported films in Table I, except entries 9, 10, 24) are indicative of oxidative attack of the Ge substrate, accompanied by migration of the reaction products across the film onto its outer surface.

Taken together, the present findings, and particularly the striking differences between ionic and covalently bonded monolayers, suggest a mechanism of surface wetting involving lateral diffusion of the wetting liquid (water) in the film–substrate interfacial region. The process is, apparently, facilitated by the surface mobility of the film molecules adjacent to the substrate, under the action of the wetting liquid. Wetting of a film-coated surface may thus be expected to affect the molecular architecture of the film. A critical evaluation of the extent of structural damage produced to a wettable film by its exposure to a wetting liquid is, therefore, required.

From the moderate drop in the HD and BCH contact angles of the acid films on ZnSe following 3 min of exposure to H_2O and/or to the $KMnO_4$ solution (Table I, entries 16–19, 21, 22, 25; Figure 4) we may infer that, although their structural integrity must have been affected to a certain degree, the initial packing and orientation of the film molecules on the surface are largely preserved in these films. This conclusion is corroborated by the analysis of the ATR (see below) and polarized ATR[24] spectra of some of the acid salt films as well as by the reflection–absorption (RA) spectra of a $L_n(t\text{-}17)C_{18}(u)/Al$ monolayer recorded prior and after exposure to water and to the $KMnO_4$ solution.[8] Finally, spectral features indicative of long-range crystalline order, detected in the spectra of a number of monolayer and multilayer acid films (see below), do not vanish upon their exposure (for 3 min) to the $KMnO_4$ solution. This clearly indicates that the initial molecular organization is preserved in these films, at least within film domains containing a large number of molecules.

A last important point to be emphasized is that, although wetting of a film-coated solid substrate by water (or by the $KMnO_4$ solution) seems to require both permeation through the film and lateral diffusion of the liquid in the film–substrate interfacial region, wetting does not effect detachment of the organic film from the solid surface. This was demonstrated by the failure of repeated attempts to remove supposedly floating film material by suction of the thick water layer left on the surface of wetted specimens. Partial removal of film material from C_{20} monolayers adsorbed on ZnSe could be achieved by this procedure only immediately following their treatment with aqueous HCl (5%) or KOH (1%) solutions. As demonstrated by the ATR spectra of HCl- or KOH-treated monolayers (Figure 1), under these circumstances, the removable film fraction consists of C_{20} molecules converted from the initial zinc salt (COO^- peak at ca. 1540 cm^{-1}) to the free acid (COOH peak at 1700–1740 cm^{-1}) or the potassium salt (COO^- peak at ca. 1576 cm^{-1}), respectively. HCl- or KOH-treated monolayers were also found to loose completely their oleophobicity (zero contact angles for HD and BCH), which suggests a major deterioration of their initial organization.

The thick films prepared by casting a volume of chloroform solution of $(t\text{-}13)C_{22}(u)$ on the surface of ZnSe are polycrystalline conglomerates, as may be deduced from their IR spectra (see below) and SEM micrographs. Contact angles measured on such films immediately after placing the test drops on their surface are close to those characteristic of ordered acid monolayers. This suggests that the crystallites have a layered structure and are oriented on the ZnSe surface in such a manner that their outer layer mimics the appearance of an oriented monolayer of $(t\text{-}13)C_{22}(u)$ molecules. Spreading of the test liquids in interstices between the crystallites leads to a rapid drop in the contact angles with time, thus revealing the heterogeneous nature of these films (Table I, entry 29).

Analysis of the IR Data. Oxidation of monolayer double bonds under the present conditions does not lead to the formation of significant amounts of carbonylic functions (see Figures 5–7). As will be shown in the following paper in this issue, even after much longer exposure times (and quantitative oxidation of the ethylenic functions) there is no evidence for cleavage of the C=C bond in the *trans*-13-docosenyl chain. The fraction of reacted double bonds (Δn in Figures 2 and 4) is thus determined from the relative peak intensity of the ethylenic bending band at 964 cm^{-1}, solely.

The reproducibility of the present ATR measurements and the observed sample-to-sample spreading of data[2,32] allow Δn to be determined with an estimated confidence not better than ca. 5–10% of a complete monolayer. This figure may vary, depending on the presence of overlapping bands, the noise level of the measurement (see Figures 3

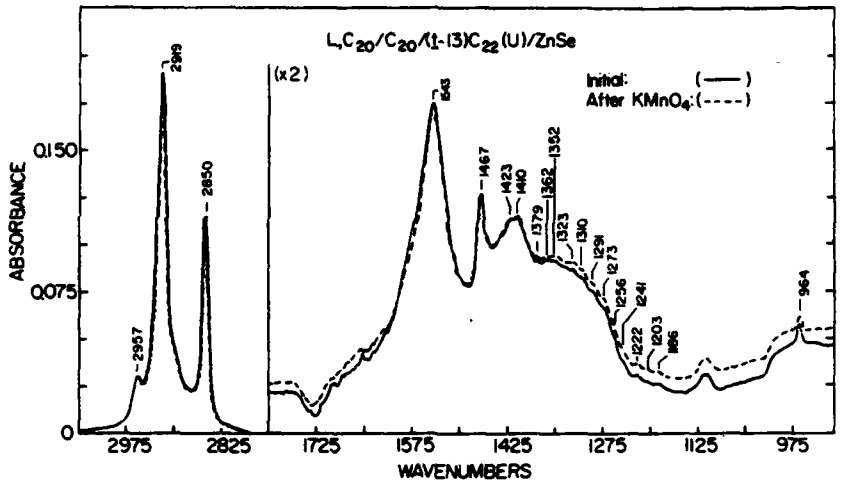

Figure 6. ATR infrared spectra of the L,C_{20}/C_{20}/(*t*-13)C_{22}(u)/ZnSe trilayer listed in Figure 4, column 3: (—) before and (---) after a 3-min exposure to the $KMnO_4$ solution.

and 5–7), and the peak intensity of the measured band[50] (see Figures 2 and 4).

Another source of error in the quantitative evaluation of the ATR data is related to the limited structural stability of part of the investigated films and to the expected modification of their optical properties upon exposure to $KMnO_4$. As shown previously,[2] a direct correlation of the measured IR–ATR band intensities with the surface concentrations of the respective functional groups is strictly valid only for films having similar indices of refraction and molecular orientation. While these conditions are well satisfied for the presently investigated films in their initial state, deviations from the initial molecular orientation and/or variations in the index of refraction associated with the oxidation of the double bonds may affect to some extent the ATR band intensities of $KMnO_4$-treated films, independent of real changes in the surface concentrations of the functional groups responsible for the respective bands. For example, complete randomization of the paraffinic chains is expected to result in lower absorbance intensities for the CH_2 stretch modes by ca. 30%.[2] In addition, broadening of the bands has also been observed to occur to a certain extent in part of the investigated specimens following the H_2O and $KMnO_4$ treatments. In order to account for possible such variations in the IR band intensities as well as for eventual losses (desorption) of film material upon treatment of the films with H_2O and $KMnO_4$, we have also calculated corrected Δn values, normalized with respect to the observed variations in the peak intensity of the respective 2919-cm^{-1} (CH_2) bands (Figures 2 and 4).

As can be seen from Figures 2 and 4, there may be quite large differences between corrected and uncorrected Δn values in films undergoing partial oxidation of their double bonds. Therefore, except for Δn close to 0 or 1 (no change, or complete disappearance of the measured C=C band, respectively), which can be determined with an accuracy of the order of 5% of a complete monolayer, the other Δn values listed in Figures 2 and 4 should be regarded as semiquantitative, enabling certain general trends to be established on a comparative basis, within the various studied systems.

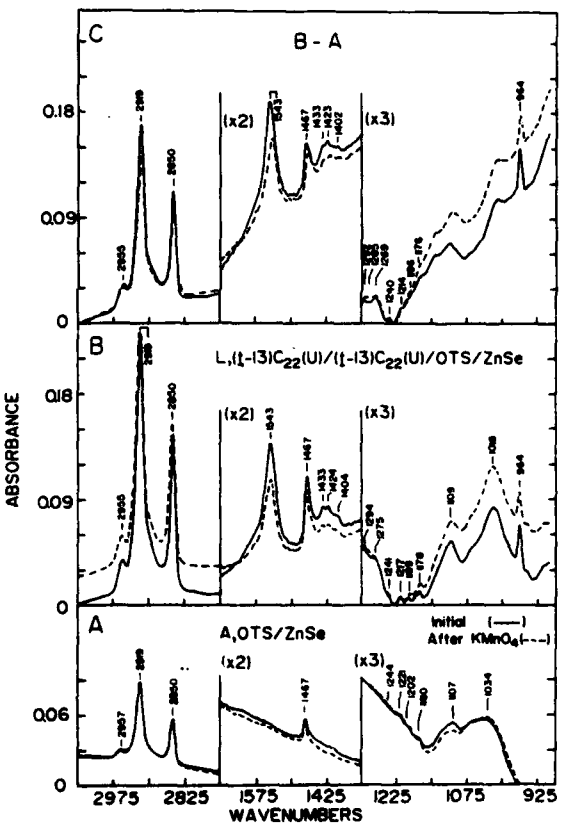

Figure 7. ATR infared spectra of the L,(*t*-13)C_{22}(u)/(*t*-13)C_{22}(u)/OTS/ZnSe trilayer listed in Figure 4, column 4: A, spectra of the OTS first layer; B, spectra of the trilayer; C, difference spectra, B – A, showing the net contribution of the (*t*-13)C_{22}(u) bilayer. Curve notations are as in Figure 6.

Oxidation of the Terminal Double Bond in Film Assemblies Containing (*t*-17)C_{18}(u). Figure 2 summarizes IR and contact angle data obtained for a number of LB film assemblies containing terminal double bond

(50) As a rule, sharper C=C bands, with higher peak absorbances, are observed in films displaying long-range crystalline order[24] (Figure 4, columns 6a, 6b; see spectrum of a crystalline sample in Figure 8). However, considerable sample-to-sample variations in the peak intensity of the *trans*-ethylenic bending band at 964 cm^{-1} have been occasionally observed when no other differences between the spectra of the respective specimens could be identified (Figure 4, columns 6 and 7).

functions, deposited on ZnSe.

The oxidation of unprotected double bonds, in a L,(*t*-17)C_{18}(u)/ZnSe monolayer, is seen to be almost quantitative (Δn = 0.83) within a 3-min exposure to the $KMnO_4$ reagent (column 1 in Figure 2). According to the intensities of the CH_2 and COO^- bands, the monolayer does not appear to be depleted upon immersion in the $KMnO_4$ solution. In fact, we observe a significant increase in the intensity of the CH_2 bands as well as the appearance of a CH_3 band, which may originate in traces of HD retained on the surface of the film during the contact angle measurements.[51]

The second and third columns in Figure 2 show results obtained for mixed monolayers of (*t*-17)C_{18}(u) with (*t*-13)C_{22}(u) and C_{20}, respectively. The molecular packing in these monolayers is less tight than that attained in monolayers of each of the respective pure acids, presumably due to sterical hindrance introduced by the terminal double bond of the C_{18} acid in the packing of the longer C_{22} and C_{20} acids. This is indicated by the lower contact angles measured on these two monolayers (Figure 2; Table I, entries 2, 3) and by their more expanded compression isotherms on the water subphase (not shown).

The oxidation of the terminal double bonds in the monolayer listed in column 2 is seen to be as efficient as in a pure (*t*-17)C_{18}(u) monolayer, while some protection seems to be provided to the terminal double bond in the mixed monolayer with C_{20} (column 3, Figure 2).[52] As indicated by the intensities of the CH_2, CH_3, and COO^- bands, both monolayers in columns 2 and 3 suffer only minor structural modifications and/or desorption of film material upon immersion in the $KMnO_4$ solution. A clear broadening of the COO^- band in the monolayer in column 2, accompanied by a shift of its peak from 1539 to 1547 cm^{-1} and the appearance of a shoulder around 1558 cm^{-1}, following the $KMnO_4$ treatment, may be due to partial exchange of the zinc ions for potassium, with the formation of potassium carboxylate species.

Remarkable protection of the terminal double bonds is achieved in the trilayer structures shown in columns 4 and 5 of Figure 2. The arrangement in column 5 appears to be somewhat more efficient than that in column 4.[53] The structure of the trilayer in column 5 is seen to be particularly well preserved following exposure to the $KMnO_4$ reagent. This is evident from the very small drop in the HD and BCH contact angles (Figure 2) and the invariance of all spectral features in its ATR spectrum (Figure 3), including the two bending vibrations of the terminal double bond, at 910 and 990 cm^{-1}, and the progression of weak bands in the 1100–1300-cm^{-1} region.[54]

From the data in Figure 2 we may conclude that burying the reactive double bonds into a compact hydrophobic environment provides, as expected, significant protection against their attack by aqueous $KMnO_4$. A dense C_{20} bilayer is thus found to efficiently prevent the oxidation of the terminal double bonds in an underlying (*t*-17)C_{18}(u) monolayer exposed to the permanganate reagent for a time long enough to ensure almost quantitative oxidation of a layer of unprotected terminal double bonds. It is also apparent that drastic deterioration of the planned architecture of the investigated films does not occur during a 3-min exposure to the $KMnO_4$ solution, in spite of their complete wetting by the reagent.

Oxidation of Intrachain Double Bonds in Film Assemblies Containing the *trans*-13-Docosenyl Moiety. Figure 4 summarizes IR and contact angle data obtained for 12 film assemblies, including LB (L) and self-assembled (A, adsorbed) monolayers, LB trilayer structures, and a trilayer comprised of an LB bilayer deposited on an underlying self-assembled OTS monolayer. The films are arranged in the order of decreasing reactivity (decreasing Δn) toward $KMnO_4$.

As expected, the mixed LB monolayer in column 1 (Figure 4) is one of the most susceptible to attack by the $KMnO_4$ reagent (Δn = 0.40–0.50). However, the internal double bond is definitely more protected than the terminal one ($\Delta n \sim 1.0$) in the same monolayer (Figure 2, column 2).

The estimated extent of double bond oxidation (Δn) in the LB assemblies on ZnSe (columns 2–5, Figure 4) varies between ca. 10% and ca. 50% of a complete monolayer. A comparison of the reactivity of these films suggests that neither a (*t*-13)C_{22}(u) monolayer (column 4, Figure 4) nor an inert C_{20} bilayer (column 3) provides significant extra protection to the internal double bonds of an underlying (*t*-13)C_{22}(u) monolayer. It is interesting to note that the highest resistance to attack by the $KMnO_4$ reagent among these films is exhibited by the trilayer assembly in column 5 of Figure 4 ($\Delta n \sim$ 0.10–0.20), where the reactive monolayer is positioned on the outer film surface,[57] as compared with the lower resistance of the film in column 3 ($\Delta n \sim$ 0.30–0.35), where the reactive monolayer is covered by an inert C_{20} bilayer.

It was further surprising to find that, although more wettable, films on Ge (columns 6, 7, Figure 4) appear to be less reactive toward $KMnO_4$ than their counterparts on ZnSe (Δn values between 0.04 and 0.36). As on ZnSe, the outer (*t*-13)C_{22}(u) monolayer in the assembly in column 6b of Figure 4 is seen to be less affected by the reagent ($\Delta n \sim$ 0.04) than that in the assembly in column 7 ($\Delta n \sim$ 0.05–0.20), which is covered by a C_{20} bilayer. From the data in Figure 4 it is also apparent that relatively large variations in the Δn values may be found between different specimens with supposedly identical film architecture (see columns 2a, 2b, 6a, 6b, Figure 4).

Contrary to the LB monolayer and multilayer assemblies, the stability and chemical inertness of the self-assembled monolayers (columns 8 and 9, Figure 4) are remarkable. Within the precision of the IR measurements (±5% of a complete monolayer), both the silane and the acid monolayers appear to be totally unaffected by the 3-min exposure to the $KMnO_4$ reagent.[58] All spectral features in the ATR spectra of these self-assembled monolayers are practically invariant upon exposure to the

(51) Contrary to the general procedure used for the other films (see Experimental Section) the contact angles on this film were measured prior to the IR measurements.

(52) It should be noted that because of the very low absorbances of the C=C band in these mixed monolayers, the uncertainty of the calculated Δn values may be as high as 40–50% of the displayed figures.

(53) The reactive monolayer is adjacent to the surface of the substrate in the assembly in column 5 and may thus be more susceptible to the wetting of the substrate by the reagent. In column 4 it resides on top of a first C_{20} monolayer but is covered by a (*t*-13)C_{22}(u) monolayer, which is itself reactive toward $KMnO_4$, as compared with the inert C_{20} bilayer covering the underlying reactive one in column 5.

(54) This progression of weak twist and wag CH_2 bands, characteristic of hydrocarbon chains in the fully extended all-trans conformation, is observed only in IR spectra of linear paraffinic compounds in the solid state–three-dimensional crystalline phases[55] or ordered solidlike monolayers.[4,6,56]

(55) Snyder, R. G. *J. Mol. Spectrosc.* **1961**, *7*, 116 and references cited therein.

(56) Nuzzo, R. G.; Rabolt, J. F.; Swalen, J. D. *J. Chem. Phys.* **1986**, *82*, 2136.

(57) The fraction of reacted intralayer double bonds in this outer (*t*-13)C_{22}(u) monolayer is similar to that of the terminal double bonds in the underlying (*t*-17)C_{18}(u) monolayer in the same assembly (Figure 2, column 4).

(58) Exposure to aqueous $KMnO_4$ for longer times affects the acid but not the silane monolayers.[34]

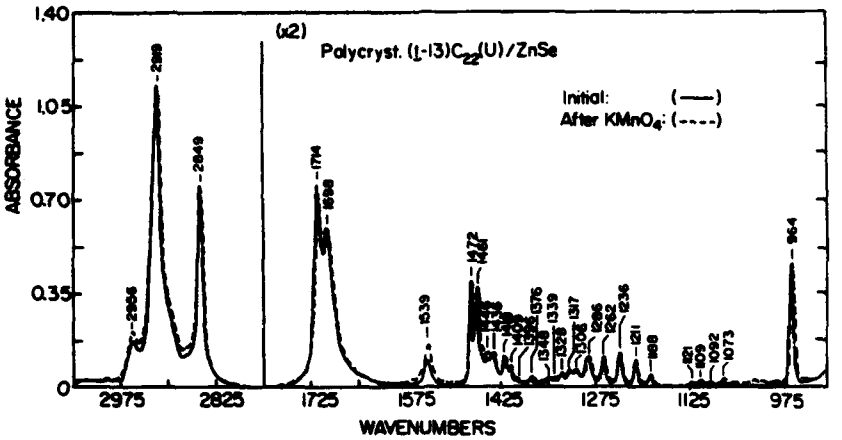

Figure 5. ATR infrared spectra of a thick polycrystalline film of $(t\text{-}13)C_{22}(u)$ on ZnSe (see text for details on film preparation): (—) before and (---) after a 3-min exposure to the $KMnO_4$ solution.

reagent.[59] The contact angles of the silane monolayer (column 9, Figure 4) are also invariant, while the drop in the HD and BCH contact angles of the acid salt monolayers (column 8) is smaller than that observed for their LB counterparts (column 2).

Taken together, the data in Figure 4 suggest a defect-controlled mechanism for the permanganate attack on double bond functions embedded in the hydrophobic region of a dense monolayer or multilayer film assembly. Apparently, the oxidant molecules cannot penetrate into the inner core of a highly ordered and tightly packed monolayer structure, oxidative attack of the double bond functions being possible only at disordered sites in the film. According to this mechanism, the extent of double bond oxidation is determined by the size and density of defects present in the initial film structure and by the extent of structural damage produced to the film upon exposure to the reagent. This explains the observed lack of correlation between film reactivity (in films containing the *trans*-13-docosenyl moiety) and the planned molecular architecture of the film. In a defect-free closely packed monolayer structure, the eight carbon atoms portion of the film extending above the reactive ethylenic function is sufficient to block completely the access of the oxidant molecules into the film. Placing an additional C_{20} bilayer on top of such a monolayer can obviously have no effect on its reactivity, whereas the observed reactivity of a defect-containing assembly with supposedly identical structure may not, in general, be expected to reflect its planned three-dimensional architecture.[60]

Support for this interpretation of the data in Figure 4 comes from a closer analysis of some characteristic spectral features in the IR–ATR spectra of the investigated assemblies.

All acid salt films on Ge display spectral features ascribable to long-range crystalline order.[55,56] This is less obvious on ZnSe. For example, a comparison of the ATR spectra of the rather inert assembly (on Ge) listed in Figure 4, column 6b, with those of the more reactive one (on ZnSe) in Figure 4, column 3 (Figures 5 and 6, respectively), reveals a sharper carboxylate (COO^-) band on Ge (at 1541 cm^{-1}), the splitting of the CH_2 bending band at 1467 cm^{-1} (on ZnSe) into a doublet (at 1464 and 1472 cm^{-1} (on Ge)), and the presence of a triplet, at 1407, 1423, and 1433 cm^{-1}, on Ge, as compared with a poorly resolved doublet, at 1410 and 1423 cm^{-1}, on ZnSe. A long progression of weak bands between ca. 1100 and 1350 cm^{-1} is detectable in both spectra;[54] however, these bands are sharper and better resolved on Ge. Finally, the "crystallinity" of the film on Ge appears to improve following the H_2O and $KMnO_4$ treatments (compare the 1541-cm^{-1} bands and the doublets around 1467 cm^{-1} in the two curves in Figure 5), while no such transformations are detectable on ZnSe (Figure 6).

According to these observations, the films on Ge are ordered crystalline (or polycrystalline) structures, while less order and uniformity of the molecular arrangement are apparent in films on ZnSe. Crystallization of the films on Ge is possibly facilitated by the weaker anchoring to this substrate, as suggested by the more wettable nature of films on Ge (see discussion above). The mobility of the film-forming molecules is, presumably, enhanced by the H_2O and $KMnO_4$ treatments, thus promoting further crystallization of the film.

The acid salt bilayer residing on top of a stable OTS underlayer (Figure 4, column 4) is expected to differ from all other acid films, as it has no direct contact with the underlying solid substrate. ATR spectra of this assembly are depicted in Figure 7. Some of the spectral features displayed by the $(t\text{-}13)C_{22}(u)$ bilayer in this film (see difference spectrum, C, in Figure 7), such as the triplet at 1402, 1423, and 1433 cm^{-1}, resemble corresponding features in the spectra of the acid salt trilayers on Ge (Figure 5), while the 1467- and 1543-cm^{-1} bands resemble corresponding bands in the spectra of acid salt trilayers on ZnSe (Figure 6). These observations point to variations in the detailed molecular organization within each of these acid salt films. Exposure of the acid bilayer on OTS to the permanganate solution does not produce any changes in the appearance of its IR spectrum (Figure 7). However, part of the film material is, apparently, removed from the surface of the substrate, as indicated by the decreased intensities of all IR bands following the $KMnO_4$ treatment (compare the solid and broken curves in Figure 7C). The corrected Δn of this film, normalized relative to the 2919-cm^{-1} (CH_2) band, indicates oxidation of ca. 19% of the double bonds (Figure 4, column 4), while considering

(59) The acid monolayer in column 5b displays "unusual" spectral features, indicative of possible long-range crystalline order in the layer plane of this specimen.[54]

(60) As indicated by the wetting properties of multilayer structures of gradually increasing thickness (Table I, entries 6–10), a sufficiently thick multilayer film should, ultimately, provide efficient protection to the surface underneath it. However, the thickness of such a multilayer barrier reflects the probability of holes or other film defects being covered or filled by material supplied by each additional monolayer in the film rather than an intrinsic structural property ascribable to its specific molecular architecture.

the reduced intensity of the carboxylate (COO^-) band at 1543 cm^{-1} one would obtain $\Delta n = 0$. This means that the observed decrease in the intensity of the C—C band in this film may equally be ascribed to loss of material from the surface and possible orientational effects as to partial oxidation of the double bonds.

Two important conclusions emerge from the above analysis: (a) No matter how the observed changes in the spectra of the LB assemblies are interpreted, it is evident from the mere presence of such changes that the respective films undergo either structural or chemical modifications, or both, upon exposure to the permanganate solution. (b) The lower reactivity of the assemblies on Ge may be ascribed to their crystallinity, which is, however, not necessarily related to their planned architecture.

That the tight packing of the reactive (t-13)C_{22}(u) molecules in a three-dimensional polycrystalline structure precludes their oxidation by the aqueous $KMnO_4$ reagent[44] is demonstrated in Figure 8, showing spectra of a thick polycrystalline conglomerate of (t-13)C_{22}(u) on ZnSe, recorded before and after exposure to the $KMnO_4$ solution. The amount of material in this film, estimated from the peak absorbance of the CH_2 bands around 2900 cm^{-1}, is equivalent to ca. 15 monolayers. Except for the first monolayer, which chemisorbs on the surface as the zinc salt (see carboxylate band at 1539 cm^{-1}), the rest of the material in the film is polycrystalline free acid (carboxylic bands at 1696 and 1714 cm^{-1}). The crystallinity of the film is obvious from the sharpness of all its IR bands, the characteristic splitting of the 1467-cm^{-1} (CH_2) bending band into a doublet, at 1461 and 1472 cm^{-1}, and the well-resolved progressions of twist and wag bands, extending from 1070 to 1350 cm^{-1}. As suggested by its wetting properties and SEM micrographs, the crystallites composing the film have layered structure and are arranged with the layer planes parallel to the ZnSe surface (see discussion above). Exposure of this film to the $KMnO_4$ solution for 3 min is seen to leave its ATR spectrum virtually unchanged (Figure 8), with no measurable fraction of the double bonds being oxidized by the reagent.

Summary and Conclusions

Wetting of a monolayer- or multilayer-covered polar solid by water or by the aqueous permanganate solution requires establishment of direct contacts between the bulk liquid and the solid surface, through the organic film, and lateral diffusion of the liquid in the film–solid interface. The process depends on the presence of voids or channels extending across the film down to the underlying solid surface and on the mobility of the film molecules in the first layer adjacent to the solid. Solid substrates coated with surface-immobilized (covalently bonded) silane monolayers are not wetted by water or by the permanganate solution (except on Ge), regardless of the presence of additional acid salt overlayers.

No correlation of film penetrability, as probed by the aqueous permanganate oxidation of intralayer ethylenic double bonds, with the planned three-dimensional architecture and total thickness of the films could be established for a series of LB built-up films ranging from one to three superimposed monolayers. Monolayers produced by self-assembly were found to be more stable and definitely less penetrable than each of the presently investigated LB films.

A combined analysis of the reactivity and wetting properties of the investigated film assemblies leads to the conclusion that passage of ions from an aqueous phase across a tightly packed monolayer or multilayer assembly of oriented long-chain surfactants occurs only through fortuitous structural defects in the assembly or through defects generated under the action of the penetrating species. An eight carbon atoms thick submonolayer barrier may, apparently, block completely the passage of the aqueous permanganate ion, provided it is free of structural defects and does not deteriorate upon contact with the permanganate solution.

These findings suggest the necessity of a thorough investigation of monolayer penetrability in films not thicker than a single monolayer. Results of such a study are reported in parts 2[34] and 3[35] of this series.

Acknowledgment. We gratefully acknowledge the support of this work by grants from the Schmidt Fund and the European Research Office of the U.S. Army.

Registry No. $KMnO_4$, 7722-64-7; MnO_4^n, 14333-13-2; C_{20}, Cd salt, 14923-81-0; OTS, Cd salt, 112-04-9; (t-13)C_{22}(u), Cd salt, 110174-27-1; (t-13)C_{22}(u)Si, 103941-63-5; (t-17)C_{18}(u), Cd salt, 92601-91-7; BCH, 92-51-3.

Reprinted from LANGMUIR, 1987, 3, 1045.

Penetration-Controlled Reactions in Organized Monolayer Assemblies. 2. Aqueous Permanganate Interaction with Self-Assembling Monolayers of Long-Chain Surfactants

Rivka Maoz and Jacob Sagiv*

Department of Isotope Research, The Weizmann Institute of Science, 76100 Rehovot, Israel

Received December 6, 1986. In Final Form: May 26, 1987

This paper presents a study of the penetrability of solid-supported monolayers as a function of their molecular packing density and mode of binding to the solid surface. Methods described in the preceding paper in this issue are applied to a detailed investigation of films of saturated and unsaturated long-chain acids (ionic bonding) and silanes (covalent bonding) in the submonolayer to complete monolayer range, produced via spontaneous adsorption (self-assembly) from solution. It is shown that ordered monolayers prepared in their tightest modes of packing behave as impenetrable barriers with respect to the passage of the aqueous permanganate ion, provided their initial rigid structure does not deteriorate under exposure to the $KMnO_4$ solution. The leaky nature of ionic acid salt monolayers is found to correlate with their limited structural stability in aqueous media, while the remarkably higher barrier efficiencies of analogous silane monolayers is a consequence of their rigidization and stabilization through intralayer and layer-to-surface covalent bonding.

Introduction

A study of the penetrability of a series of solid-supported film assemblies, including Langmuir–Blodgett (LB) and self-assembled (SA) monolayers, and LB multilayers of some saturated and unsaturated long-chain acids and silanes, under exposure to $KMnO_4$ in aqueous solution, was reported in part 1 (preceding paper in this issue).[1] All films described in part 1 were prepared in their tightest modes of packing and were exposed to the permanganate solution for a fixed period of time (3 min), within which almost complete oxidation of unprotected (surface-exposed) double bonds was observed. A comparative analysis of the penetrability of these assemblies, as deduced from the extent of double bond oxidation in the unsaturated film components and from changes in their surface wettability, suggests a defect-controlled mechanism for the passage of the permanganate ion across the films. In general, SA monolayers, and particularly those stabilized by intralayer and layer-to-surface covalent bonding (silanes), were found to exhibit barrier efficiences remarkably higher than those of acid salt LB films in the range from one to three superimposed monolayers. A sharp decrease in the latter's penetrability was observed in films thicker than seven monolayers. These results lend support to the notion that the role of total film thickness is important only inasmuch as it contributes to healing of defects in a structure made of intrinsically leaky monolayers.

The main factors determining the penetrability of the monolayer films reported in part 1 appear, thus, to be the degree of film structural perfection and its structural stability under the action of the penetrating reagent. This paper (part 2) focuses on the roles of the above two factors in the process of monolayer penetration by the aqueous permanganate ion. Advanatage has been taken in the present study of the possibility of controlling both the strength of anchoring to the underlying solid surface and the packing density of monolayers produced via self-assembly.[2] The investigation was confined to ionically bonded acid salts and covalently bonded silanes, in the submonolayer to complete monolayer range. Variable times of exposure to the permanganate solution were employed in order to check the long-term structural stability of the studied films. For comparison, data previously obtained for a number of representative LB acid salt monolayers[1] were also included in the discussion of the results.

As before,[1] FTIR–ATR spectroscopy (including also measurements with linearly polarized radiation[2]) and wettability (contact angle) observations were used to follow the chemical and structural transformations produced upon exposure of the films to the permanganate solution.

Experimental Section

All materials and experimental procedures employed in this work were described in part 1.[1]

The unsaturated silane surfactant (t-13)C_{22}(u)Si (see Part 1[1] and ref 2 for the abbreviated notations of the surfactants and respective monolayer systems) was prepared from brassidic acid according to the following synthetic route:

$$CH_3(CH_2)_7CH{=}CH(CH_2)_{11}COOH \xrightarrow{\text{DMAP, DCC}}$$
$$CH_3(CH_2)_7CH{=}CH(CH_2)_{11}CO_2CH_3 \xrightarrow{LiAlH_4}$$
$$CH_3(CH_2)_7CH{=}CH(CH_2)_{11}CH_2OH \xrightarrow[CBr_4]{(C_4H_9)_3P}$$
$$CH_3(CH_2)_7CH{=}CH(CH_2)_{11}CH_2Br \xrightarrow{Mg/THF}$$
$$CH_3(CH_2)_7CH{=}CH(CH_2)_{11}CH_2MgBr \xrightarrow[C_6H_6]{SiCl_4}$$
$$CH_3(CH_2)_7CH{=}CH(CH_2)_{11}CH_2SiCl_3$$

The esterification with 4-(dimethylamino)pyridine (DMAP) and N,N-dicyclohexylcarbodiimide (DCC) and the reduction to alcohol with $LiAlH_4$ were carried out according to standard procedures (ref 3 and 4, respectively). The bromination of the alcohol, with carbon tetrabromide (CBr_4) and tri-n-butylphosphine ($(C_4H_9)_3P$), was performed according to the method of Hooz and Gilani,[5] and the conversion of the bromide to the trichlorosilane was performed via addition of its Grignard reagent in tetrahydrofuran (THF) to an excess of tetrachlorosilane ($SiCl_4$) in benzene (C_6H_6), as described in ref 6.

Purification of the ester and bromide intermediates was done by chromatography on silica with n-hexane as eluent, and the alcohol was recrystallized from ethanol. The final trichlorosilane product was isolated from the reaction mixture after decantation and vacuum evaporation of the excess $SiCl_4$ and the benzene.

The intermediates and the final product were analyzed by standard proton NMR and IR spectroscopy. A number of weak, broad features identified between 1500 and 1750 cm^{-1} in the IR

(1) Maoz, R.; Sagiv, J. *Langmuir*, preceding paper in this issue.
(2) Maoz, R.; Sagiv, J. *J. Colloid Interface Sci.* **1984**, *100*, 465.
(3) Nisse, B.; Speiglich, W. *Angew. Chem., Int. Ed. Engl.* **1978**, *17*, 523.
(4) Vogel, A. *Practical Organic Chemistry*; Wiley: New York, 1956; p 879.
(5) Hooz, J.; Gilani, S. S. H. *Can. J. Chem.* **1968**, *46*, 86.
(6) Netser, L.; Iscovici, R.; Sagiv, J. *Thin Solid Films* **1983**, *99*, 235.

0743-7463/87/2403-1045$01.50/0

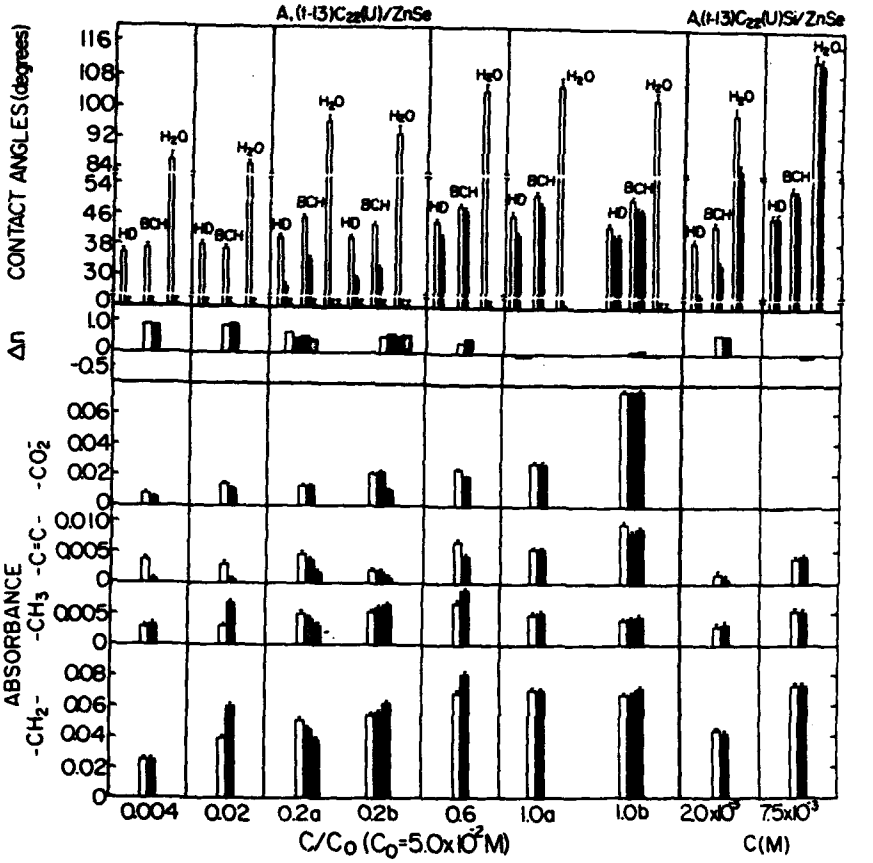

Figure 1. IR absorbance and contact angles of SA monolayers with variable packing density, measured before and after a 3-min exposure to pure water and/or the $KMnO_4$ solution. The first seven columns from the left represent brassidic acid absorbed on ZnSe from solutions of relative concentrations C/C_0, C_0 being the concentration of a saturated solution of brassidic acid in BCH.[2] The last two columns represent monolayers of the corresponding unsaturated silane adsorbed on ZnSe at solution concentrations (C) below and above (last column) the critical concentration required for the formation of complete monolayers[2] of this compound, respectively. Lower part: $-CH_2-$, $-CH_3$, $-C{=}C-$, and $-CO_2^-$ represent ATR peak absorbances at ca. 2919, 2957, 964, and 1544 cm^{-1}, respectively. (See Figures 5 and 6. The monolayer of column 1.0b displays "unusual" spectral features,[7] as illustrated in Figure 2.) □, initial absorbance; ▨, absorbance after exposure to H_2O; ■, absorbance after exposure to $KMnO_4$. The enhancement of the CH_2 and CH_3 peak absorbances upon exposure to $KMnO_4$, observed in columns 0.02, 0.2b, and 0.6, is, most probably, due to traces of organic contaminants picked up from the surface of the permanganate solution (these specimens were exposed to $KMnO_4$ by immersion in the bulk liquid, followed by withdrawal through the liquid–air interface—see description of experimental procedures in the preceding paper[1]). Middle part: Δn is the fraction of reacted double bonds, determined from the decrease in the absorbance of the 964-cm^{-1} peak. □, relative to the initial absorbance, uncorrected; ▨, relative to the initial absorbance, normalized with respect to the observed change in the absorbance of the respective 2919-cm^{-1} (CH_2) peak after exposure to $KMnO_4$; ■, relative to the absorbance of the H_2O-treated film, uncorrected; ▨, relative to the absorbance of the H_2O-treated film, normalized with respect to the observed change in the absorbance of the respective CH_2 peak after exposure to $KMnO_4$. Small negative Δn values (within ca. −0.05), indicating an increase in the absorbance of the 964-cm^{-1} peak following the $KMnO_4$ treatment, may arise from the statistical spreading of the IR measurements. Upper part: Advancing contact angles for *n*-hexadecane (HD), bicyclohexyl (BCH), and water. □, initial values; ▨, after exposure to H_2O; ■, after exposure to $KMnO_4$.

spectra of the final trichlorosilane product as well as its bromide and alcohol precursors may originate in some residual ester and carboxylate impurities. These impurities adsorb on ZnSe, along with the silane surfactant (see Figure 6), but not on silicon (spectra on Si are not shown). No measurable effect of these impurities on the contact angles or the barrier efficiency of the (t-13)C_{22}(u)Si monolayers could be detected (see Results and Discussion, below).

Results and Discussion

Monolayers with Variable Packing Density. Exposure to $KMnO_4$ for 3 min. Experiments were performed with a series of SA monolayers of brassidic acid on ZnSe, in the range from ca. 36% to complete surface coverage, and two monolayers of the corresponding unsaturated silane, at ca. 60% and complete surface coverage, respectively. Figure 1 summarizes the IR and contact angle data obtained before and after exposure of these films to H_2O and/or the aqueous $KMnO_4$ solution.

As discussed in part 1,[1] the fraction of reacted double bonds (Δn) determeined form the relative peak intensities of the ethylenic bending band at 964 cm^{-1} is subject to an uncertainty of the order of at least 5% of a complete monolayer. At partial surface coverages, the uncertainty in the Δn values is correspondingly higher. Despite this limiation, it is still possible, from the IR data plotted in Figure 1, to draw a clear qualitative picture of the trends relating film penetrability to its molecular packing density.

Thus, an upper limit value of $\Delta n \approx 0.85$ is reached at ca. 36% and 55% surface coverage (incomplete monolayers of brassidic acid prepared with solution concentrations $C = 0.004C_0$ and $0.02C_0$, respectively). It then drops to about 0.60–0.40, at ca. 73% surface coverage (solution concentration $C = 0.2\ C_0$) and finally to 0 (no measurable oxidation of the double bonds) at 100% surface

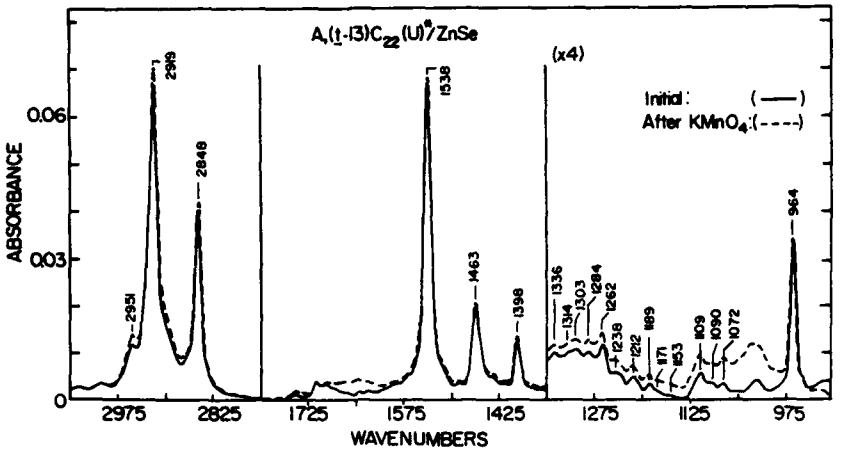

Figure 2. ATR infrared spectra of the brassidic acid monolayer of Figure 1, column 1.0b: (—) before and (---) after a 3-min exposure to the $KMnO_4$ solution.

coverage ($C = C_0$). Significant oxidative attack ($\Delta n \approx 0.30$–0.35) is observed at $C = 0.6C_0$, although the surface coverage reached at this concentration appears to approach completion too. For the silane monolayers, Δn values of about 0.60 and 0 are observed at ca. 60% and 100% surface coverages, respectively (last two columns in Figure 1).

Further evidence for the penetration of the $KMnO_4$ solution in the monolayer–substrate interfacial region is provided by the changes observed in the carboxylate (COO^-) region in the spectra of the incomplete acid monolayers. These consist in a variable drop in the peak absorbance, broadening of the initial carboxylate band, and the appearance of new, broad bands around 1600 cm^{-1}. No such changes are observed in the spectra of the complete acid salt monolayers (compare the COO^- peak absorbances in Figure 1).

These results confirm the expected dependence of film penetrability on its molecular packing density. If prepared in their tightest modes of packing, both the acid salt and silane monolayers are seen to provide efficient protection to intralayer double bonds during a 3-min exposure to the $KMnO_4$ solution. The substantial double bond oxidation observed under identical experimental conditions in the incomplete monolayers of the same compounds is evidently associated with the leaky structure of these films.

The changes in the contact angles, plotted in the upper part of Figure 1, reflect not only the reactivity of the respective films toward $KMnO_4$ but also their sensitivity to water and aqueous permanganate, related to their specific modes of binding of the surface.[1]

The incomplete acid salt monolayers listed in the first three columns of Figure 1 are seen to be wetted by each of the three test liquids following their exposure to permanganate. A drastic drop in the contact angles of the hydrocarbon liquids is also observed following the exposure of these films to pure water (see columns 0.2a and 0.2b in Figure 1). Identical treatments applied to the complete acid salt monolayers cause only a moderate drop in their BCH and HD contact angles (see columns 1.0a and 1.0b in Figure 1). All acid salt monolayers are wetted by the permanganate solution and by water following their exposure for 3 min to $KMnO_4$ or pure H_2O. The wetting of these monolayers may not be ascribed to the presence of the double bonds, as similar behavior is displayed also by monolayers of saturated acids, such as arachidic acid on ZnSe (C_{20}/ZnSe).[1]

The behavior of the unsaturated silane monolayers (last two columns in Figure 1) is distinctly different from that of the acid salt films. There is practically no effect of the $KMnO_4$ treatment on the wettability of the complete silane monolayer (Figure 1, last column), while a large drop is observed in all contact angles of the incomplete one. However, unlike the acid salt films, complete wetting by water was never observed with surfaces coated by silane monolayers. The water contact angles displayed by the incomplete silane monolayer remain, thus, relatively high even after its treatment with permanganate.

We may conclude, on the basis of these observations, that only covalently bonded (silane) monolayers allow a direct relationship to be established between the extent of double bond oxidation and the drop in their water contact angles. The wettabilty of the ionic (acid salt) monolayers is a more complex function of their reactivity, the penetration of water into the film, and its lateral diffusion in the monolayer–substrate interface.[1] The latter process clearly depends on the surface mobility of the monolayer-forming molecules under the influence of an aqueous environment.[1] This interpretation is consistent with the observed insensitivity of surface-immobilized monolayers of saturated silanes to treatments by water and/or aqueous $KMnO_4$, regardless of their degree of compactness. Thus, exposure of an incomplete (ca. 78% surface coverage) monolayer of *n*-octadecyltrichlorosilane (OTS) on Si to the $KMnO_4$ solution for 3, 10, and 60 min produced no detectable changes in its contact angles (H_2O, 103°; BCH, 46°; HD, 43°).

Finally, it would be of interest to note that, as far as IR spectroscopy may reveal, no major structural modifications appear to necessarily accompany the wetting of acid salt monolayers by the aqueous permanganate solution. This is particularly well demonstrated in Figure 2, showing IR–ATR spectra of the complete brassidic acid monolayer listed in Figure 1, column 1.0b, taken before and after its exposure to $KMnO_4$.

The appearance of the spectra in Figure 2 is "unusual", displaying features normally not observed in acid salt monolayers on ZnSe[2,7] (compare with curve a in Figure 5). Thus, all spectral bands in Figure 2 are sharper, the COO^-

(7) SA acid salt monolayers displaying "unusual" spectra, as in Figure 2, were occasionally produced on ZnSe plates when used for the first time in monolayer adsorption. Attempts to reproduce such spectra on a particular plate after removing a first-adsorbed monolayer have constantly failed. The conditions required to promote formation of such "unusual" monolayers are under current investigation.

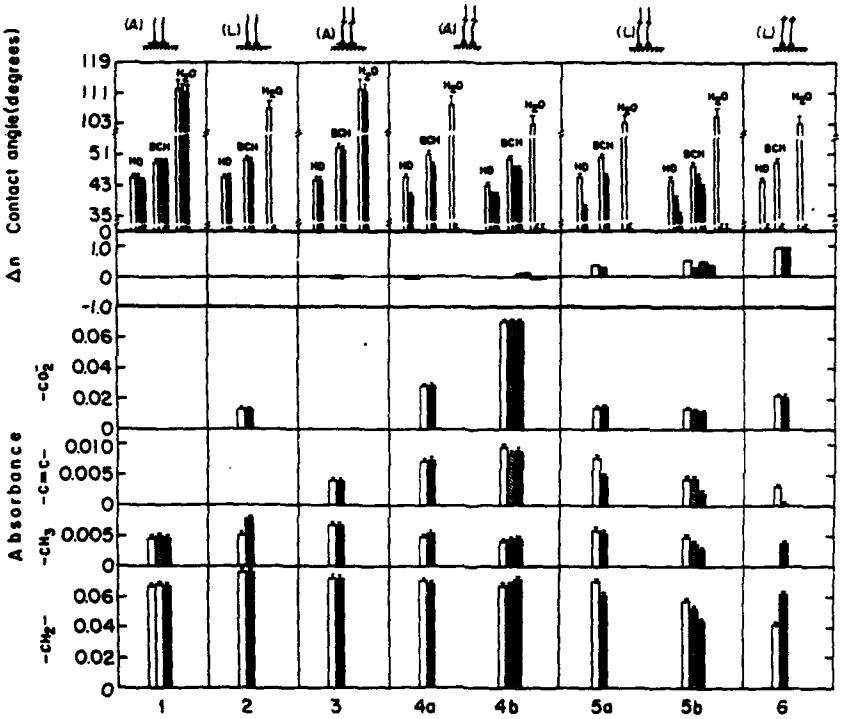

Figure 3. IR absorbance and contact angles of SA and LB complete monolayers, measured before and after a 3-min exposure to pure water and/or aqueous $KMnO_4$: 1, A,OTS/ZnSe; 2, L,C_{20}/ZnSe; 3, A,(t-13)C_{22}(u)Si/ZnSe; 4a and 4b, A,(t-13)C_{22}(u)/ZnSe; 5a and 5b, L,(t-13)C_{22}(u)/ZnSe; 6, L,(t-17)C_{18}(u)/ZnSe. The films in columns 3, 4a, and 4b are the same as in the last column and columns 1.0a and 1.0b of Figure 1, respectively. All other notations are as in Figure 1.

band is shifted ca. 4–6 wavenumbers to the red and its peak absorbance (at 1538 cm^{-1}) is almost threefold higher than that usually observed (Figure 1), the CH_2 bending band is shifted from 1467 to 1463 cm^{-1}, the 1409-cm^{-1} band, ascribed to the bending vibration of the CH_2 group adjacent to the carboxylate[2] (see curve a, Figure 5) is missing, and a new band is now present at 1398 cm^{-1}. The peak absorbance of the C=C band at 964 cm^{-1} is also higher than that normally observed (Figure 1), and an unusually long progression of well-resolved twist and wag methylene bands is visible between 1072 and 1336 cm^{-1}. All these features are indicative of a highly ordered and rigid monolayer structure, possibly displaying long-range crystalline order in the layer plane.[2,8,9]

The initial ordered structure of the acid salt monolayer in Figure 2 appears to be preserved upon treatment with aqueous permanganate, as the two curves, taken before and after the exposure to $KMnO_4$, are virtually identical. Additional evidence, indicating only minor alterations in the orientation of the paraffinic chains of this monolayer upon treatment with aqueous permanganate, is furnished by ATR measurements with linearly polarized radiation.

The dichroic ratios[2] ($A_\perp/A_\parallel$) in Table I, measured for a number of representative films of brassidic acid on ZnSe, are indicative of preferential perpendicular orientation (on the layer plane) of the chains in the complete monolayers.[2] Significantly lower dichroic ratios were obtained for the "unusual" monolayer as compared with those of "normal" ones, particularly in the 2919-cm^{-1} band (see also ref 2), which would suggest a tilted chain arrangement in the former. The normal SA monolayer in Table I also displays somewhat better perpendicular chain orientation than the LB monolayer.[10] As expected, the incomplete SA mon-

Table I. Polarized ATR Measurements of Some Representative (t-13)C_{22}(u) Monolayers on ZnSe: Dichroic Ratios ($A_\perp/A_\parallel$) at the Peak Absorbance of the Antisymmetric (ca. 2919 cm^{-1}) and Symmetric (ca. 2850 cm^{-1}) Methylene Stretching Bands[a]

film[b] (% of complete monolayer)	$A_\perp/A_\parallel$					
	ca. 2919 cm^{-1}			ca. 2850 cm^{-1}		
	initial[c]	H_2O[c]	$KMnO_4$[c]	initial[c]	H_2O[c]	$KMnO_4$[c]
L (100%)	1.102		1.002	1.123		0.966
A (100%)	1.186	1.160	1.060	1.222	1.166	1.080
A[e] (100%)[d]	1.046	1.064	1.066	1.139	1.194	1.172
A (73%)	0.980	1.000	1.020	1.000	1.030	1.030

[a] The theoretical dichroic ratios expected for perfect perpendicular and random orientation of the paraffinic chains are 1.237 and 0.970, respectively.[2] [b] L stands for LB and A for SA (adsorbed) monolayers. [c] Dichroic ratios were determined before (initial) and after a 3-min exposure to pure H_2O and then to the $KMnO_4$ solution. [d] The "unusual" brassidic acid monolayer of Figure 2.

(8) Gun, J.; Iscovici, R.; Sagiv, J. *J. Colloid Interface Sci.* 1984, *101*, 201.

(9) It should be noted that the spectra in Figure 2 differ from those of crystalline LB multilayer films of the Cd^{2+} salt of brassidic acid on Ge.[2] The doublets centered at 1467 and 1428 cm^{-1} in the multilayer spectra (Figure 19 in ref 2) are characteristic of a multilayer crystal structure with two molecules per unit cell. No such band splittings are observed in Figure 2, which would suggest the existence of a distinct monolayer crystalline structure with only one molecule per unit cell. The present spectral data are first indications for possible long-range crystalline order in self-assembled monolayer films.[2,8]

(10) A quantitative evaluation of the chain orientation from polarized ATR measurements, as those presently reported, is subject to considerable uncertainty due to the low sensitivity of such measurements to orientational effects and the relatively large experimental error associated with the determination of the dichroic ratios.[2]

(11) A similar peak at 1745 cm^{-1} was previously observed following treatment of a saturated acid salt monolayer (C_{20}/ZnSe) with aqueous KOH.[1] This band may represent a base line artifact originating in residual ZnSe contributions.[1,12]

olayer (ca. 73% surface coverage) is less ordered than each of the complete ones (lowest dichroic ratios in Table I).

The significant drop in the dichroic ratios of the LB and normal SA monolayers following the water and permanganate treatments suggests significant deviations from the initial orientation or partial randomization of the paraffinic chains in these films. An opposite trend, i.e., a small increase in the dichroic ratios, is observed for the unusual and incomplete monolayers, suggesting that only minor orientational changes, possibly leading to slightly improved perpendicular orientation of the chains, occur in these films upon treatments with water and permanganate. This improvement in the chain orientation, particularly in the incomplete monolayer, may arise from a hydrophobic effect inducing chain association in the water-treated films.

The main results of the experiments with dense (complete) monolayers exposed to $KMnO_4$ for 3 min are summarized in Figure 3. Figure 3 lists both SA and previously investigated[1] LB monolayers, arranged in the order (from left to right) of increasing susceptibility to $KMnO_4$. The first two columns include monolayers of the saturated surfactants, OTS and C_{20}, and the last one an acid salt monolayer with exposed outer double bonds.[1]

A point of interest in Figure 3 is the significantly lower penetrability of the SA unsaturated acid salt monolayers (columns 4a, 4b) as compared with their LB counterparts (columns 5a, 5b). The drop in the CH_2 absorbance of the LB monolayers in columns 5a and 5b of Figure 3 points to the structural damage produced to these films by the permanganate treatment. No such changes are observed in the spectra of the saturated (C_{20}) LB monolayer (column 2). The latter monolayer also exhibits invariant BCH and HD contact angles, although its complete wetting by water following the $KMnO_4$ treatment is similar to that of the unsaturated acid salt monolayers.

The superior behavior of the silane monolayers (columns 1 and 3 of Figure 3) is evident from the invariance of both their IR spectra and contact angles upon exposure to $KMnO_4$.

Exposure to $KMnO_4$ for Times Longer Than 3 min. Figure 4 summarized IR and contact angle data obtained during exposure of complete SA monolayers of brassidic acid and the corresponding unsaturated silane to aqueous permanganate for periods of time varying between 3–60 and 90 min, respectively.

The gradual disappearance of the double bond band at 964 cm^{-1} (reaching $\Delta n \approx 0.87$ at 60 min of exposure) and the concomitant monotonic drop in the respective BCH and HD contact angles (the H_2O contact angle falls to zero already at 3 min of exposure) provide unequivocal evidence for the slow oxidation of the double bonds in the acid salt monolayer. The oxidation process does not involve cleavage of the paraffinic chains[12] or depletion of the film, as indicated by the invariance of the CH_2 band absorbance ($\Delta n \approx 0$ for CH_2).

In contradistinction to the acid salt monolayer, no significant oxidation of the double bonds could be detected in the silane monolayer, up to a total exposure time of 90 min. The contact angles are also seen to be stable, except for a slight decrease that might be due to eventual adsorption of trace impurities on the exposed film surface.

It is clear from these results that only covalently bonded silane monolayers maintain their barrier efficiency over long times of exposure (hours) to the penetrating reagent, although densely packed acid salt monolayers may show

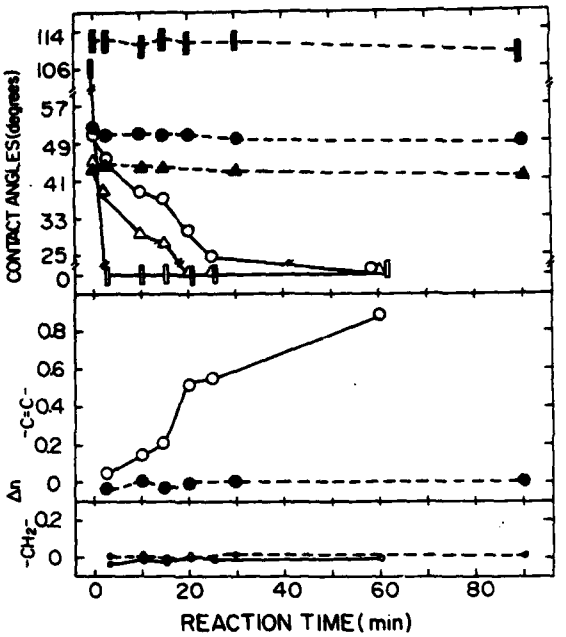

Figure 4. Spectral and contact angle changes measured upon exposure of complete monolayers of A,(t-13)C_{22}(u)/ZnSe (open points) and A,(t-13)C_{22}(u)Si/ZnSe (solid points) to the $KMnO_4$ solution, for the indicated periods of time. Lower part: Δn defines the observed decrease in the IR absorbance relative to the respective absorbance measured before exposure to $KMnO_4$, with $-CH_2-$ and $-C{=}C-$ representing ATR peak absorbances at ca. 2919 and 964 cm^{-1}, respectively. Upper part: Advancing contact angles. ● and ○, bicyclohexyl (BCH); ▲ and △, n-hexadecane (HD); ■ and □, H_2O. The size of the displayed data points indicates the estimated reproducibility of the IR and contact angle measurements.

similar behavior over times of the order of several minutes.

IR spectra corresponding to part of the data points in Figure 4 are given in Figures 5 and 6. For comparison, spectra of incomplete monolayers of the respective compounds, taken before and after 3 min-exposure to the permanganate solution, are also reproduced in the upper parts of Figures 5 and 6.

The gradual disappearance of the double bond band at 964 cm^{-1} and a slight broadening of the CH_2 bands around 2900 cm^{-1}, pointing to partial disordering of the paraffin chains, are clearly seen in the spectra of the complete acid salt monolayer (curves a–d in Figure 5). The 964-cm^{-1} band of the incomplete acid salt monolayer disappears almost quantitatively within a 3-min exposure to $KMnO_4$ (upper curves in Figure 5).

In addition, major changes are also visible in the 1500–1750-cm^{-1} spectral region in Figure 5. There is a drop in the peak absorbance of the carboxylate band at 1544 cm^{-1} with the appearance of a new peak at 1556 cm^{-1}, which becomes dominant after a 60-min exposure to $KMnO_4$ (curve d). A strong, broad band around 1618 cm^{-1} is visible in the curves recorded after 15, 20, and 25 min of exposure to $KMnO_4$ (curve c). Finally, a new band centered at 1745 cm^{-1} is present in curve d[11] of Figure 5.

The peak at 1556 cm^{-1} may be ascribed to the formation of potassium carboxylate species.[1,13] The origin of the

(12) Maoz, R.; Sagiv, J. *Thin Solid Films* **1986**, *132*, 135.

(13) Carboxylate peaks at 1558 cm^{-1} were observed in the IR spectra of bulk potassium stearate as well as of a surface-immobilized potassium carboxylate species produced by the organic $KMnO_4$ oxidation of (t-13)C_{22}(u)Si/ZnSe.[12]

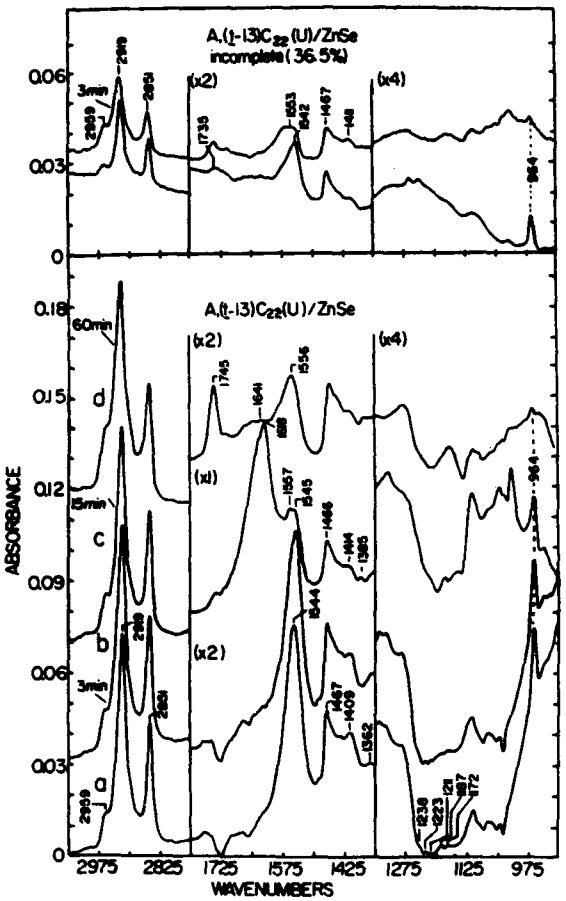

Figure 5. Lower part: ATR infrared spectra of the brassidic acid monolayer of Figure 4 corresponding to (a) 0, (b) 3, (c) 15, and (d) 60 min of exposure to the $KMnO_4$ solution. Upper part: Spectra of the incomplete brassidic acid monolayer of Figure 1, first column, taken before (lower curve) and following a 3-min exposure to the $KMnO_4$ solution.

other spectral features in this region is not well understood; however, most of them appear to originate in interactions of the $KMnO_4$ solution with the ZnSe surface rather than with the monolayer double bonds. Thus, the strong 1618-cm^{-1} band in curve c of Figure 5 may not be attributed to double bond oxidation products, as ca. 80% of the double bonds are still intact at this stage of the reaction (Figure 4; see also the C=C peak at 964 cm^{-1} in curve c of Figure 5). Furthermore, broad spectral features of variable intensity and distribution are found between 1500 and 1750 cm^{-1} in all spectra of incomplete acid salt monolayers following their treatment with aqueous permanganate (see spectra of the incomplete monolayer in Figure 5) as well as in the spectrum of an uncoated ZnSe plate after being exposed to an identical $KMnO_4$ treatment. No correlations could be established between the intensity and spectral distribution of these bands and the density of reactive double bonds in the respective films.

Except for the drop in the 964-cm^{-1} (C=C) absorbance of the incomplete monolayer, practically no other changes are observed in the spectra of the silane monolayers following their treatment with permanganate (Figure 6). The CH_2 and CH_3 bands around 2900 cm^{-1} are invariant in both the complete and incomplete silane monolayers, like the broad bands around 1102 and 1033 cm^{-1}, ascribable to

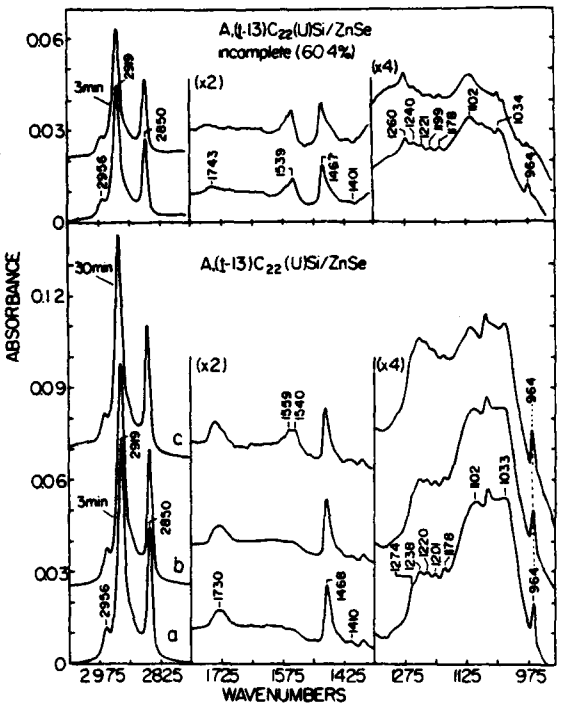

Figure 6. Lower part: ATR infrared spectra of the unsaturated silane monolayer of Figure 4 corresponding to (a) 0, (b) 3, and (c) 30 min of exposure to the $KMnO_4$ solution. A curve similar to c was recorded after 90 min of exposure to $KMnO_4$. Upper part: Spectra of the incomplete silane monolayer of Figure 1 taken before (lower curve) and following a 3-min exposure to the $KMnO_4$ solution.

Si–O–Si and Si–O–surface bonds,[2,14] and the progression of weak bands between 1178 and 1274 cm^{-1}, characteristic of paraffinic chains in the extended all-*trans* conformation.[2,8,14] These observations provide evidence for the structural stability of the silane monolayers under exposure to aqueous $KMnO_4$. The presence of the band progression between 1178 and 1274 cm^{-1} also in the incomplete silane monolayer (Figure 6, upper part) is indicative of a partially ordered islandlike molecular distribution in this film.[15,16]

The assignment of the weak features visible in all curves in Figure 6 between 1500 and 1750 cm^{-1} is more problematic. The band around ca. 1730 cm^{-1} was previously ascribed to a residual ZnSe contribution.[12] However, a weak band centered at about the same wavelength, in addition to some broad features around 1575 cm^{-1}, has also been identified in the spectra of bulk (*t*-13)C_{22}(u)Si as well as of its bromide and alcohol precursors. These features might originate in some residual ester and carboxylate impurities carried along with the (*t*-13)C_{22}(u)Si material (see the Experimental Section, above). The presence of these impurities does not appear to have any measurable effect on the penetrability or the stability of the respective silane monolayers.

Summary and Conclusions

Conclusive experimental evidence has been provided demonstrating the dependence of monolayer penetrability

(14) Sabatani, E.; Rubinstein, I.; Maoz, R.; Sagiv, J. *J. Electroanal. Chem.* **1987**, *219*, 365.
(15) Garoff, S.; Hall, R. B.; Deckman, H. W.; Alvarez, M. S. *Proc. Electrochem. Soc.* **1986**, *86-8*, 112.
(16) Cohen, S.; Naaman, R.; Sagiv, J. *J. Phys. Chem.* **1986**, *90*, 3054.

on its molecular packing density and structural rigidity. Densely packed monolayers of long-chain amphiphiles could be produced on solids by spontaneous self-assembly from solution, behaving as efficient impenetrable barriers with respect to the passage of the aqueous permanganate ion. Permeation of ionic species from aqueous media through such solid-supported monolayers is demonstrated to be a defect-controlled process.[17] The barrier efficiency of highly ordered monolayers of this type is, ultimately, determined by their long-term structural stability, which is, in turn, a function of their specific mode of binding to the solid surface. Thus, the performance of covalently bonded monolayers (silanes) is remarkably superior to that of analogous ionic films (acid salts), the differences between the two types of films correlating with former's structural stability versus the latter's deterioration upon prolonged contact with the solution of the penetrating species.

Complete monolayers of unsaturated long-chain acid salts prepared for the present study by spontaneous self-assembly (SA) from solution were found to be less penetrable than their LB counterparts. This is a consequence of the higher degree of perfection and structural stability of the SA monolayers.

Taken together, the present and previously reported[1] spectral and wettability data suggest a rather intricate mechanism for the wetting of acid salt films by water and aqueous $KMnO_4$. The wetting process obviously involves both penetration through voids across the film and lateral diffusion of the wetting liquid in the monolayer–substrate interface. This requires sufficient surface mobility of the film-forming molecules. However, as demonstrated by the IR data, wetting of a film-covered surface by the $KMnO_4$ solution is not necessarily accompanied by detectable alterations of the initial film structure or by significant oxidation of intralayer double bonds. It thus appears that the passage of the wetting liquid across the film occurs through a limited number of pinhole defects, while its lateral diffusion in the film–substrate interface is mediated by the coupled motion of relatively large numbers of film-forming molecules. Electrostatic factors might also play a role in the wetting of the ionic films. Finally, the nonwettable character of the silane monolayers, including the incomplete ones, is, obviously, a consequence of their surface immobility, resulting from intralayer and layer-to-surface covalent bonding.

The present results emphasize the key roles of film structural stability, besides its structural perfection, in the engineering of efficient monolayer barriers.[17] The usefulness of "penetration-controlled" reactions, in conjunction with wettability observations, as indicators of the penetrability of monolayer films is demonstrated.

Acknowledgment. We gratefully acknowledge the support of this work by grants from the Schmidt Fund and the European Research Office of the U.S. Army.

Registry No. MnO_4^-, 14333-13-2; $KMnO_4$, 7722-64-7; (*t*-13)C_{22}(u)Si, 103941-63-5; ZnSe, 1315-09-9; (*t*-13)C_{22}(u), 506-33-2; C_{20}, 14923-81-0; OTS, 112-04-9; C_{18}, Cd salt, 2223-93-0.

(17) These conclusions are confirmed by recent results of an electrochemical study of the water permeation through organized SA monolayers on gold electrodes.[14]

Thermally Induced Disorder in Organized Organic Monolayers on Solid Substrates

Sidney R. Cohen, Ron Naaman,* and Jacob Sagiv*

Department of Isotope Research, The Weizmann Institute of Science, Rehovot 76100, Israel
(Received: March 5, 1986)

Observation of melting in solid-supported organic monolayers of long-chain amphiphiles using FTIR spectroscopy and wettability measurements is reported. Three different substrate–monolayer interactions—covalent, ionic, and physical bonds—were investigated. Both Langmuir–Blodgett and self-assembly techniques were used. With the exception of covalently bound octadecyltrichlorosilane, all species underwent a large, irreversible randomization at around 110 °C. Although heating affected slight disorientation of the chains in OTS, no sharp phase transition characteristic of a melting process could be detected for temperatures up to 140 °C. The importance of head group immobilization in the thermal stabilization of monolayer structures is demonstrated.

Introduction

Ordered monolayers of long-chain organic amphiphiles are of interest theoretically, for potential applications, and because of their similarity to biological membranes. The chains can be attached to hydrophilic or hydrophobic substrates through the polar head or the alkyl tail. There exist many variations in the polar head groups and the type of bond made to the substrate. The effect of these variations on monolayer structural stability has not been thoroughly studied. The effect of temperature on such films is of particular interest. Thermally induced phase transitions in solid-supported monolayer films have been detected by changes in the friction coefficient[1] and observed by electron diffraction[2] and Penning ionization spectroscopy.[3] In addition, melting of a seven-layer built-up film has recently been reported by using FTIR (Fourier transform infrared) spectroscopy.[4] The literature lacks information on the effect of the substrate–mon-

(1) Bowden, F. P.; Tabor, D. *The Friction and Lubrication of Solids*; Clarendon: Oxford, 1950; Chapter X.
(2) Chapman, J. A.; Tabor, D. *Proc. R. Soc. London, A* **1957**, *242*, 96.
(3) Harada, Y.; Ozaki, H.; Ohno, K. *Surf. Sci.* **1984**, *147*, 356–60.
(4) Nuzzo, C.; Rabolt, J. F.; Swalen, J. D. *J. Chem. Phys.* **1985**, *82*, 2136.

0022-3654/86/2090-3054$01.50/0

TABLE I: Advancing Contact Angles (deg) Measured before (Initial) and after Heating and Cooling to Ambient Temperature (Final)[a]

	initial			final		
film type	H_2O	HD	BCH	H_2O	HD	BCH
trilayer	115 ± 2	47 ± 1	53 ± 1	109 ± 2	42 ± 1	48 ± 1
C_{20} (LB)	108 ± 2	43 ± 1	49 ± 1	100 ± 2	32 ± 2	41 ± 2
C_{20} (SA)	105 ± 2	45 ± 1	51 ± 1	97 ± 2	30 ± 2	39 ± 2
OTS (SA)	113 ± 2	46 ± 1	51 ± 1	113 ± 2	46 ± 1	51 ± 1
OTS (SA, P[b])	102 ± 2	42 ± 1	42 ± 1	102 ± 2	42 ± 1	42 ± 1

[a] Test liquids used were H_2O, hexadecane (HD), and bicyclohexyl (BCH). [b] Partial (ca. 60% surface coverage).

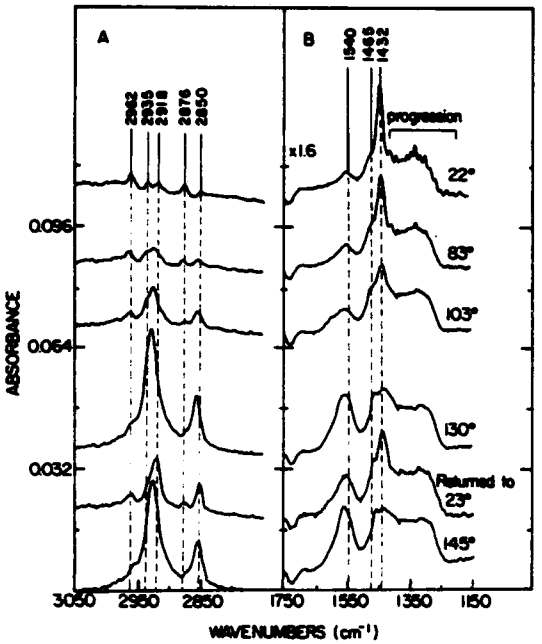

Figure 1. Spectra of the cadmium(II) arachidate bilayer on OTS obtained by mathematical subtraction of OTS/Al spectra from those of the cadmium(II) arachidate/cadmium(II) arachidate/OTS/Al trilayer. Effect of temperature (indicated on spectra) in the two spectral regions is seen. Approximate positions of the observed peaks are as follows: (A) CH_3 ν_a (2962 cm^{-1}) and ν_s (2935 and 2876 cm^{-1}); CH_2 ν_a (2920 cm^{-1}) and ν_s (2850 cm^{-1}); (B) CH_2 δ (1465 cm^{-1}), COO^- ν_s (1432 cm^{-1}), and ν_a (1540 cm^{-1}); progression (1150–1450 cm^{-1}).

olayer bonding in such phase transitions. In this Letter, we wish to present preliminary results of an FTIR and wettability study on the effect of temperature on the structure of organized organic monolayers of long-chain amphiphiles. Emphasis has been placed on the influence of monolayer–substrate and intralayer interactions.[5]

The utility of FTIR spectroscopy, in the reflection–absorption mode, for detecting orientational changes in monolayers on metal mirrors has been well documented.[4,6,7] Because only those vibrational modes with components perpendicular to the surface are excited, any changes in a long chain's orientation relative to the substrate can be easily observed. When an alkyl tail is oriented normal to the surface, the methylene stretching modes are parallel to it and thus cannot be detected. As the orientation is lost, these modes gain a component in the perpendicular direction and their absorption increases dramatically.

Contact angle measurements can complement the FTIR results. For long-chained amphiphilic monolayers exposing CH_3 groups, disorientation results in contact angles significantly lower than

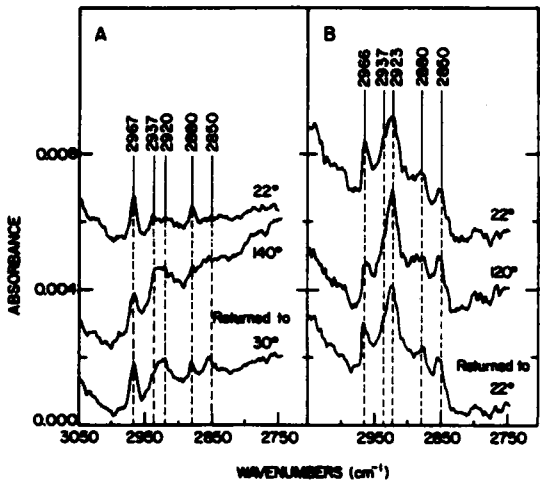

Figure 2. Spectral changes in the C–H stretch region of OTS/Al upon heating and recooling, showing complete (A) and partial (B) monolayers (see text). Peaks are identified in Figure 1 caption.

the values characteristic of well-oriented layers.[6,8] The wettability of monolayer-covered surfaces may thus be used as a valuable tool in the detection of structural transformations in such films.

Experimental Section

Sample preparation was by techniques previously described.[6,8] Briefly, the mirror substrates were formed by vacuum evaporation (Edwards evaporator) of the pure metal onto specially cleaned glass microscopic slides. Self-assembled (SA) monolayers of *n*-octadecyltrichlorosilane (OTS) and arachidic acid (C_{20}) were prepared on Al by adsorption from solutions in bicyclohexyl. Langmuir–Blodgett (LB) monolayers of cadmium(II) arachidate were transferred to Al and Ag substrates by using standard techniques. A trilayer film was also prepared by building up two LB monolayers of cadmium(II) arachidate on top of a SA OTS monolayer. Thus, the alkyl tail of the first LB layer faces the alkyl tail of the OTS, and the alkyl tail of the second LB layer points outward, leaving the polar head groups of the two chains situated in the center of the LB bilayer.

Spectral measurements were made with a Nicolet MX-1 FTIR spectrometer, as described previously.[6] A constant purge of cleaned nitrogen prevented IR-absorbing contaminants from entering the spectrometer and lessened any probability of oxidation at the higher temperatures. A polarizer was used to select the parallel to the plane of incidence component. Signals were averaged for 20 min, 640 scans, and are shown here after subtracting the appropriate reference (blank mirrors + polarizer). The sample mirrors were backed by resistively heated copper blocks. Temperature was monitored with a thermocouple.

Contact angle measurements were performed by placing drops of the respective liquids on the slides under ambient conditions and measuring the contact angle with a goniometer.[8] The readings were made both before heating and after heating to the maximum temperature used in the FTIR measurements and then recooling.

(5) Cohen, S.; Naaman, R.; Sagiv, J. In *Proceedings of the 2nd International Conference on Langmuir–Blodgett Films*, Schenectady, NY, July 1–4, 1985; *Thin Solid Films*, in press.
(6) Gun, J.; Iscovici, R.; Sagiv, J. *J. Colloid Interface Sci.* **1984**, *101*, 201.
(7) Allara, D. L.; Nuzzo, R. G. *Langmuir* **1985**, *1*, 52.
(8) Maoz, R.; Sagiv, J. *J. Colloid Interface Sci.* **1984**, *100*, 465.

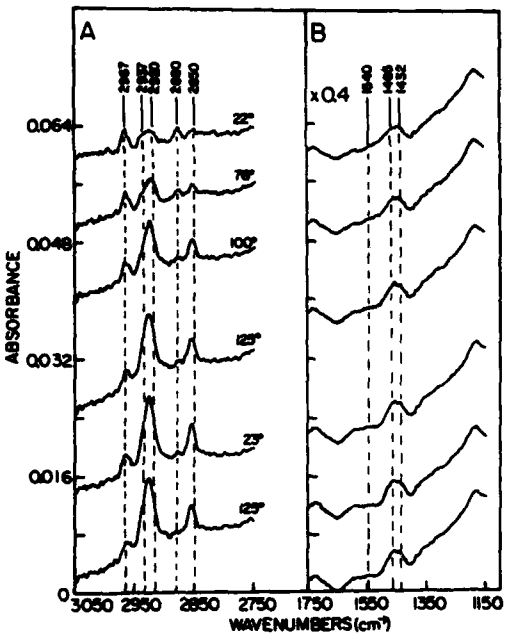

Figure 3. Spectral changes in cadmium(II) arachidate monolayer on aluminum upon heating and recooling. For description of peak identities, see Figure 1 caption.

The results are displayed in Table I for the monolayers on Al substrates.

Results and Discussion

Representative spectra of two extreme cases—cadmium(II) arachidate bilayer on OTS and OTS monolayer—are shown in Figures 1 and 2, respectively. Contact angles are displayed in Table I. The cadmium(II) arachidate bilayer in the trilayer sample represents the weakest film-to-substrate bonding: van der Waals attraction between the hydrocarbon tails of the respective (OTS and cadmium(II) arachidate) chains. The results (Figure 1) are similar to those obtained for the seven-layer cadmium(II) arachidate LB film on Ag.[4] The progression between 1150 and 1450 cm^{-1}, characteristic of fully extended chains, as well as the COO^- stretching at 1431 and 1540 cm^{-1} and the CH stretching bands around 2900 cm^{-1}, changes moderately up to ca. 100 °C. Between 100 and 130 °C, a more abrupt change in the respective band intensities occurs, indicative of randomization of both the hydrocarbon chains and the COO^- head groups. Significant reversibility in the orientation of the cadmium(II) arachidate bilayer is observed upon recooling (see also Table I).

The C_{20} monolayers, both SA and LB, represent an intermediate case of bonding. By using LB monolayers of cadmium(II) arachidate on two different substrates, Al and Ag, and additionally a C_{20} SA arachidic acid monolayer on Al, we prepared three monolayer types with minor variations between them. The self-assembled C_{20} monolayer is either physisorbed or ionically bound.[6,7] The cadmium salt, although transferred as a neutral species, carries potential for ionic bonding.[9] LB monolayers of the salt were transferred to both aluminum and silver substrates in order to distinguish between varying substrate influences. Although the COO^- stretch spectral region varied among these different monolayers, the main features of the randomization process observed in the C–H region were essentially the same. The cadmium(II) arachidate monolayer on aluminum is shown here in Figure 3 as a representative example. The COO^- stretch region in Figure 3B shows broad features, presumably due to the interaction of the head groups with the Al surface, as discussed in ref 6. No significant variations are observed in this spectral region up to 125 °C, suggesting that randomization of the paraffinic chains is not accompanied by significant changes in the orientation of the head groups. In this case reversibility is observed neither in the spectral features nor in the contact angles (Table I) upon recooling.

The covalent bonding of OTS represents the strongest film–substrate and intralayer interactions.[6,8] Both complete and less-ordered partial (ca. 60% coverage) monolayers were prepared. The partial monolayer appears to have an orientation only slightly worse than that of the full monolayer (Figure 2). This supports evidence that incomplete monolayers form in partially ordered islands rather than as a sparse, homogeneous layer.[10] Spectral changes upon heating are far less dramatic for both the complete and partial OTS monolayers, no discontinuities ascribable to significant disorientation being detected. In accord with the spectral data, the contact angles were invariant.

In summary, several effects were observed upon heating and recooling of the films. The first effect, below certain critical temperatures, is gradual disorder—largely reversible upon recooling as in multilayer assemblies.[4] This probably corresponds to thermal excitation of vibrations. For the covalently bound OTS monolayers this effect was very weak and the only observed change up to 140 °C. The second effect, identified in the C_{20} monolayers above ca. 100 °C by randomization of the paraffinic chains, is indicative of complete collapse of the monolayer structure. This may be ascribed to a melting phase transition.[4] The C_{20} bilayer on OTS also undergoes this melting transition above ca. 100 °C. However, it displays significant structural reversibility upon recooling from the melted state (130 °C), probably induced by the stable OTS monolayer.

Melting of an oriented and densely packed array of long-chain amphiphiles implies a finite volume expansion, which would require some degree of mobility of the polar head groups. Immobilization of the head groups by covalent intralayer and layer-to-substrate bonding, as in the OTS/Al monolayers, may thus be expected to prevent melting of such films. The higher thermal stability presently reported for the OTS monolayers supports this notion. Further work is now in progress in an attempt to elucidate the role of head group immobilization in the thermal stabilization of monolayer structures.

Acknowledgment. We gratefully acknowledge the support of the U.S.–Israel Binational Foundation and partial support by a grant from the European Research Office of the U.S. Army.

(9) Barraud, A.; Rusaudel-Teixier, A.; Rosilio, C. *Ann. Chim.* **1975**, *10*, 195.
(10) Garoff, S.; Hall, R. B.; Deckman, H. W.; Alvarez, M. S. *Proc.—Electrochem. Soc.* **1985**, *85–6*, 112.

Thin Solid Films, *132* (1985) 153–162
PREPARATION AND CHARACTERIZATION

COVERAGE OF Si SUBSTRATES BY SELF-ASSEMBLING MONOLAYERS AND MULTILAYERS AS MEASURED BY IR, WETTABILITY AND X-RAY DIFFRACTION*

M. POMERANTZ† AND A. SEGMÜLLER
IBM Research, Yorktown Heights, NY 10598 (U.S.A.)
L. NETZER AND J. SAGIV
Isotope Department, The Weizmann Institute of Science, 76100 Rehovot (Israel)
(Received June 11, 1985; accepted July 4, 1985)

A study is presented of the amount of coverage of Si substrates by monolayers and multilayers of molecules deposited by the self-assembling technique. Self-assembly was achieved by chemisorption of silane compounds from solutions, on to smooth n-Si substrates. The coverage was examined by IR absorption, wettability and X-ray diffraction. For n-octadecyltrichlorosilane (OTS), prepared as a single layer, the coverage appears to be close to 100%. For a monolayer of a silane–methyl ester, containing 24 carbons (C_{24}SME), the coverage is at least 90%. A film comprising three layers of C_{24}SME molecules could be modeled by a mixture of two- and three-layer regions.

1. INTRODUCTION

Spontaneous adsorption (chemisorption) of appropriate amphiphiles from organic solution has been shown to allow the formation of ordered monolayer films on a variety of polar solid surfaces[1–3]. Recently, this monolayer self-assembly process, combined with a chemical activation procedure serving as an externally controllable trigger, was used to construct planned multilayer structures similar, in some respects, to solid-supported Langmuir–Blodgett (LB) built-up films[4]. An important difference between the two types of films, aside from their fundamentally different mode of assembly, is related to the fact that the self-assembling multilayer structures are obtained as covalently bonded (both intra- and interlayer) networks of remarkable physical and chemical stability. The molecular arrangement and final overall architecture of such systems may thus be expected to reflect the interplay between the various weak as well as the strong forces operating during the spontaneous formation of each monolayer on the solid substrate. Sterical and electrostatic factors should play important roles in the process.

The present paper addresses the question of whether the coverage of the

* Paper presented at the Second International Conference on Langmuir–Blodgett Films, Schenectady, NY, U.S.A., July 1–4, 1985.
† Address correspondence to this author.

0040-6090/85/$3.30

substrate by such a self-organized monolayer is complete. For this purpose we have applied X-ray diffraction methods[5], complemented by quantitative Fourier-transform IR attenuated total reflection (FTIR–ATR) and wettability measurements. The substrates chosen were Si because polished wafers that are excellent for X-ray measurements are readily available, and the ATR plates were also of Si.

The adsorbed molecules chosen were n-octadecyltrichlorosilane (OTS, CH_3—$(CH_2)_{17}$—$SiCl_3$) and a long-chain silane–methyl ester (C_{24}SME, CH_3—O—CO—$(CH_2)_{22}$—$SiCl_3$), and of a trilayer film of the latter. OTS is, to date, the amphiphile for which the largest body of data is available regarding the formation of covalently bonded self-assembling monolayers[2,6]. Evidence derived by a number of different techniques[2,6] points to the structure of complete OTS monolayers as consisting of arrays of fully extended and densely packed hydrocarbon chains, with essentially perpendicular orientation of their axes on the layer plane (mean deviation of the chain axes within less than 10° from the surface normal). C_{24}SME is representative of a new series of bifunctional silane–ester surfactants, recently synthesized for the purpose of studying the self-assembling properties of long-chain amphiphiles containing a relatively polar and bulky function at different positions along their chains[7]. OTS can form only monolayers, but the ester group of C_{24}SME can be chemically activated and used to form multilayers.

2. PREPARATION AND CHARACTERIZATION OF THE FILMS

The general methods employed in the preparation of self-assembling monolayers and in the ATR and contact angle measurements were described before[2]. Solutions of the respective amphiphiles (2.0×10^{-3} M) in 80% bicyclohexyl (BCH) + 12% CCl_4 + 8% $CHCl_3$ were used for the adsorption of the present films. All materials, except C_{24}SME, were identical to those employed in previous work[2]. The synthesis of C_{24}SME is described elsewhere[7]. The low oleophobicity of C_{24}SME monolayers (see contact angles in Table I) made difficult the dry retraction of such films from the adsorption solution. Liquid retained on top of the monolayer-coated substrates was removed by Soxhlet extraction with hot chloroform. In order to ensure formation of solvent-free, complete monolayers, all presently reported samples (both C_{24}SME and OTS) were exposed to several adsorption (10 min)–hot $CHCl_3$ extraction (20 min) cycles, until invariant maximal contact angles and IR signals were reached[6].

Multilayer films were constructed via a two-step chemical procedure involving the conversion of the ester functions of each layer to terminal hydroxyls (the chemical activation step[4]), followed by covalent coupling of the silane functions of the subsequent layer to the exposed hydroxyls of the underlying one (the chemisorption step[4]). The ester carbonyls were reduced to terminal hydroxyls by immersing the film-covered substrates for 15–30 min in a saturated solution of $LiAlH_4$ in dry diethyl ether at ambient temperature, followed by rinses with distilled water, concentrated HCl (30%), distilled water, and final Soxhlet extraction with hot $CHCl_3$ (20 min).

Polished n-type Si wafers were employed as film substrates in the X-ray diffraction experiments, while the IR data were collected from a separate set of films

prepared by an analogous experimental procedure on a silicon ATR plate. A qualitative comparison of the two sets of samples is possible through their contact angles[2].

Figures 1 and 2 depict ATR–IR spectra recorded after each step in the construction of a C_{24}SME/C_{24}SME/Si bilayer and an OTS/C_{24}SME/Si bilayer respectively. The spectrum of an OTS/Si monolayer is also shown in Fig. 2. The corresponding contact angles measured for n-hexadecane (HD), bicyclohexyl (BCH) and H_2O are listed in Table I. Inspection of the IR spectra and the respective contact angle data leads to the following conclusions regarding the composition and structure of the films.

1. The intensities of the (H—C—H) stretching bands around 2900 cm^{-1} in the C_{24}SME/Si and OTS/Si monolayers (compare Figs. 1(a), 2(a) and 2(e)) are proportional to the number of (—CH_2—) groups in the chains of the respective compounds (22/17), suggesting that similar molecular packing densities (areas/molecule) are reached in both films[2]. This estimation is subject to an uncertainty of the order of about 5% of a complete C_{24}SME monolayer, associated with the sample-to-sample data spreading characteristic of the present ATR measurements[2,6]. A comparison of the contact angles measured on complete C_{24}SME and OTS monolayers (Table I) is not conclusive in this respect, as the proximity of the relatively polar ester function to the outer film surface results in significantly lower contact angles on the former, irrespective of its packing density and the orientation of the chains in the film[2].

2. The quantitative conversion of the ester function to a terminal hydroxyl is evident from both the disappearance of the ester carbonyl band at 1742 cm^{-1} (Fig. 1(b)) and the contact angles measured on the respective reduced films (Table I)[4]. The ester reduction is seen to be accompanied by a certain depletion of material (about 20%) from the C_{24}SME monolayer shown in Fig. 1, while the corresponding monolayer in Fig. 2 is not affected by the $LiAlH_4$ treatment. In general, silane monolayers on Si were found to be stable under exposure to $LiAlH_4$ in ether[7]. However, as the present examples demonstrate, molecules less tightly anchored to the surface may be occasionally removed under these conditions. Such partial depletion of the film is easily detected by IR, but not by the contact angle measurements (see Table I).

3. The second adsorbed layers in both the C_{24}SME/C_{24}SME/Si and OTS/C_{24}SME/Si bilayer films appear to be identical to monolayers of the respective compounds adsorbed directly on the bare silicon substrate. This is indicated by their IR spectra (compare Figs. 1(a) with 1(d) and 2(d) with 2(e)) as well as by the respective contact angle values (Table I). It is further apparent from Fig. 1 that part of the C_{24}SME material adsorbed as a second layer (about 12%) is, in fact, used to refill the depleted first layer, so that the final bilayer film is actually composed of two almost complete monolayers.

A comparison of the contact angles measured on the films prepared on Si wafers for the X-ray diffraction experiments with those measured on the films used in the IR experiments allows the following inferences to be made, in a general, qualitative way, about the structure of the former.

1. The contact angles measured on the OTS/Si-wafer monolayers are excep-

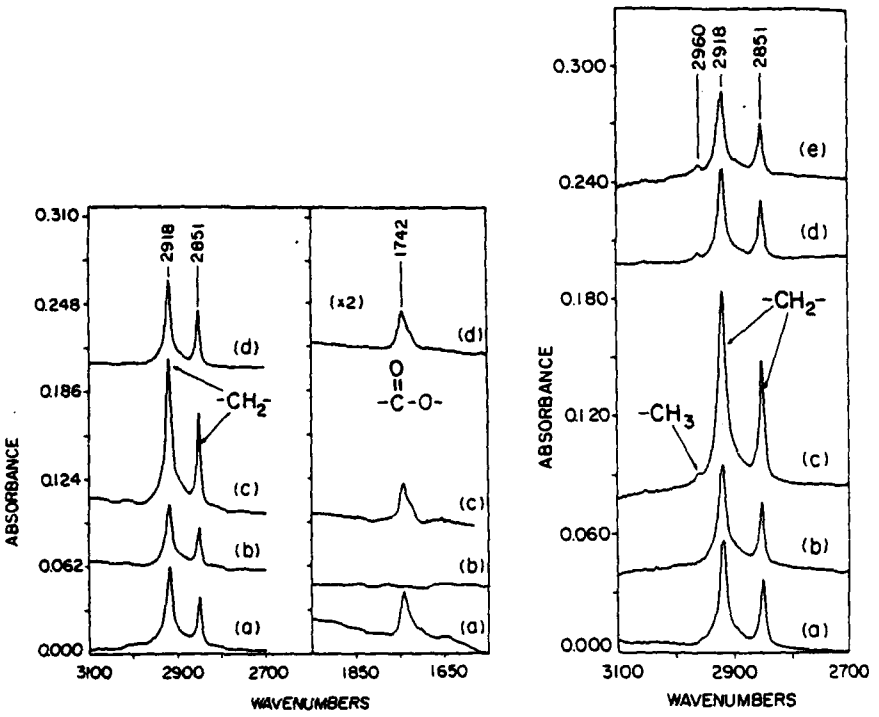

Fig. 1. ATR-IR spectra of films on silicon plate (45°, 17 reflections), recorded with a Nicolet MX-1 FTIR spectrophotometer, at a resolution of 4 cm^{-1}: (a) C_{24}SME/Si monolayer; (b) C_{24}SME/Si reduced monolayer (after treatment with ethereal $LiAlH_4$); (c) C_{24}SME/C_{24}SME/Si bilayer; (d) C_{24}SME second monolayer, subtraction (c) − (b).

Fig. 2. Spectra as in Fig. 1, showing only the (—CH_2—) stretching bands around 2900 cm^{-1}, for: (a) C_{24}SME/Si monolayer; (b) C_{24}SME/Si reduced monolayer; (c) OTS/C_{24}SME/Si bilayer; (d) OTS second monolayer, subtraction (c) − (b); (e) OTS/Si monolayer.

TABLE I

CONTACT ANGLES ON MONOLAYER AND BILAYER FILMS BUILT ON SILICON ATR PLATE AND ON GLASS SLIDES

Film	*Advancing contact angle*[a]			*IR spectrum (Fig.)*
	HD	*BCH*	*H_2O*	
C_{24}SME/glass[b]	22°–24°	30°–32°	70°–72°	—
C_{24}SME/Si	26°	32°	72°	1(a)
C_{24}SME/Si, reduced	0°	0°	50°	1(b)
C_{24}SME/C_{24}SME/Si	Not measured	31°	74°	1(c)
C_{24}SME/Si	23°	32°	73°	2(a)
C_{24}SME/Si, reduced	0°	0°	50°	2(b)
OTS/C_{24}SME/Si	46°	51°	112°	2(c)
OTS/Si	46°	51°	112°	2(e)

[a] The precision of the contact angle measurements is of the order of ± 1°.

[b] Maximum contact angle values measured on complete C_{24}SME monolayers on glass.

tionally high (compare the values in Tables I and II with those in refs. 2 and 6). These OTS monolayers appear, therefore, to be almost perfect in terms of surface coverage and chain orientation and packing, possibly displaying long-range two-dimensional crystalline order[2,6].

2. The contact angles measured on the C_{24}SME/Si-wafer monolayer sample (entry 2 in Table II) are close to those determined on the corresponding monolayers on an Si ATR plate (Table I), except for the water contact angle which is somewhat higher. This might point to a larger deviation of the hydrocarbon chains from the surface normal in this particular monolayer, thus causing a larger proportion of inner (—CH_2—) groups to be exposed on the outer film surface.

3. The contact angles measured after each step in the construction of the C_{24}SME trilayer film on the Si wafer (Table II) indicate the formation of a complete first layer, similar to the C_{24}SME monolayers on the ATR plate, followed by less ordered second and third layers (compare values in Tables II and I). Thus, the somewhat lower contact angles displayed by the second layer for the organic liquids, in particular for BCH, may be taken as evidence for a less compact and ordered structure, although not very much different from that of the first one[2,6]. A drastic disordering effect is further observed in the formation of the third layer. This is obvious from the large drop in the BCH and HD contact angles, which may be interpreted as indicating the formation of an incomplete monolayer[2,6]. It is to be noted that the water contact angles are not sensitive to these structural differences (Table II). This behavior can be rationalized by considering the opposite variation tendencies expected for water contact angles on C_{24}SME monolayers of variable density. Usually, lower film densities lead to lower contact angles[2,6], however, in the present case, increasing the area/molecule should result in an outer film surface poorer in relatively hydrophilic ester groups and richer in more hydrophobic chain methylenes, which should thus tend to raise the water contact angles.

The origin of the disordering effect observed in the formation of the third layer in the C_{24}SME trilayer film is not entirely clear. A number of film-building experiments carried out with C_{24}SME on glass, quartz and silicon have shown rather poor reproducibility in the formation of high-quality monolayers of this compound, regardless of the substrate. We suspect that partial misorientation of the film-forming molecules at the liquid–solid interface, caused by the relatively polar

TABLE II

CONTACT ANGLES ON FILMS BUILT ON SILICON WAFERS

Film	*Advancing contact angle*		
	HD	*BCH*	*H_2O*
OTS/Si (two samples)	48°	54°	113°–114°
C_{24}SME/Si (monolayer sample)	27°–28°	30°	79°
C_{24}SME/Si (trilayer sample)	26°	32°	72°
C_{24}SME/Si, reduced (trilayer sample)	0°	0°	50°
C_{24}SME/C_{24}SME/Si (trilayer sample)	24°	28°	72°
C_{24}SME/C_{24}SME/Si, reduced (trilayer sample)	0°	0°	50°
C_{24}SME/C_{24}SME/C_{24}SME/Si (trilayer sample)	About 12°	23°–24°	71°

nature of the terminal ester function, may be responsible for the difficulties encountered in the self-assembly of C_{24}SME. Results of film-forming experiments performed with several other silane–ester surfactants, having the ester function located at different positions along the chain, support this interpretation[7].

3. X-RAY DIFFRACTION

It has been demonstrated that X-ray diffraction can be used to get structural information about LB films even for a single monolayer[5]. It is possible to measure such small (microgram) samples because the Bragg angles are about 1° (the molecules are long and stand nearly perpendicular to the surface), hence the diffraction is occurring near total external reflection from the solid samples. The X-rays that are reflected from the atomic planes are thus relatively intense and their interference produces large modulations in the diffracted beams. This high sensitivity makes it feasible to measure the monolayers deposited by the method of spontaneous adsorption. The most definite information extracted from the measurement is the thickness of the film. This is relevant to the question of the coverage by the film, because if the observed thickness is equal to the known length of the molecules then the molecules must be closely packed. If the thickness is less than the length, the molecules must be leaning, which implies that the packing is not maximal. This case needs to be examined to learn if it arises from incomplete coverage. Our procedure of fitting the data also gives information about the chemical composition of the layers, but this is not very precise. As will be explained below, for rather featureless patterns like that from a monolayer, a good fit to the data can be achieved with a range of parameters; however, some models of the molecule seem incapable of explaining the data and thus may be rejected.

Our experimental and interpretational methods were published earlier[5]. The only change from those techniques is that we now[8] can optimize the fit to the data by use of the simplex method of variation of an initial set of parameters. This is done with the constraint that the correct number of electrons in each lamina is maintained as their thicknesses and refractive indices are varied. The data were taken on a diffractometer possessing a highly collimated and monochromatic X-ray beam. A θ–2θ scan in steps of about 0.01° and counting times of minutes is made under computer control. The resulting spectrum for OTS is shown in Fig. 3. Note that the intensity scale is logarithmic so that the rounded peak at about 1.5° is only 10^{-4} of the incident intensity. This peak is absent on Si substrates that are uncoated; it is caused by the adsorbed OTS. The full line that passes through the data was computed by considering the interference of waves reflected from plane laminae representing the chemical structure of the OTS molecule. The model is shown in Table III, with the parameters used for the various molecules we examined. The structure of the molecules is shown on the left side. The procedure used to find the parameters was to first estimate the index of refraction, $n = 1 - \delta + i\beta$ where δ and β are directly proportional to the electron density, N; $\delta = 1.06 \times 10^{-6} \times N$. We assume that the maximum density is for the alkane packing, because there are no bulky groups to separate the chains. We can then calculate the alkane densities from known structures. When alkane chains are closely packed they occupy an area of about

18 Å^2. The separations of the atoms along the chains and the numbers of electrons are known. Thus for the CH_2 groups, which have $N = 8$ electrons in a volume of 18 Å$^2 \times 1.3$ Å, we find a value of $\delta = 3.9 \times 10^{-6}$. If the molecules are not tightly packed we assume that the deltas will be decreased, but probably not by much. The major effect of loose packing will be a reduction in the thickness of the layer. The tilted molecules will probably pack to a smaller, but approximately the same, density than for close packing. Using known covalent radii, and models of the molecule, we estimate the length of the chain to be 26 Å. From the data of Fig. 3 we derived a thickness of the film of 23 Å, about 13% less than the extended chain length. Incomplete coverage may be the cause of the reduced thickness, but somewhat looser packing in films is probably the cause. In LB films the typical area/molecule of carboxylic chains is 20 Å^2, slightly larger than in bulk paraffins. The packing of our films is unknown, but previous IR and wettability measurements[2] on OTS showed that its density on Si was the same as LB films of carboxylic acids. An area/molecule of 20 Å^2 would allow the chains to tilt the observed extent. The parameter β in Table III represents the lossy part of the refractive index. The values given are only estimates, but in such very thin films they have very little influence on the diffraction pattern.

For the C_{24}SME, similar considerations lead to an estimated length of the chain of 35 Å. The measurements, shown in Fig. 4, give a film thickness of 28 Å. This decrease of 20% is noticeably larger than for OTS. If we attribute a decrease of 13% to steric effects, as in OTS, then here the additional decrease in thickness of about 7% implies a maximum 7% lack of coverage.

The trilayer of C_{24}SME gave the data shown in Fig. 5. We attempted to fit the data using the same parameters used for the successful fit of a monolayer, but repeating it for three layers. We also included the modifications in the structure introduced by the chemical binding of the layers to each other. The result was the curve labeled "3 layers" in Fig. 6. It can be seen that the predicted diffraction has sharp decreases near 0.2° and 1.0°, which appear only vaguely in the experiment. We were unable to find any reasonable parameters that satisfactorily reproduced the data using a three-layer model. We therefore considered the possibility that only part of the film has three layers, and part might have two. The predicted diffraction from a two-layer film is also shown in Fig. 6. The tendency is for the peaks in the three-layer diffraction to occur at the minima of the two-layer diffraction. A superposition of the two patterns smooths the features. By trial we arrived at the fit shown by the full line in Fig. 5. To achieve this fit the ratio of the areas covered by two layers to three layers was 0.55/0.45, and slight adjustments of the thicknesses of the layers were made (as listed in Table III). This fit was not optimized because we felt that a more perfect fit would not be very meaningful, considering the number of parameters. It does seem clear that a mixture of two- and three-layer regions provides an explanation of the data.

Table III also lists the values of the refractive index parameter δ. These values are not to be regarded too seriously, because good fits to the data could be obtained with values of δ of the CH_2 layer (the thickest and thus most important) that differed by 25% from those in Table III. The corresponding change in the thickness of the CH_2 layer was only -3% so the thicknesses are much more strongly determined

TABLE III

SCHEMATIC DIAGRAM OF THE MODEL USED TO CALCULATE THE DIFFRACTED INTENSITIES IN FIGS. 3–6. THE MOLECULAR STRUCTURE DEFINES LAMINAE WHOSE THICKNESSES AND REFRACTIVE INDICES ($= 1 - \delta + i\beta$) ARE GIVEN (DELTAS AND BETAS, IN UNITS OF 10^{-6}, ARE LISTED). n IS THE NUMBER OF $-CH_2-$ GROUPS. FOR THE TWO- AND THREE-LAYER CALCULATIONS OF FIGS. 5 AND 6, THE CENTRAL CHAIN UNIT WAS REPEATED ONCE AND TWICE RESPECTIVELY.

Lamina	*OTS*			*C_{24}SME*			*C_{24}SME multilayer*				
	Thickness (Å)	$\frac{\delta}{10^{-6}}$	$\frac{\beta}{10^{-6}}$	*Thickness* (Å)	$\frac{\delta}{10^{-6}}$	$\frac{\beta}{10^{-6}}$	*Lamina*	*Thickness* (Å)	$\frac{\delta}{10^{-6}}$	$\frac{\beta}{10^{-6}}$
Si	∞	7.6	0.2	∞	7.6	0.2	Si	∞	7.6	0.05
Si Oxide	47	7.8	0.2	45	7.8	0.2	Si Oxide	45	7.8	0.2
O	2.4	1.5	0.04	1.3	2.6	0.04	O	1.6	2.6	0.02
—Si—O—	3.2	2.8	0.07	2.0	4.8	0.07	—Si—O—	1.1	4.8	0.08
$(HCH)_n$	16.3 ($n = 18$)	3.7	0.08	20.8 ($n = 22$)	3.6	0.08	$(HCH)_n$	19.2 ($n = 23$)	3.6	0.06
O—C=O	Not present			2.3	4.0	0.02	O	1.1	2.6	0.02
HCH	Not present			1.1	3.2	0.02	—Si—O—	1.7	4.8	0.08
H	1.1	0.4	0.02	0.7	0.6	0.01	$(HCH)_n$	18.4 ($n = 22$)	3.6	0.06
							O—C=O	1.4	5.8	0.10
							(HCH)	0.8	3.6	0.06
							H	0.6	0.6	0.01
Roughness (Å)		0.25			3.0				3.0	

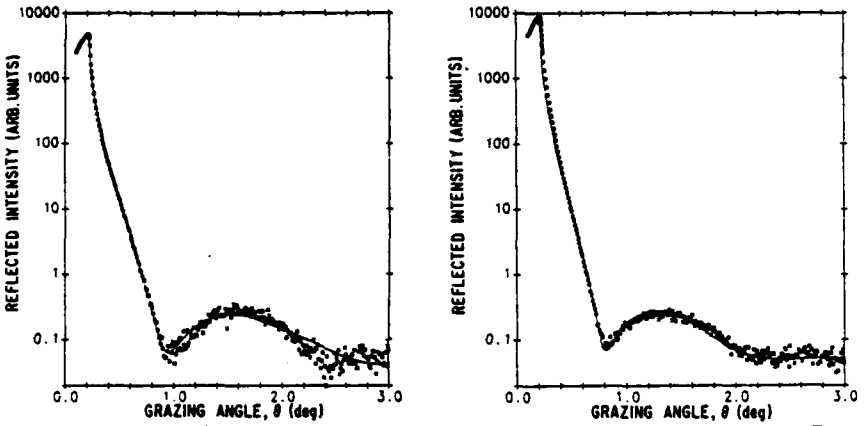

Fig. 3. X-ray diffraction from a single layer of OTS on a Si substrate. The squares are the data points. The full line is calculated from a model described in the text and in more detail in ref. 5.

Fig. 4. Same as Fig. 3 except for one layer of C_{24}SME.

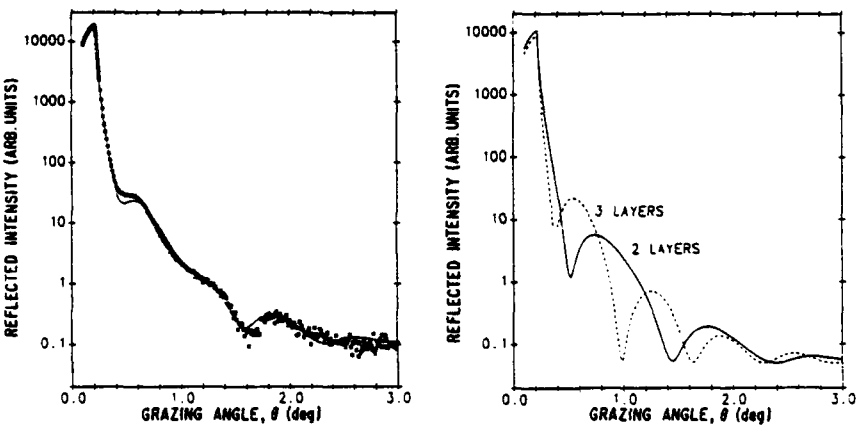

Fig. 5. Same as Fig. 3 except for C_{24}SME prepared as a trilayer. The full curve is the superposition of the diffraction from two- and three-layer films assumed in the ratio of 55% to 45%.

Fig. 6. Calculated diffraction from two- and three-layer C_{24}SME films.

than are the δ values. Nevertheless, we found that some models did not seem to be capable of providing a good fit. For example, if we assumed that the Cl of the original chlorosilane remained attached instead of being replaced by O, this added such a large electron density that only poor fits were found. This model can be rejected on chemical grounds as well.

4. CONCLUSIONS

We have used three independent methods to study the degree of coverage of Si surfaces by chemisorbed OTS and C_{24}SME monolayers, and a trilayer of C_{24}SME,

deposited by the method of spontaneous adsorption. The IR absorption, contact angles, and X-ray diffraction all suggest that the monolayer of OTS is complete. In fact, the contact angles are larger than any values previously reported; this indicates exceptionally good coverage and smoothness. The thickness of this C_{24}SME film is noticeably less than the length of the molecule. This can be interpreted as a lack of coverage of $\leqslant 7\%$, which is compatible with the results of the other methods. In some other samples, IR and wettability indicate complete monolayers of C_{24}SME. For the trilayer of C_{24}SME all the methods allow for an incomplete upper layer. IR showed that, in some cases, when a second layer is added it also helps to complete the first layer. The X-ray diffraction does not seem explicable by a three-layer model. Using parameters not much different from those of the monolayer, we find a good fit by assuming that about 45% of the area has three layers and 55% has two layers. Work is in progress to substantiate the idea that the variability noted for C_{24}SME may result from the proximity of the hydrophilic ester group to the end of the tail.

The X-ray diffraction gives another result which tends to confirm the interpretation that the OTS gives good coverage and that C_{24}SME gives somewhat less. The roughness, r, needed to explain the results differs drastically in the two cases. For OTS we deduced a value of $r = 0.25$ Å, which indicates a very smooth film. For C_{24}SME, we needed $r = 3$ Å, rather like that of a single LB film[5]. A possible interpretation is that the OTS forms a very complete polymer network, linked by Si—O—Si—O— chains. Such chains might have sufficient sidewards strength to allow the film to bridge over the roughness of the substrate, like a membrane. It seems to do this better than LB films, as might be expected. The C_{24}SME bridges less well, perhaps because its coverage is less and the polymer network does not support the film everywhere. Such films would follow the contours of the substrate, and be rougher than well-polymerized films.

It should be noticed the different molecules in this study had somewhat different adsorption properties. Thus the behavior of one or the other cannot be readily generalized. Perhaps after more studies of this kind, on a variety of molecules, we shall achieve greater predictive ability. However, it seems that the method of spontaneous adsorption can be expected to give coverages in excess of 90%, approaching 100% in some cases.

REFERENCES

1 W. C. Bigelow, D. L. Pickett and W. A. Zisman, *J. Colloid Sci.*, *1* (1946) 513.
2 R. Maoz and J. Sagiv, *J. Colloid Interface Sci.*, *100* (1984) 465, and references cited therein; J. Gun, R. Iscovici and J. Sagiv, *J. Colloid Interface Sci.*, *101* (1984) 201.
3 R. G. Nuzzo and D. L. Allara, *J. Am. Chem. Soc.*, *105* (1983) 4481; D. L. Allara and R. G. Nuzzo, *Langmuir*, *1* (1985) 45, 52.
4 L. Netzer, R. Iscovici and J. Sagiv, *Thin Solid Films*, *99* (1983) 235; *100* (1983) 67.
5 M. Pomerantz and A. Segmüller, *Thin Solid Films*, *68* (1980) 33, and references cited therein.
6 J. Sagiv, J. Gun, R. Maoz and L. Netzer, *Proc. 5th Int. Symp. on Surfactants in Solution, Bordeaux, France, July 9–13, 1984*, Plenum, in the press.
J. Gun and J. Sagiv, *J. Colloid Interface Sci.*, in the press.
7 L. Netzer and J. Sagiv, to be published.
8 A. Segmüller in J. M. Cowley, J. B. Cohen, M. B. Salamon and B. J. Wuensch (eds.), *Modulated Structures—1979 (Hawaii)*, *AIP Conf. Proc. 53*, American Institute of Physics, New York, 1979, p. 78.